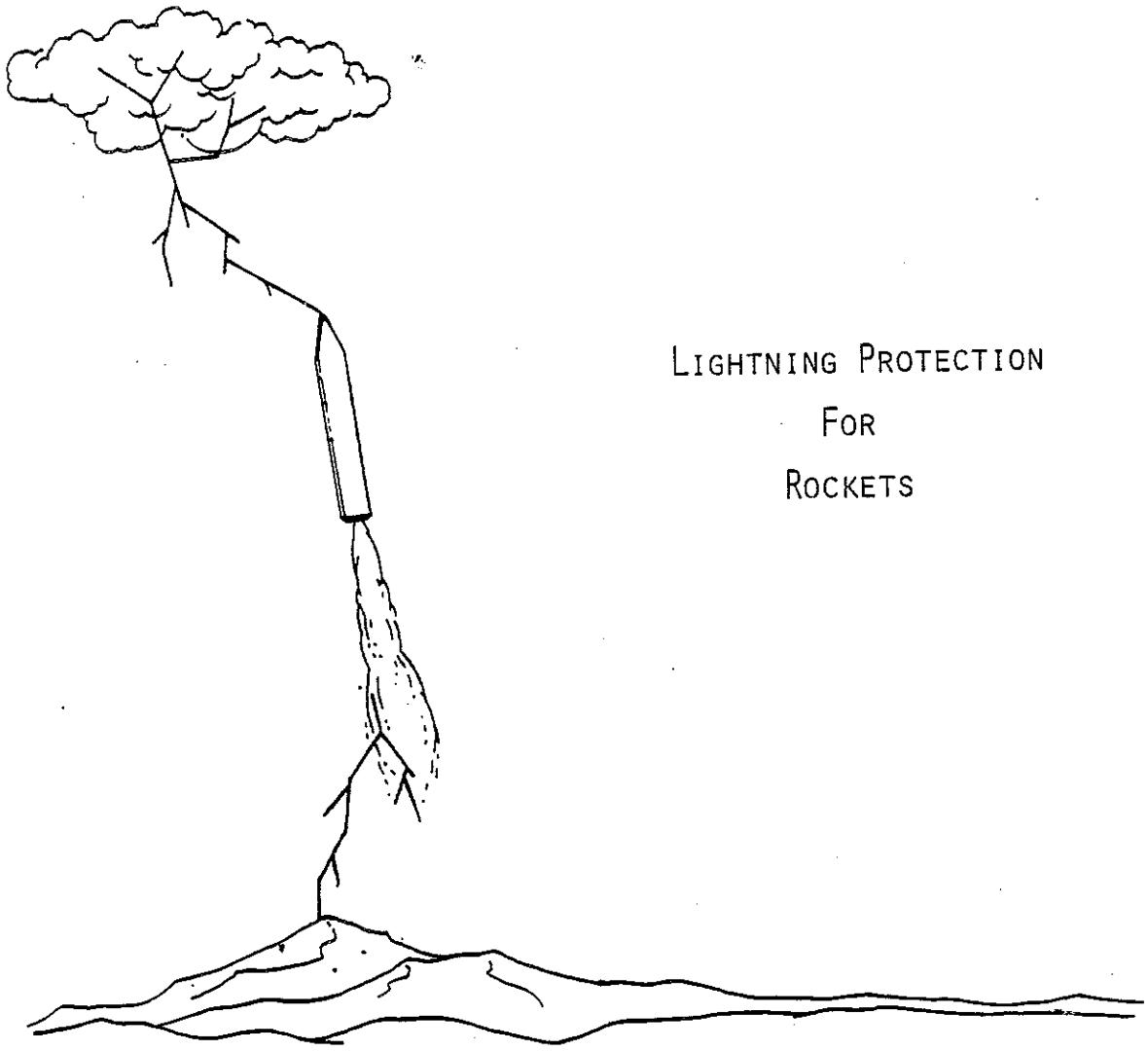

Lightning Protection For Rockets

Bruce C. Gabrielson

1982

ABSTRACT

The lightning threat to airborne vehicles and electrical equipments has become an increasing concern, particularly in view of the trend toward using composite materials and extremely sensitive integrated circuits.

This report presents a generalized approach to designing lightning protection for large modern rockets. Theoretical analyses and state-of-the-art protection techniques are discussed. Data published previously in relation to ongoing rocket test programs is presented.

No classified information or proprietary data has been used.

TABLE OF CONTENTS

LIST OF TABLES

LIST OF FIGURES

INTRODUCTION

Background

Lightning is simply a long spark that discharges regions of excess electrical charge developed in clouds. Little research has been done in the area of lightning effects as they relate to rocket design; the waveform of lightning current that could strike a rocket in vertical flight has been defined a number of times in different ways. A waveform is developed as an example in this document so future designers will have a model when developing their own threat waveforms. No standard methodology for analyzing the effects of lightning on airborne rocket electronics has been developed. The majority of available research and experience deals with aircraft interaction, resulting in design techniques that are not always applicable to rockets. Several large rockets have been designed over the past 35 years, but only subsequent to their design have the equipment and techniques become available to properly examine natural lightning parameters. The U. S. Minuteman program represents the most recent experience in designing a rocket to prevent failures due to static charging or lightning mishaps. Lightning technology was not well understood at the time of design and it was believed the use of an all metal outer skin and heavy, conductive, internal parts would provide sufficient protection from all possible lightning threats.

Apollo 12 was the first important rocket launch affected by lightning. Thirty-six and one-half seconds after launch, at an altitude of 2 km, the Saturn V vehicle was struck by lightning. At the same time, four cameras photographed a stroke to the ground that hit near the launch pad. Quoting

from Brook, Holmes, and Moore,[1]

> "The fuel cells were disconnected from the main power bus, an undervoltage condition prevailed, and numerous alarms and warning lights were activated in the command module. Signal conditioning equipment dropped out for a period of about 60 seconds. About nine temperature and pressure sensors were permanently damaged.
>
> At 52 seconds after launch a second major disturbance occurred. The spacecraft was now at an altitude of 4.2 km, 651 m above the freezing level. This time no visible evidence of lightning was photographed, but a spherics receiver at the ground was saturated. Equipment malfunctions were again noted (battery power was in use at this time), most noteworthy of which was the computer-directed tumbling of the inertial measurement unit in the spacecraft. Fortunately, the inertial unit was not providing guidance at this time."

Based on an analysis prepared for the Office of Naval Research,[2] it was concluded that the rocket triggered the lightning flash. The astronauts on board were able to reset the guidance computers so a major disaster was averted. If one considers that the combined time of all the Apollo launches below the maximum altitude where lightning strikes occur was only 12 minutes, two strikes during a 12-minute period is important from a probability viewpoint.

Modern rockets, weather manned or unmanned, that encounter guidance problems create a hazard to population centers, and must be totally

controlled under any conditions. The use of strong, lightweight, non-conductive materials and extremely sensitive integrated cirucits has made lightning effects a hazard that must be understood and regulated in any modern system. Some lightning protection design experience from the aircraft industry is useful in rocket design; however, the mechanics of an actual strike are only slightly similar. Aircraft strikes involve attachments to an insulated metallic object in near horizontal flight while rocket strikes involve attachment to an object in vertical flight having a metallic tip and trailing a long, conductive plume. Aircraft are physically configured with many attachment points while a rocket has two major points, the nose and exhaust port. Enough information is now available that the natural lightning threat to large modern rockets can be characterized, and a methodology to solve lightning-related design problems can be defined.

The approach presented examined the unique characteristics of a large rocket in flight, then applied the most recent information available concerning lightning phenomena and protection techniques to achieve a cost effective means to evaluate and design any rocket. Theoretical information on lightning phenomena was available from many sources, as was electromagnetic theory and related analysis information. Protection design techniques were extrapolated from aircraft information where applicable.

All major compoents of any standard rocket were examined in detail. The shroud that protects the nose of the rocket was analyzed to determine its influence on current distribution and magnetic field penetration. Information gathered allowed examination of electronics contained therein.

Guidance and control electronics, including plated wire and core memories inside computers, and telemetry systems received a thorough analysis. Downstage electronics and the protection provided by standard downstage cable designs were also examined. An examination of the rocket skin was performed to determine its response or any damage modes that could result from a direct strike attachment. The results of this study can be used to design a lightning survivable rocket by providing both theory and example. Further, information concerning the probability of rocket induced strikes, the use of transfer impedance in lightning analysis, thunderstorm day distribution information and strike characterization has been developed and is presented in this report. Only natural lightning strikes are addressed.

Approach

First, the nature of the threat is determined. The author has developed cumulative distribution functions for the probability of receiving a strike while explaining the properties of the waveform such as rise time, peak current, fall time, dwell time, and energy in the stroke. In each case, a consensus was sought based on a number of studies. When a consensus could not be established, a model was developed and the arguments for it are presented. Also identified are areas of relative susceptibility to the threat.

Second, a methodology for identifying the hardware elements affected and for evaluating the impact of the threat on the design is developed. The lightning threat poses complex dynamic field problems. A number of simplified solutions are presented that are adequate for these assessments.

Chapter 1

EFFECTS OF LIGHTNING ENCOUNTER

Nearby Lightning Effects

There are two aspects of the lightning threat that are significant: voltages produced by direct strikes and voltages induced by nearby strikes. The effects of a nearby strike can be determined by first calculating the magnetic field existing at the rocket a distance r from the stroke. Treating the lightning stroke as a line current of amplitude I, and assuming a perpendicular orientation, the worst case flux density, B, derived from Ampere's law, is

$$B = \mu_o \frac{I}{2\pi r} \quad \text{(Tesla)}$$

where

I = lightning current, amps

μ_o = permeability of free space $4\pi \times 10^{-7}$ Henries/meter

r = distance in meters from the lightning current

In free space, magnetic field strength H is related to flux density by

$$B = \mu_o H \text{(Tesla)}$$

so

$$H = \frac{I}{2\pi r} \quad \text{for a line current.}$$

For a current coil

$$H = \frac{NI}{\ell}$$

where

N is the number of turns,

ℓ is the length of a turn = $2\pi r$

For a specific circuit to be analyzed, using a one turn loop of area A in the same orientation as above; radian frequency of ω.

The total flux, F, for a single turn in free space is:

$$\overline{F} = \vec{B}\vec{A} = \frac{IA}{2\pi r} \quad \text{(webers)}$$

where

$\mu = \mu_o \mu_r$ $\quad$ μ_r is relative permeability

The total voltage V, induced into a one turn loop is:

$$\overline{V} = \frac{d\overline{F}}{dt} = \frac{-\mu IA\omega}{2\pi r}$$

When needed, shielding is used to control magnetic field strength inside the rocket. The incident wave impedance must be taken into account when determining the shielding effectiveness. The penetration of the field through structural apertures must also be considered in determining the field strength inside the structure. Field penetration through apertures has been addressed extensively.[3,4,5]

Effects of Lightning Strikes on Rockets

Once the waveform of lightning striking the rocket has been characterized, the most obvious question to ask is, "What will the effects be?" Since little information is available on rocket strike effects, related aircraft information is used to provide basic guidelines. Two types of lightning effects are discussed: direct and indirect. Direct effects are physical damage, and usually include high voltage and current related damage to metallic or composite structures and other hardware. Indirect effects

are malfunctions, either temporary or permanent, that affect avionics and electrical systems. These effects arise from voltages and/or currents induced in the avionics equipment.

Direct Effects on Electrical Systems

Direct effects of lightning are the burning, eroding, blasting, and structural deformation caused by lightning arc attachment, as well as the damage produced by the high-pressure shock waves caused by the high currents. Structural damage effects are typically localized in the immediate area of the arc attachment point since the current density is highest there. As the current enters a conductive structure it rapidly spreads so the current density is quickly reduced to harmless levels. This localization effect is particularly true for the lower level continuing current phases of a strike.

Damage may be far reaching if current dispersion is prevented, or if there is limited current-carrying capacity in the path taken by the lightning currents. Rockets are often made with a substantial amount of composite nonconductive material for weight reduction. To provide communication between the stages, a cable is sometimes attached along the outside of the skin for accessibility. The cable is housed in a conductive conduit known as a raceway running from the aft skirt to some point near the nose. When lightning attaches to the nose its current is restricted to traveling down the raceway until it reaches the plume. The energy involved could cause harmful or improper signals on wires within the cable if the raceway does not protect it.

Examples of points in the design that might limit the current-carrying capacity include bonding straps, adhesively bonded structures, or high resistance coatings of the type designed for prevention of static charge buildup. Ignoring resistance changes due to temperature, the Joule heating developed can be represented mathematically as:

$$J = \int_0^t RI^2(t)dt$$

Where:

J = heat developed in test part (Joules)

t = time (seconds)

R = electrical resistance (ohms)

I(t) = electrical current (amps) as a function of time

When the electric current is introduced into the conducting material by means of an electric arc, heat is generated in the material due to normal Joule heating and to heating at the arc/metal interface. If the current has a fast rise time, the initial current will essentially remain on the surface of the metal (skin effect). As the time period increases, the current and the heat will diffuse and spread into the matierial. This can be compared to an arc weld except that electrical currents are several orders of magnitude greater for lightning, and the time can be several orders of magnitude shorter.

The nature of localized structural damage to electrical hardware is dependent upon the construction and geometry of the part, as well as on the type of lightning current flowing. The high peak current surge

exerts shock and mechanical bending forces because of the intense magnetic fields and the explosiveness of the channel. However, on large conductors such as thick aluminum, very little effect is noted; typically just small pits or etch marks on the surface. Conversely, the continuing current is capable of melting sizable holes through relatively thick, metal parts if allowed to deposit its energy at one point for a few tenths of a second.[6]

The shock and blast effects of the high peak current phase may shatter coverings, allowing the current direct access to the electrical system. The high peak currents tend to flow in straight lines so conductors with sharp bends will either be magnetically distorted, or the lightning may flash across the corner or find an alternate path. Magnetic forces are proportional to the square of the current producing them, and the damage produced is related to both the magnetic forces and to the response time of the affected system.

In areas where the current density is high, such as at the attachment of protective bonding jumpers or at an arc root, the magnetic forces can become large. This problem has been addressed by James and Phillpott[7] who determined that an arc rising in a few microseconds to a peak current of 200 kA will have a diameter of about 2 mm; hence, its maximum magnetic field will be about 40 Tesla. This will produce a magnetic pressure approaching $6.3 \times 10^8 n/m^2$ (150,000 lbs/in^2).

Indirect Effects on Electrical Systems

Indirect effects are caused by lightning induced electromagnetic fields coupling currents into internal electrical equipment. The effects may cause problems even if the lightning flash does not directly strike the

rocket. Direct and indirect effects often occur simultaneously.

The mechanism whereby lightning currents induce voltages in electrical circuits is illustrated in Figure 1-1. As lightning current flows through the chassis, strong, rapidly changing magnetic fields surround the conducting path. Some of the magnetic flux will penetrate the structure and joints. Other fields may arise inside the rocket when lightning current diffuses to the inside surfaces of skins. These internal fields interact with rocket electrical circuits and induce voltages in them proportional to the rate of change of the magnetic field. These magnetically induced voltages may appear between both wires of a two-wire circuit or between either wire and the raceway of other conductors. The former are referred to as line-to-line or differential-mode voltages and the latter as common-mode voltages.

In addition, resistive voltage drops occur along the raceway as lightning current flows through it. If any part of a circuit is connected anywhere to the raceway these voltage drops may appear between circuit wires and the raceway. For rockets made of highly conductive aluminum these voltages are seldom significant except when the lightning current must flow through resistive joints or hinges. However, the resistance of titanium is ten times that of aluminum and the resistance of composite materials may result in resistive voltages significantly higher.

Rocket Physical Characteristics

Figure 1-2 shows magnetic flux lines for typical rocket profiles. When the rocket is built in stages with a raceway design, current is constrained causing maximum flux density.

MAGNETIC EFFECTS

ϕ_c - COMMON MODE FLUX
ϕ_d - DIFFERENTIAL MODE FLUX

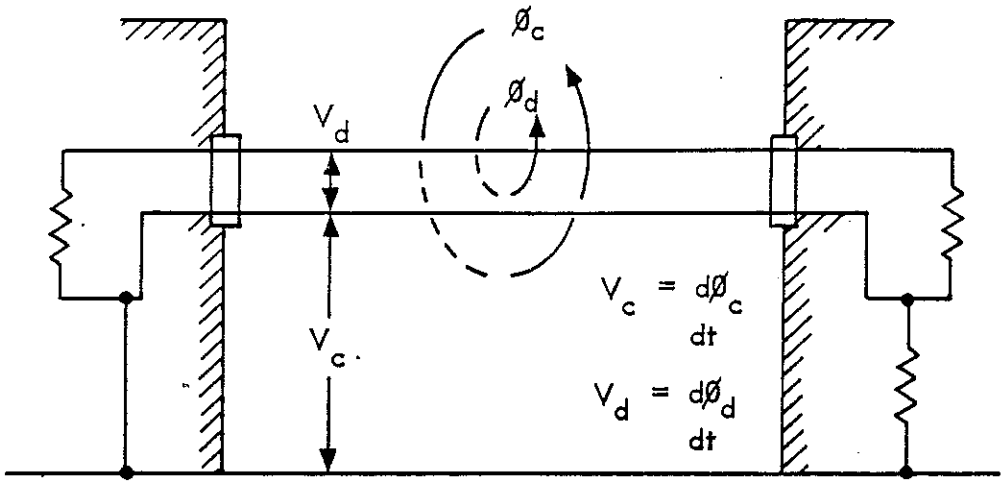

- INDUCED VOLTAGE IS PROPORTIONAL TO di/dt (FOR APERTURE COUPLING)
- VOLTAGES ARE INDUCED BY BOTH COMMON AND DIFFERENTIAL MODE FLUX

E-FIELD EFFECTS

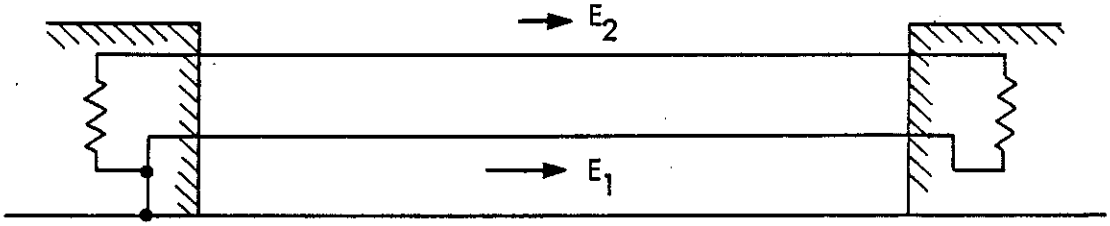

- VOLTAGES CAN BE COUPLED INTO CIRCUIT LOOPS BY E-FIELD GRADIENTS

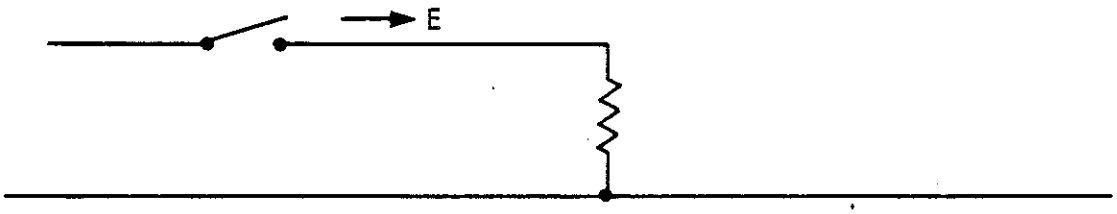

- VOLTAGES CAN BE PRODUCED IN OPEN CIRCUITED IMPEDANCES BY AN E-FIELD (VOLTAGE GRADIENT)

Figure 1-1. Electrical and Magnetic Field Coupling to Electrical Circuits[8]

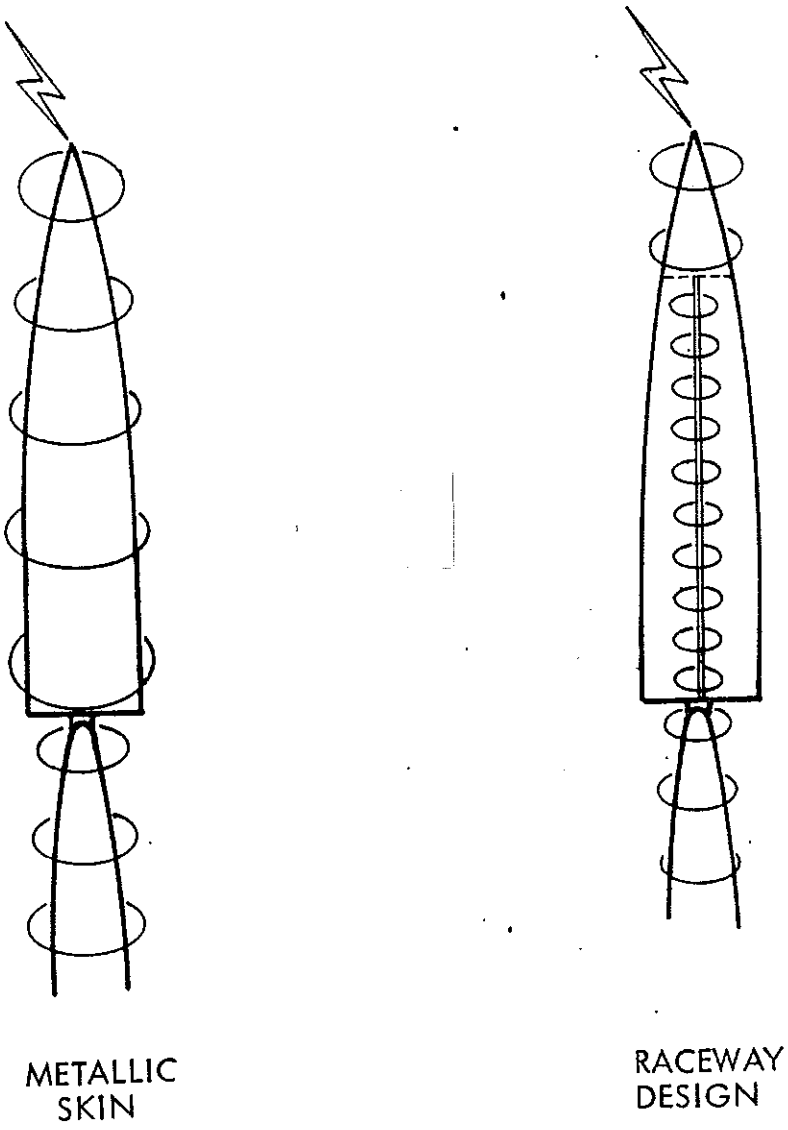

Figure 1-2. Magnetic Flux Lines

Guidance electronics are usually located in the upper stages, since guidance is needed throughout powered flight. Rocket motors or other propulsion mechanisms comprise most of the lower stages. Electronics in the lower stages often consist of ordnance firing devices and flight test instrumentation circuitry.

Chapter 2

THE LIGHTNING THREAT

Lightning Strike Probability

It is difficult, if not impossible, to establish a probability for lightning strikes that one can have high confidence in. The literature and tests performed to establish probability are primarily oriented to a special case, rather than the generalized case that is required. Further, the probabilities will depend on factors such as location, time of year, surrounding terrain and structures, and orientation of the rocket to the charge center.

The primary reason for wanting to do a probability analysis is to determine whether there is a reasonable chance that lightning will hit the rocket, and if there are major costs associated with accommodating the rocket to lightning strikes. Since the increased cost of accommodating lightning strikes varies with the type of rocket designed, the importance of a probability analysis is dependent on the individual project.

If it is necessary to establish such a probability, the data supplied in the subsequent paragraphs of this chapter is provided to assist the reader. The numbers are nominal values only included as examples. A specific analysis would involve selecting values within the ranges specified.

Thunderstorm Days

The parameter commonly used throughout the world for lightning information is the thunderstorm-day data tabulated by the World

Meteorological Association. A thunderstorm-day is defined as a calendar day on which thunder is heard.

There are problems related to using thunderstorm-day data because it is possibly inaccurate for lightning predictions. Thunder is rarely heard at distances exceeding 25 km from the lightning channel,[9,10,11] and the average practical limit of audibility seems to be about 15 km. One of the reasons for this limit is acoustic refraction. Fleagle[12] has estimated that according to the various atmospheric refractive circumstances normally encountered, the range of audibility of thunder lies between 5 and 25 km. The problem, therefore, is that except for heavily populated areas, not many people have been around to hear the thunder.

A second problem with thunderstorm-day data is that it contains no information on the intensity or duration of a storm or if one or several flashes occurred. A. S. Dennis[13] suggests that the average rate of flashing in a thunderstorm cell is about three per minute regardless of storm location. A typical storm can be made up of several cells, and according to Cianos and Pierce[14] the average flashing rate may not change with more cells, only the duration of the storm. Typically, an active single cell storm lasts about one hour,[15] and the average tropical thunderstorm lasts about three hours. A rough approximation of the flash incidence can be made if A is the storm area (radius estimated between 300 km and 500 km on the average[16]), D is the storm duration, and F is the average flashing rate. The flash density per unit area in a thunderstorm-day is DF/A.

Appendix A summarizes atmospheric information in a sparsely populated area of the U.S. These data show that the number of cloud-to-ground lightning stokes occurring in a given area will be substantially greater than current thunderstorm-day data predicts. Listed below are typical thunderstorm activity values for selected locations.

Thunderstorm days per year - $T\gamma$

West Coast (5)	Southeast U.S. (93)
Kwajalein Island (2)	Asia (20)
Southwest U.S. (40)	Eastern Europe (20)
Northwest U.S. (40)	Europe (3)
Midwest U.S. (60)	

Flash Density

Intercloud discharges and flashes to earth ground are primarily controlled by altitude and by the separation of the individual charge centers. Charge-center distributions are at least partially attributable to local topography and latitude.[17]

Pierce[18] has represented the latitudinal variation by:

$$p = 0.1 \left[1 + (\lambda/30)2\right]$$

where p is the proportion of discharges that go to ground, and λ is the geographical latitude in degrees. Muhleisen[19] states that in middle latitudes, about the same number of discharges occur between clouds as there are flashes to ground. Figure 2-1 shows the strike relationship.

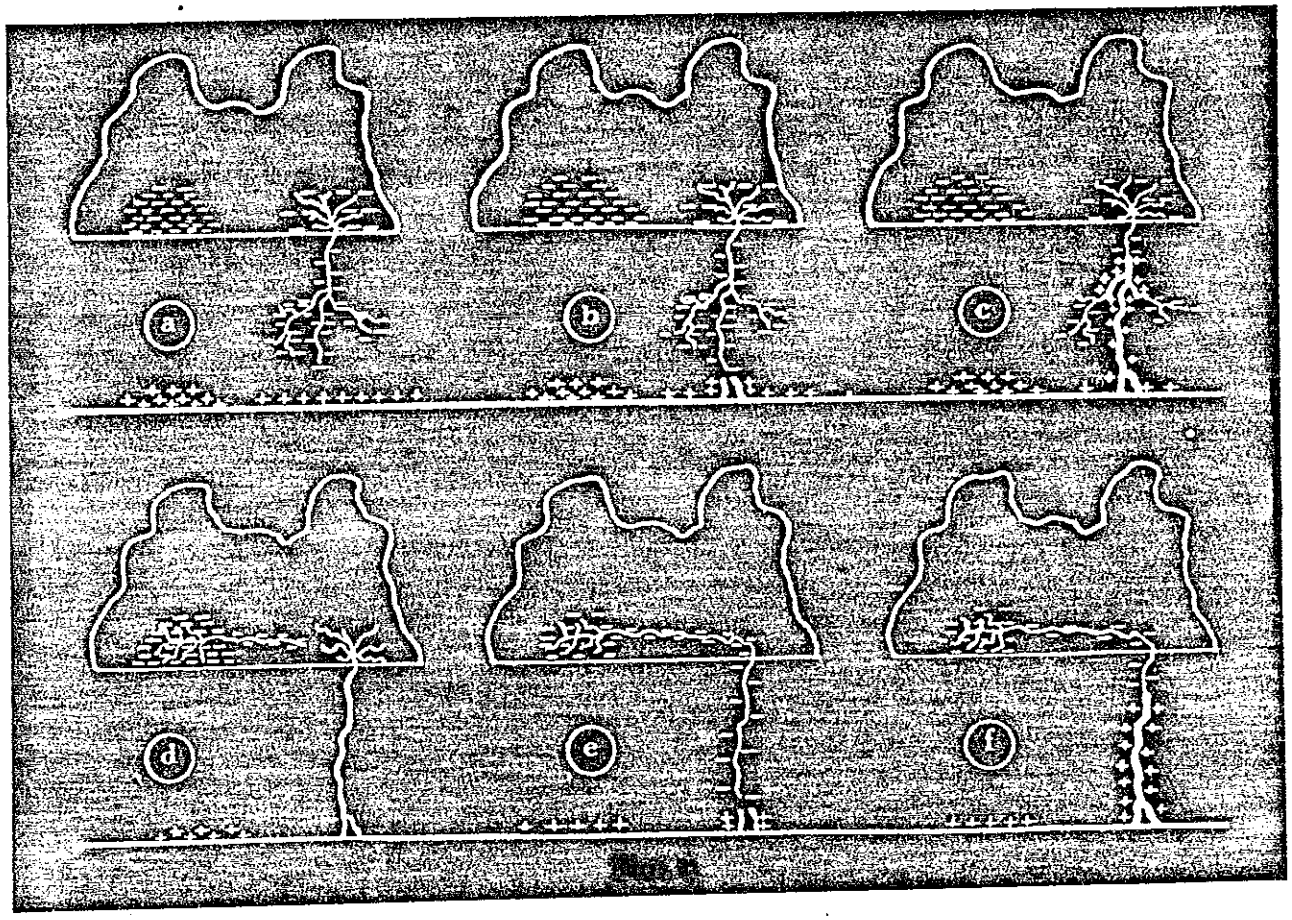

Ratio of cloud- and ground-flashes 1975

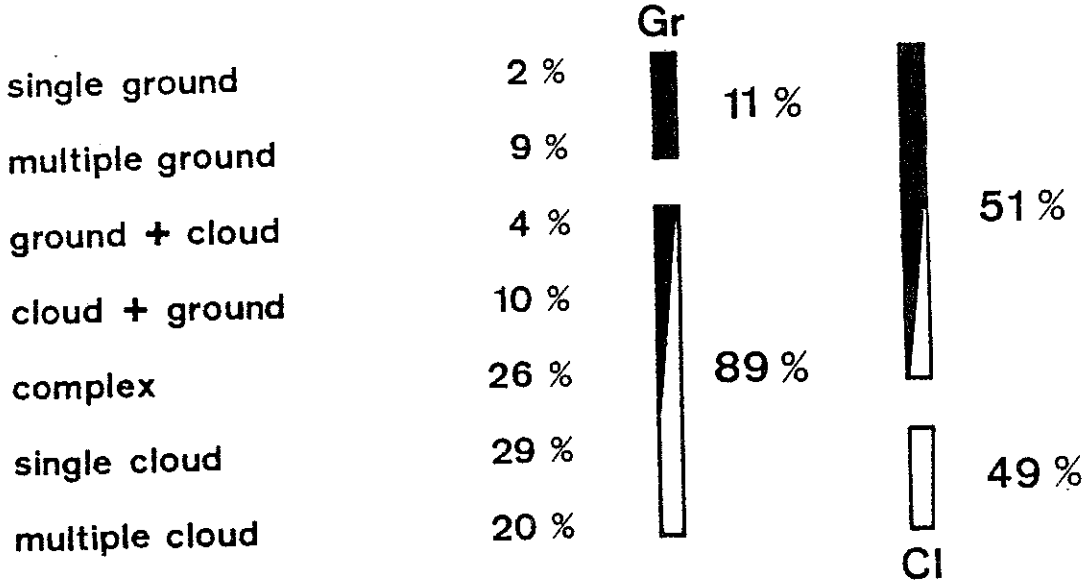

ground flash = cloud to ground

cloud flash = intra cloud or cloud to cloud or cloud to air

Figure 2-1

Combining the equation for the average density of lightning to ground for any location:

$$\sigma gy = 0.1\ DF/A \left[1 + (\lambda/30)2\right] T\gamma$$

where σgy is the flash density, λ is the geographical latitude and $T\gamma$ is the number of thunderstorm days per year. $T\gamma$ is taken as 50 for the following examples. It is important to note that the Pierce equation is for the discharges to ground and the above figures only approximately reflect all lightning flashes that may affect rocket electronics.

Exposure Time

Exposure time is the period during which a rocket is vulnerable to the effects of a direct or nearby lightning strike. Figure 2-2 shows a vehicle altitude versus time profile for the rocket used in this example. Since lightning can occur to 20 km (65,000 ft), we can use 50 sec for the upward exposure time of the rocket. The probability of a nearby strike (P_n) affecting the rocket, based on thunderstorm days only can now be estimated using the equation:

P_n = flash density x vulnerability area x exposure time

Direct Lightning Strike Probability

Direct strike probabilities are difficult to determine. The surrounding terrain and the physical orientation of the vehicle during a thunderstorm are key considerations. To make the problem manageable, an assumption is made that the rocket will always be hit by a strike when the opportunity exists. To further simplify the calculations, we assume the probability

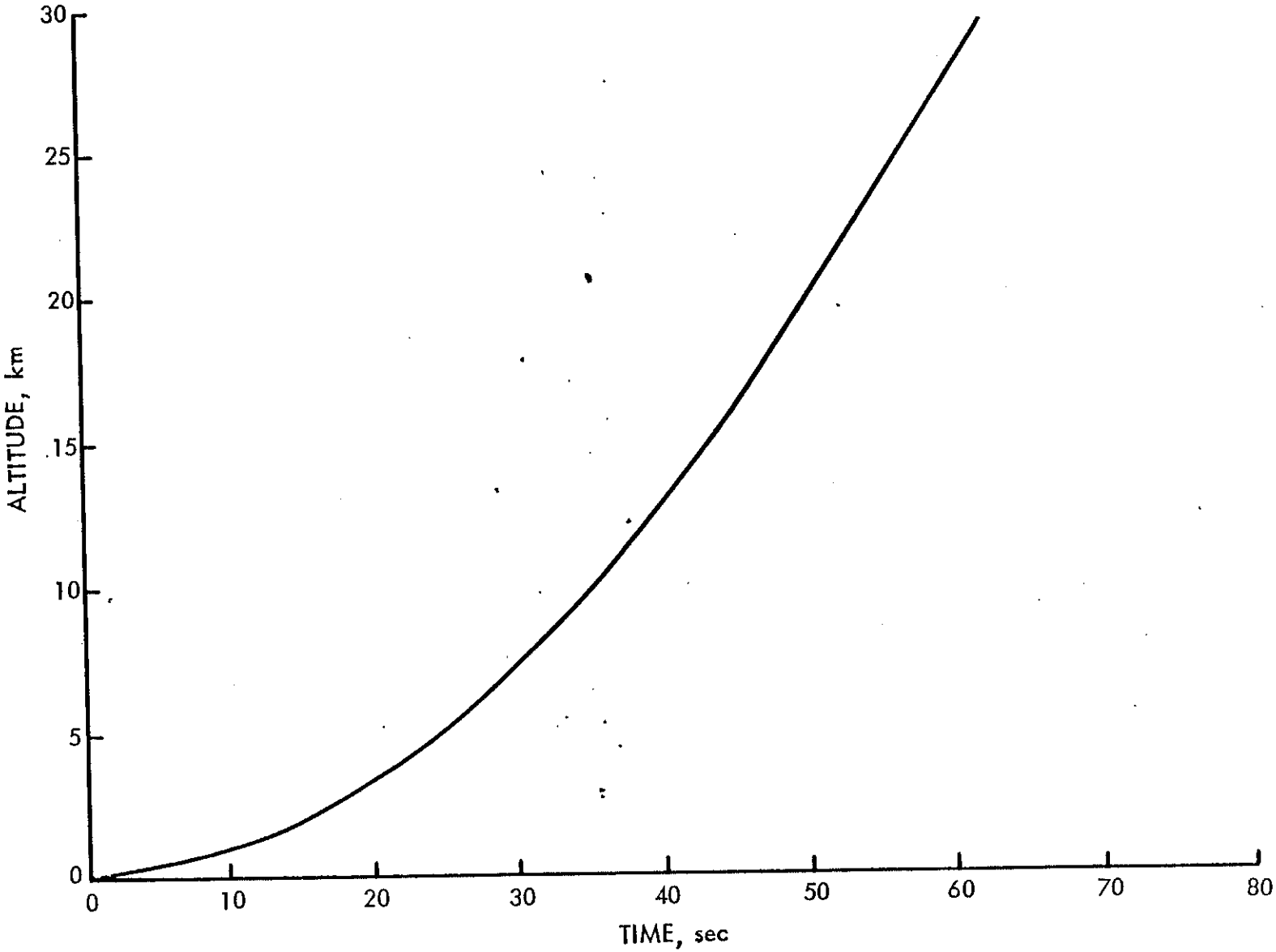

Figure 2-2 Nominal Rocket Altitude Profile

is then equal to the probability of a flash to ground over any surface area of approximately the same size as the largest cross sectional area of the rocket when vertically oriented.

According to Uman, various studies determined that the number of flashes to ground per square mile per year falls between 0.05 and 0.8 times the number of thunderstorm days per year for various geographic locations.[20] For this example we assume a value of 0.05. However, a more exact number is necessary for a specific launch location. Therefore, if a surface area of one hundredth (1/100) square mile is used for the rocket area, the minimum value of 0.05 flashes to ground is used, and 50 thunderstorm days is used, a probability can be calculated for the case in question.

$$P_d = \frac{50 \times 0.05}{100} = 0.025$$

Rocket Triggered Lightning

It would appear from the probability analysis that the likelihood of a strike to ground affecting a rocket is not large. However, the rocket does not stay on the ground and cloud-to-cloud discharges also affect vehicle performance. Therefore, a closer look at the triggering process and how the probability calculation might be modified is necessary. This is especially important if one considers that a triggered strike will actually involve the rocket and circuit upset is more likely to occur with the fields involved in a direct strike than from a nearby strike.

There is considerable evidence that a rapidly moving aircraft charged to high potentials by triboelectric processes can trigger lightning discharges by passage through freezing precipitation. If we examine this rationale and then compare the aircraft to a rocket in flight, several conclusions become significant. The following sections postulate a case for rocket triggered lightning similar to the case proposed by Clifford[21] for aircraft.

Fitzgerald,[22] in his Rough Rider Program experiments, developed evidence that the presence of an aircraft in an electrified environment initiated lightning strikes. Also, other researchers[23,24] have been able to trigger lightning strikes to ground by firing rockets into charged clouds. Grounded wires were attached to each rocket, resulting in a slightly different electrostatic situation than a considerably larger rocket in free flight.

To determine if a rocket will trigger a lightning strike with or without the presence of clouds, we will first examine the atmospheric conditions leading to the production of a lightning flash in the presence of an aircraft. Then, we will relate these to the rocket case. Commercial and military pilots agree that there are two distinct classes of lightning observed in flight.[25] The most common type usually occurs while flying in precipitation at temperatures near freezing. This type is preceded by a buildup of static noise in the communication gear and the presence of corona (St. Elmo's fire). The buildup may continue for several seconds until a violent discharge takes place. Once the discharge occurs, the

static and corona disappear. The discharge may repeat itself if the aircraft continues to fly through precipation. This precipitation does not have to be associated with a thunderstorm. Reports of these low buildup strikes typically indicate no visible lightning in the vicinity and no radar indication of thunderstorms in the region.

The second type is usually described as more violent, and occurs without any warning. It is almost always encountered in or near thunderstorms. Both types create a brilliant flash, but the abrupt type usually produces more damage.

To postulate a triggering process and determine if lightning is indeed a likely threat to an in-flight rocket, a review of lightning strike weather statistics is of value. Statistics show weather tendencies favor the slow buildup type of discharge. Figure 2-3 shows the temperature distribution for lightning strikes to aircraft. Figure 2-4 shows the environmental conditions related to clouds, precipitation, and turbulence at the time of 214 strikes reported by Fisher and Plumer.[26]

In over 80% of strikes reported, aircraft were within a cloud and were experiencing precipitation and some turbulence; the vast majority occurred at temperatures near the freezing level. Evaluation of the synoptic conditions and localized weather circumstances by Harrison,[29] in the case of the United Air Lines strikes, and Trunov[30] in a summary of USSR incidents, confirms that thunderstorm activity is usually not present at the time of a discharge.

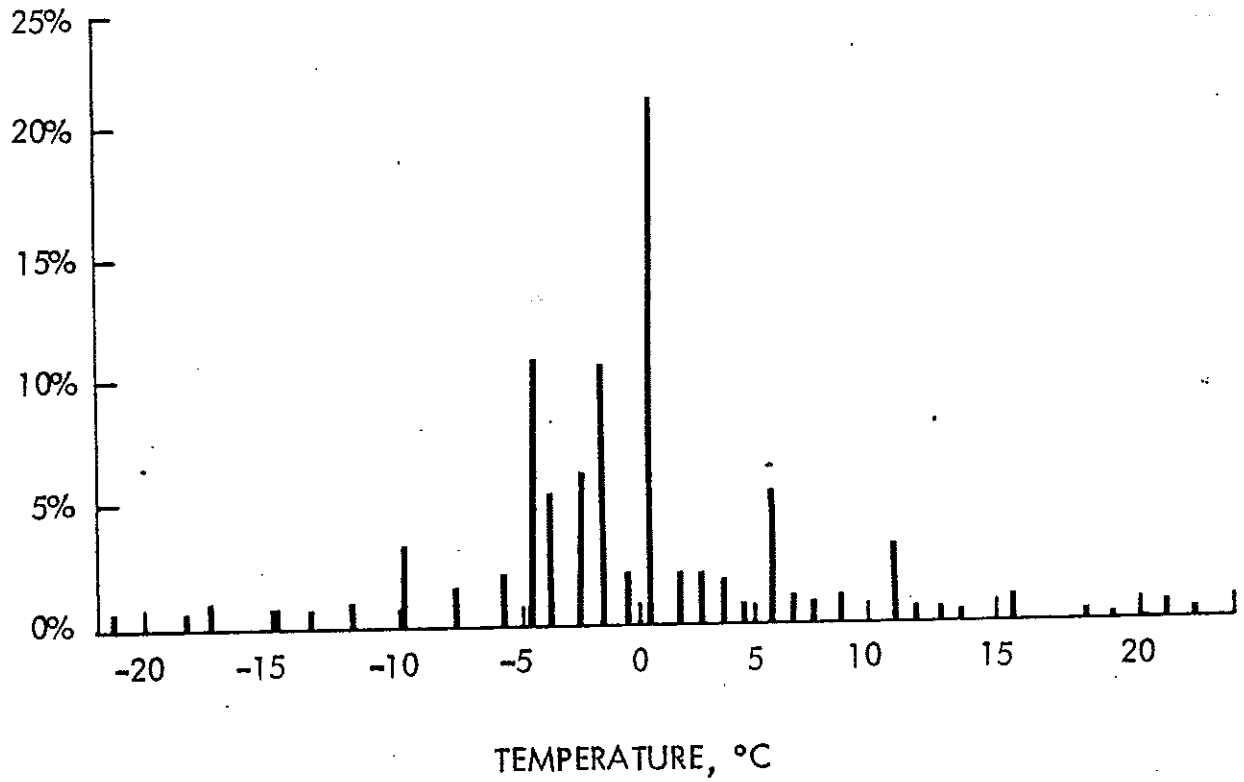

Figure 2-3. Lightning Strikes to Aircraft[27]

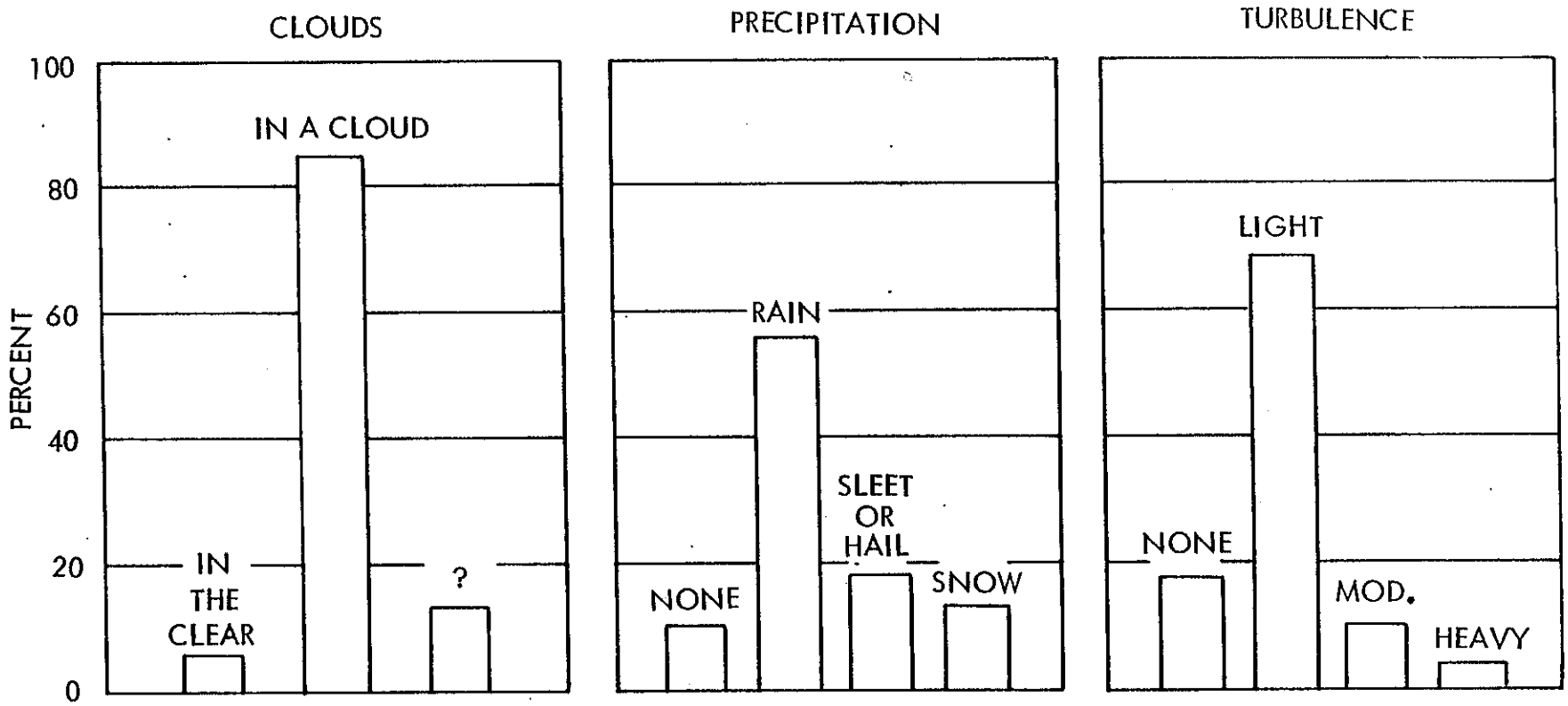

Figure 2-4 Environmental Conditions at Time of Strike[28]

Triboelectric Charging

Triboelectric charging is the exchange of charge produced by friction from precipitation or dust particles impacting a moving vehicle. This type of charging appears to either generate or increase the possibility of a lightning flash. However, the physical mechanisms and processes involved are not well understood at present.[31]

According to Nanevicz,[32] charging rates are a function of precipitation particle concentration, precipitation type, effective frontal area of the vehicle, and velocity of the aircraft. The precipitation charging current to a vehicle is given by:

$$i = q_p \; c \; v \; A_{eff}$$

where

q_p = charge per particle

c = particle concentration

v = aircraft velocity

A_{eff} = effective intercepting area of aircraft

Typical values of particle parameters for in-flight vehicles at subsonic speeds are given in Table 2-1.

Table 2-1. Precipitation Particle Parameters[33]

Cloud Type	q_p pico Coulomb	C m^3
Cirrus	1 - 10	2×10^4
Thunderstorm Anvil	1 - 35	5×10^4

In practical charging calculations Nanevicz suggests the use of the experimental results shown in Table 2-2. These values lead to total aircraft charging currents of a few hundred microamps, but values as high as 3 milliamps have been measured in flight.[34]

Table 2-2. Peak Charging Rates Encountered With KC-135 Prototype[35]

Cloud Type	Peak Charging Rate (μamp/sq ft)
Cirrus	5 to 10
Strato Cumulus	10 to 20
Frontal Snow	30

The triboelectric charging rates quoted by Nanevicz for ice particles and water droplets are values measured at temperatures away from the freezing level. Maximum charging rates quoted are for ice crystals and corona. However, no violent or abrupt discharges have been reported in cold ice crystals, contrasted to the case of precipitation at the freezing level.

If we assume that the conditions at some altitude, temperature, and humidity cause the electrical breakdown strength of air to be considerably less than the strength at sea level, and if we assume that the vehicle has some small but finite capacitance, it follows that a small charging rate can raise any vehicle to a significant potential. Potentials of over two million volts have been measured on research aircraft in the USSR.[36]

Aircraft Towing Long Conductors

According to Clifford,[37] at least ten events involving electrical discharges from the end of long steel cables being towed by aircraft have been reported. Some incidences were reported as static electrical discharge from the aircraft through the towed conductor, with no observable lightning strike to the aircraft and the possibility of lightning unlikely. Clifford concluded that although there may be an intense charge exchange activity going on in apparently stable cloud systems, there is no visible electrical activity because there is no effective mechanism for large-scale charge separation.

Ionized Gases

Even though the exact composition of a particular rocket exhaust is unknown, Shaeffer[38] has investigated engine exhausts as a possible lightning triggering mechanism. He concluded that the ion concentrations in the exhaust are too low by themselves to trigger lightning. It should be pointed out that the case of a gas containing conductive metallic particles was not examined by Shaeffer, and most solid propellent fuels contain some conductive material. Table 2-3 lists the lightning streamer head.

Table 2-3. Comparison of Electron Concentration Values

Electron Concentration In	Quantity (e/cm^3)
Free Atmosphere	$10\text{-}10^3$
Jet Exhaust	$10^3\text{-}10^5$
Rocket Exhaust	10^{12}
Lightning Streamer Head	10^{12}

In Shaeffer's study, exhaust ions were supplemented by the ionized corona streaming from protruding points on the charged aircraft. The presence of a corona tends to decrease the amount of charge the vehicle can hold. A rocket will have virtually no protruding points over most of its length, allowing very few corona locations, and creating a uniform potential gradient along the entire rocket length. Also, since the rocket is moving in a fast, nearly vertical direction, the slow corona buildup mentioned previously is unlikely to occur.

Air Conductivity

High charge densities can be postulated in an exhaust plume, but the wake itself will not act as a conductor unless the charges are mobile enough to move freely. Charges are essentially frozen in a dielectric medium. Air conductivity is lower in clouds since moisture droplets capture free vapor ions and prevent them from moving in the presence of an external field. We assume these same conditions exist in a rocket wake, and charges will attach to nearly immobile ice particles, dust, contaminants, or water droplets. Solid dielectric material will greatly reduce the materials's insulating capability. Griffiths[39] demonstrated a 20% reduction in the external field required to produce corona from ice crystals if they were initially charged to nominal values.

Electric Field

It is difficult to determine if the strong electric fields associated with thunderclouds are the result of precipitation or down-drafts. Regardless of their source, according to Muhleisen,[40] field strength as high as 2.5 kV/meter exists at distances up to about 10 km from a single thundercloud cell. Natural lightning occurs inside a cloud when the field strength exceeds about 10 kV/meter.

The natural electric field surrounding any charge center in the atmosphere is distorted by the presence of a rocket or aircraft. The distortion is mostly related to the geometric form of the aircraft body. For an ellipsoid the outer electric field near the aircraft is enlarged by a factor k depending on the ratio a/b; a is the length of the longer axis, and b is the length of the transverse axis of the ellipsoid. Table 2-4 lists various values for k. These values suggest field distortions will be greatest in the vertical axis for rockets, decreasing the potential required for triggering.

Table 2-4. Electric Field Intensification Factor
Ellipsoid-Axes a and b

a/b	2	5	10	20	50
k	5.8	16	49	148	694

Rocket Interaction

We can postulate the effects of a relatively large, possibly highly charged, mass of metal passing almost vertically through a field of charged ice crystals and supercooled water droplets, leaving in its wake a turbulent exhaust of hot ionized gases and conductive, partially charged contaminants.

To generate a spark discharge, streamers must be generated from an electrode into the surrounding atmosphere, or toward a nearby concentration of charge. Clifford[41] pointed out that streamers, once initiated, will propagate in low field regions, and free charge in the exhaust added to the external field gradient might allow streamer propagation

through the exhaust in low ambient fields. As noted by Shaeffer[42], this streamer is nearly identical in order of magnitude to the electron concentration of rocket exhaust. The rocket itself acts as an electrode of increasing potential as it increases in velocity and altitude.

When the charge density reaches a critical level, photoionization of the adjacent air in the direction of the applied field allows the charge volume to grow in that direction. The requirement for propagation is related to the ratio of field strength to pressure, E/P. This indicates that as the rocket climbs the field strength required for triggering decreases. We can postulate that the rocket will eventually charge to a potential sufficient to create a streamer and its exhaust will decrease the breakdown potential necessary for triggering to occur. The streamer would then provide a sufficient concentration of free electrons to act as a conductor and compress the external field. Figure 2-5 gives the field strength at which air breakdown occurs.

Since triggering can occur in the presence of nonstormy clouds[43], we will further postulate that triggering of some magnitude will nearly always occur in cloudy or overcast conditions, or when the rocket is launched within a few kilometers of such conditions.

For rocket induced lightning in charge concentrations where the charge is insufficient to produce natural lightning, we can assume the discharge would probably contain less energy. However, based on the previous analysis, one must conclude that the possibility exists of a lightning flash hitting an in-flight rocket, even with no thunderclouds present.

Corrected Nearby Strike Threat Estimate

Having examined the characteristics necessary for a rocket to trigger a lightning flash to ground, the earlier probability evaluation can be modified for a more realistic assessment of the threat. The analysis presented suggests a triggered strike (cloud-to-cloud or cloud-to-ground) will probably involve the rocket whenever the conditions exist for an intercloud discharge within 10 km of the craft. Noting the previous statement that the number of intercloud and cloud-to-ground strikes are about equal, and using the data in Appendix A to modify the thunderstorm day number, the following analysis is postulated.

To correct the thunderstorm day data and take into account intercloud effects, the value of the average flashing rate can be corrected:

$$T\gamma_1 = 10 \times T\gamma$$

$$F = (3 \text{ per min})(60 \text{ min per hr})(2) = 360$$

The correction still does not totally compensate for the triggering effect, but using intercloud discharges does help correct the deficiency. If an additional 5% of the total value is added to account for discharges which can be triggered on nonstormy days, the recalculated value of probability of the rocket of this example encountering a nearby strike during flight is $P_n = 0.01575$. The total maximum probability for this case is therefore $P_{n1} + P_d = P = 0.03075$.

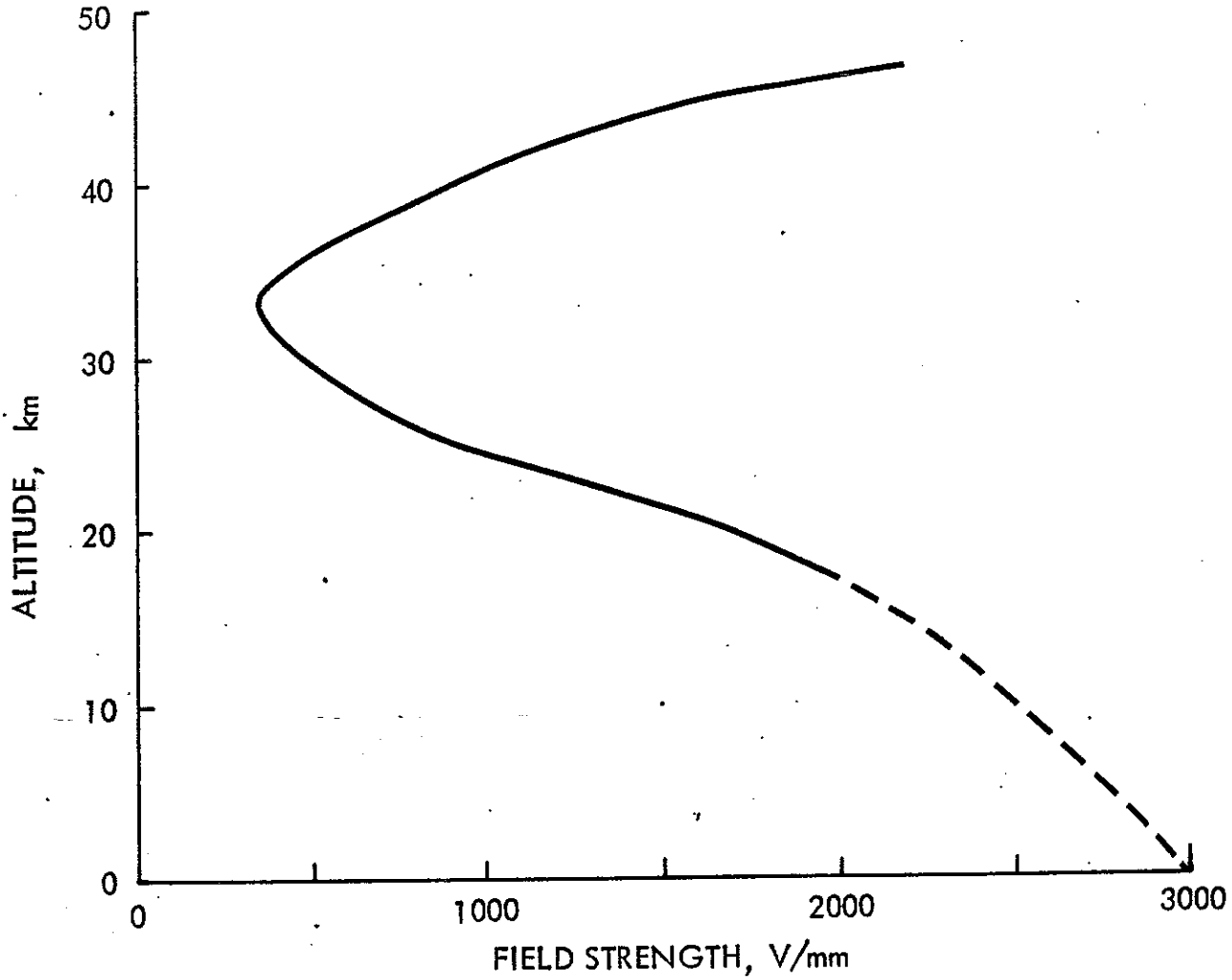

Figure 2-5. Electric Field at which Breakdown of Air Occurs

Chapter 3

LIGHTNING STROKE MODEL

Classic Lightning Strike Phenomena

To understand the lightning discharge phenomena, some discussion of what actually occurs is required. The total lightning discharge, called a flash, is initiated by a downward (or upward) traveling spark known as a stepped leader. Stepped leaders move from cloud to ground in rapid steps, each about 50 yards long. The visible flash occurs when the stepped leader contacts the ground or an oppositely charged body of equal proportions.

Each flash between cloud and ground is composed of a number of independent current pulses called strokes. Three or four strokes per flash are common and a much larger number of strokes can occur. If there is a sufficiently long time period between strokes, the lightning will appear to flicker.

Once a leader gets close to the ground, a return stroke is initiated at the ground surface that propagates back up the ionized channel left by the passage of the downward going leader. Return strokes have higher amplitude since they grow by collecting charge left by the downward traveling leader. Return strokes propagate at a velocity related to the amount of charge transfer, usually 0.1 to 0.3 times the speed of light. The relationship is shown in Figure 3-1. Velocities slower than the speed of light result from longitudinal resistance of the return stroke channel and the inductance associated with the small diameter highly conductive

central core of the return stroke channel.

Lightning may be initiated by either upward or downward moving stepped leaders. Since a rocket often exhausts a conductive plume, it can be thought of as an upward traveling lightning rod capabe of initiating either a ground-to-air or air-to-ground stepped leader.

There are two principal types of lightning discharges: flashes that occur between the thundercloud and the earth (cloud-to-ground) and flashes within the thundercloud (intracloud) discharges. Other types of discharges such as cloud-to-cloud and cloud-to-air occur infrequently. Lightning also occurs in snowstorms, sandstorms, nonthunderstorm rain and ice, in the ejected material above erupting volcanoes, near the firballs created by nuclear explosions, and even out of a clear sky.[44]

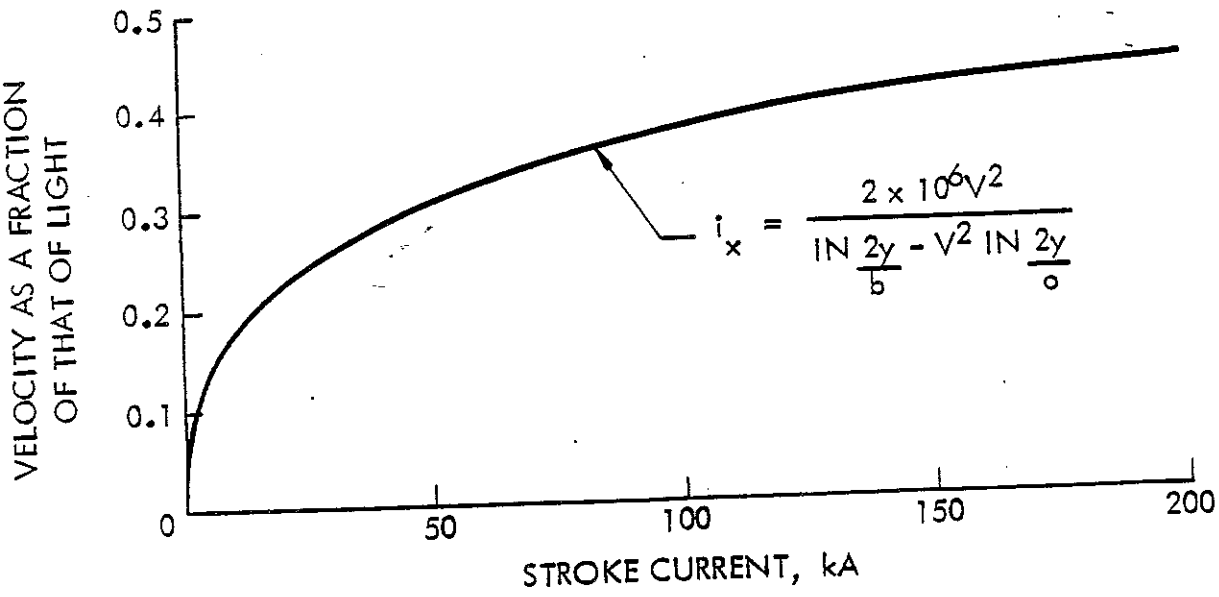

Figure 3-1. Relation Between Stroke Current and Velocity of Return Stroke[45]

To produce lightning, some portion of the atmosphere must charge sufficiently to overcome the resistivity of the air between oppositely charged regions. Static charging occurs to some degree whenever strong wind acts on dust or sand.

Inside a normal thundercloud a turmoil of wind, water, and ice exists in the presence of a temperature decreasing with height. Small particles are carried upward by the wind; large particles move downward under the influence of gravity. The various ascending and descending particles exhibit different velocities depending on their size; the particles collide with one another, causing friction and static charging.

The light, positively charged particles move upward, while the heavier, negatively charged particles move downward. In a typical thundercloud, the upper positively charged region is called the P-region, the negatively charged N-region extends vertically below this, with a smaller positively charged region, known as the p-region located at the bottom of the cloud. This probable distribution is shown in Figure 3-2.

Cloud-to-ground lightning usually occurs between the lower part of the N-region and the ground in a string of discrete strokes. Intracloud discharges are typically composed of a single, slowly moving leader between the N- and P-regions.

The first stroke of a lightning flash contains more current than subsequent strokes. Continuing current occurs in about half of all lightning flashes and is normally referred to as hot lightning. It is this hot lightning that causes severe damage to aircraft and rockets.

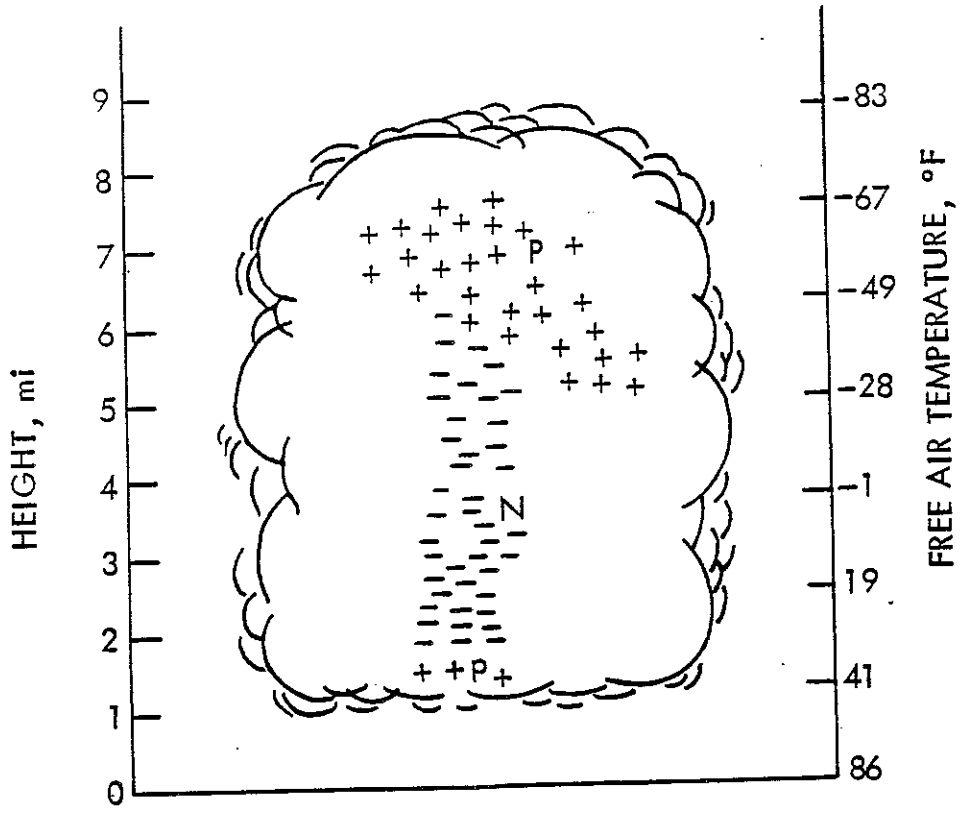

Figure 3-2. Probable Distribution of Thundercloud Charge According to D. J. Malan [46]

Initial Attachments and Swept Stroke Phenomena

Lightning will strike the rocket at one or more attach points, and leave at one or more points. Attachment point testing on a rocket shaped object at McDonnell Aircraft[47] and research performed at Bell-Northern[48] indicate the most probable strike attachment points are on the nose and exhaust port.

During the charge transfer the rocket becomes a part of the stationary lightning discharge channel. Since the plume is conductive it also becomes a part of this channel. As the rocket moves, the length of stroke and continuing currents are long enough that the vehicle may travel a considerable distance while in the channel. Voltage potential differences between the cloud and earth are large enough to insure that there is no possibility that the rocket with its long conductive plume can fly out of a channel during the life of the flash.

As the rocket moves, the channel will appear to sweep across its surface, reattaching at other points for different time periods. This is called swept stroke phenomena. After the rocket has flown a distance equal to its own length, any subsequent attachment will be on its plume, thus causing no damage to the rocket itself, other than field induced currents.

Figure 3-3 shows a rocket in a lightning channel with one reattachment point.

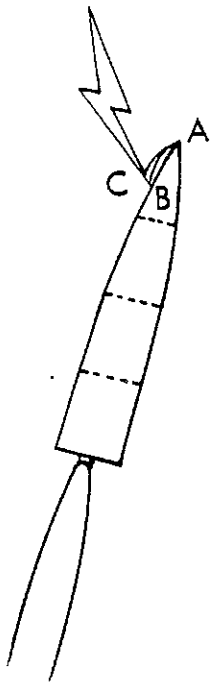

Figure 3-3. Inflight Strike With One Reattachment

A reattachment to the surface at point B is possible if the voltage across the gap BC is sufficient to break down the air gap and any insulating coating on the surface. The dwell time at any one point is therefore a complex function of the local geometry, nature of the surface, the current waveform, and the speed of the rocket. The extent of physical

damage is directly related to dwell time. The attachment point may dwell at various surface locations for differing periods of time, thus resulting in a skipping action across the rocket surface. The other initial attachment point often occurs on a trailing edge, and therefore carries the full current associated with the flash.

Both high peak current restrikes with intermediate current components and continuing currents may be experienced. Restrikes typically produce reattachment of the arc at a new location because the magnitude of the voltage across gap BC is large due to the large inductive voltage developed by the restrike current buildup, and if the flash is discontinuous for a brief period, a new leader will travel along the previous channel since it will still be hot. Consequently, a high electric stress can be produced at the rocket surface. The resulting voltage could be higher than the inductive voltage produced by the changing current, and a puncture of nonmetallic surfaces or dielectric coating is likely to occur.

Significant Parameters

Significant parameters can be delineated that are used to define a lightning waveform applicable to the requirements dictated by any design program.

A summary and analysis of measured lightning parameters was published in 1972 by Cianos and Pierce.[49] Their report presents statistical summaries of all the major return stroke parameters such as peak current, charge transfer, rate of rise, and restrike values.

Table 3-1 from Cianos and Pierce lists the statistical distribution of several lightning parameters.

Cianos and Pierce proposed the severe negative lightning flash current waveform shown in Figure 3-4. Their report summarized published measurements of cloud-to-ground return stroke current pulses that have been assumed to be the principal threat to aerospace system operation. Table 3-2 lists the parameters of the Cianos and Pierce severe current waveform. It should be noted that a significant amount of information has been published since this report in 1972.

Table 3-1. Properties of Statistical Distribution for Lightning Parameters [52]

Parameter*	Percentage of Occurrence				
	2%	10%	50%	90%	98%
Number of return strokes	10 to 11	5 to 6	2 to 3	—	—
Duration of flash (ms)	850	480	180	68	36
Time between strokes (ms)	320	170	60	20	11
Return stroke current** (kA)	140	65	20	6.2	3.1
Charge transfer per flash (C)	200	75	15	2.7	1
Time to peak current (μs)	12	5.8	1.8	0.66	0.25
Rates of current rise (kA/μs)	100	58	22	9.5	5.5
Current half-value time (μs)	170	100	45	17	10.5
Duration of continuing current (ms)	400	260	160	84	58
Continuing current (A)	520	310	140	60	33
Charge in continuing current (C)	110	64	26	12	7

*Note that not all of the parameters are independent. Some judgment must be made in using the values for consistency.

**Values for first strokes.

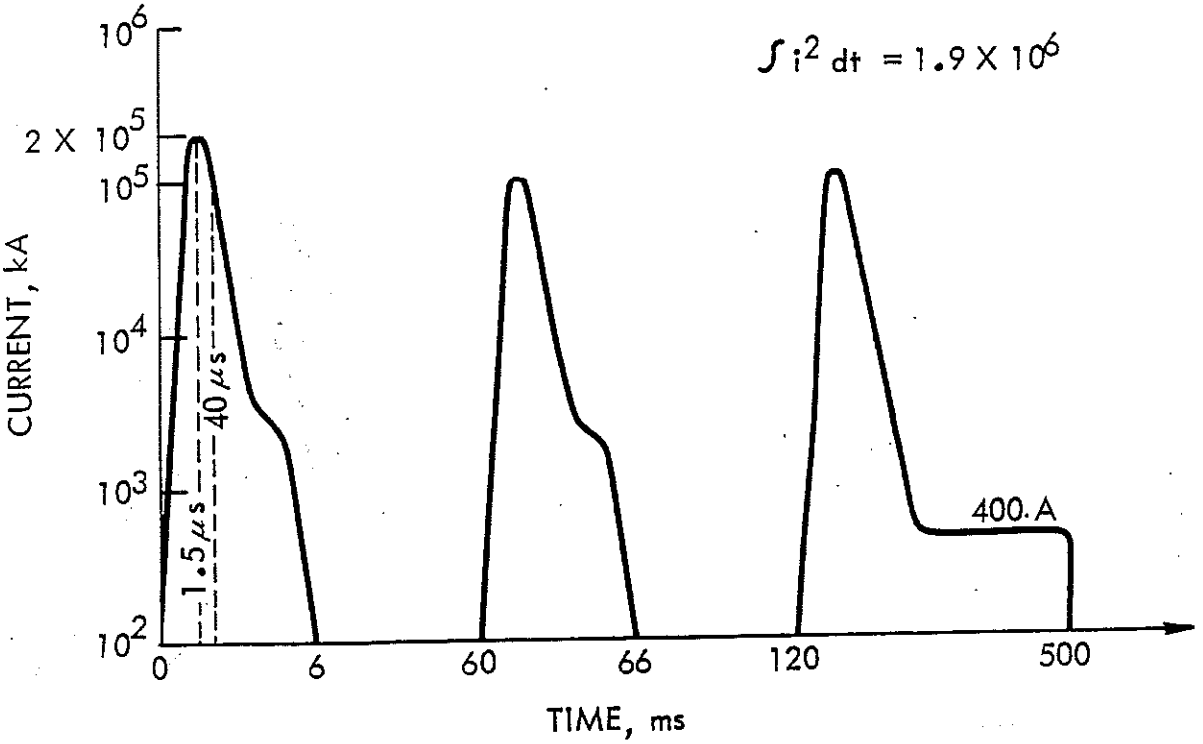

Figure 3-4. Time History of Severe Lightning Model [53]

Table 3-2. Severe Lightning Model Parameters[54]
(Basic Model)

Return Strokes					Intermediate Current Model		Continuing Current
Stroke Order	Peak Current (kA)	Charge (C)	Time Between Strokes (ms)	Model Current, I_o (kA)	I_i (kA)	Charge (C)	
1	140	~8		144	4	4	
2	70	~4	10	72	4	4	
3	30	~2	60	31	0	0	
4	30	~2	60	31	4	4	
5	30	~2	60	31	0	0	
6	30	~2	300	31	0	0	Continuing Current*
7	30	~2	60	31	4	4	
8	30	~2	60	31	4	4	
9	30	~2	60	31	0	0	
10	30	~2	60	31	0	0	Final Stage**

Tests: Charge transferred = 200 C
Duration = 0.9 s
Action integral = 10^6 A^2 s

*Continuing current = 400 A; duration = 300 ms; charge transfer = 120 C
**Final stage continuing current = 200 A; duration = 160 ms; charge transfer = 32 C.

Lightning parameters are also addressed in Uman's book, "Lightning",[50] and Golde's recent work by the same name.[51] Table 3-3 summarizes many of these important parameters and their range of values. Here again it should be noted that the data reflects values at the time of publication.

Nine existing lightning studies were used to determine typical realistic values for each significant lightning parameter evaluated in this example. These parameters are discussed below. However, it is important to note that values for each parameter can be manipulated, depending on the equipment used when the study took place.

Lightning Strike Characteristics

In studying the characteristics of a lightning flash as it affects a rocket in vertical flight, distinct phases can be identified.

Prestrike Phase. As a lightning stepped leader approaches the nose of a rocket, high electrical fields are produced at the surface of the vehicle. These electric fields produce electrical streamers that propagate away from the nose until one of them contacts the approaching lightning stepped leader. Propagation of the stepped leader will continue from other vehicle extremities until one of the branches of the stepped leader reaches the ground or another charge center. The average velocity of propagation of the stepped leader is about 1 m/μsec.

High Peak Current Phase. The high peak current associated with lightning occurs after the stepped leader reaches the ground and forms what is called the return stroke of the lightning flash. This return stroke occurs when the charge in the leader channel is suddenly able

Table 3-3. Data for a Normal Cloud-to-Ground Lightning Discharge Bringing Negative Charge to Earth[55]

	Minimum[1]	Representative	Maximum[1]
Stepped Leader			
Length of Step, m	3	50	200
Time Interval Between Steps, μs	30	50	125
Average Velocity of Propagation of Stepped Leader, m/s[2]	1.0×10^5	1.5×10^5	2.6×10^8
Charge Deposited on Stepped Leader Channel, Coul	3	5	20
Dart Leader			
Velocity of Propagation, m/s[2]	1.0×10^6	2.0×10^6	2.1×10^7
Charge Deposited on Dart-Leader Channel, Coul	0.2	1	6
Return Stroke			
Velocity of Propagation, m/s[2]	2.0×10^7	5.0×10^7	1.4×10^8
Current Rate of Increase, kA/μs[3]	<1	10	>80
Time to Peak Current, μs[3]	<1	2	30
Peak Current, kA[3]		10-20	110
Time to Half of Peak Current, μs	10	40	250
Charge Transferred Excluding Continuing Current, Coul	0.2	2.5	20
Channel Length, km	2	5	14
Lightning Flash			
Number of Strokes per Flash	1	3-4	26
Time Interval Between Strokes in Absence of Continuing Current, ms	3	50	100
Time Duration of Flash, sec	10^{-2}	0.2	2[4]
Charge Transferred Including Continuing Current, Coul	3	25	90

[1]The words maximum and minimum are used in the sense that most measured values fall between these limits.

[2]Velocities of propagation are generally determined from photographic data and thus represent "two-dimentional" velocities. Since many lightning flashes are not vertical, values stated are probably slight underestimates of actual values.

[3]Current measurements are made at the ground.

[4]A lightning flash lasting 15 to 20 sec has been reported by Godlonton (1896).

to flow into the low impedance ground and neutralize the charge attracted into the region prior to the stepped leader reaching ground.

Intermediate and Continuing Current Phases. Most of the energy associated with a lightning flash is transferred in two phases following the first return stroke. The intermediate phase occurs when decay of the initial return stroke starts to level off over some longer time period than the initial return stroke. The continuing current phase occurs when the current flow levels off and before a restrike can hit. Maximum charge is usually transferred during this contining current phase.

Restrike Phase. Restrikes occur when differently charged portions of the atmosphere discharge during the flash. They are usually one-half the amplitude of normal strikes, and occur during the continuing current phase.

A generic lightning waveform originated by NASA for the Space Shuttle program is shown in Figure 3-5. Some parameters of the lightning waveform are interdependent. For example, the rate of current rise in the wavefront is dependent on the rise time (time to peak current) and the peak current amplitude. It is desirable to base the proposed waveform on parameters that will have the most significant effect on the vehicle being designed.

If the lightning strike characteristics are coupled with the information on worst case lightning flash phenomena, five significant parameters can be identified as having the most effect on a rocket.

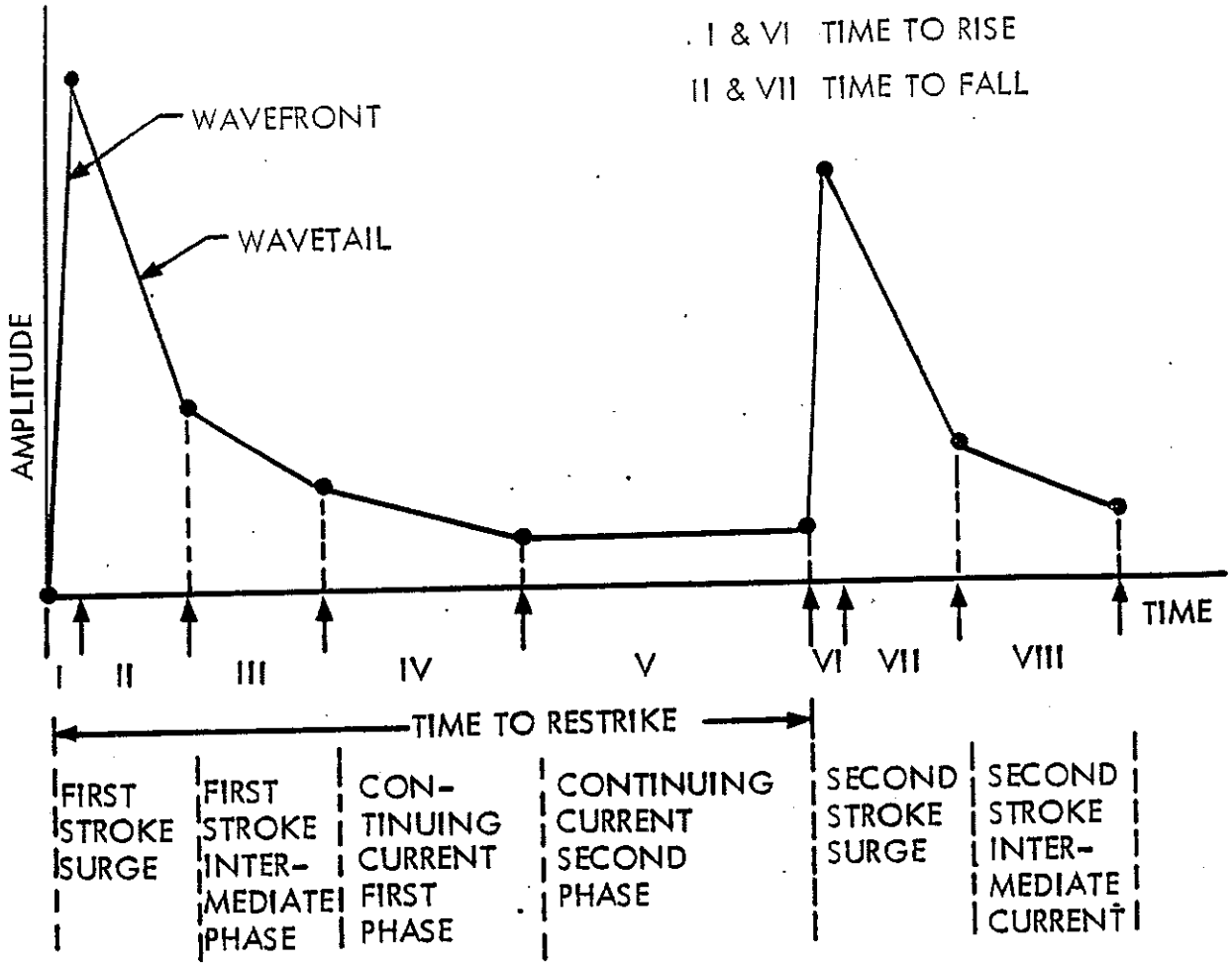

Figure 3-5. Generic Waveform Diagram

Action Integral

The total flash energy transferred by a lightning discharge is the critical parameter for direct strikes. The action integral given below is a measure of this energy transfer.

$$\theta(T) = \int_0^T i^2 \, dt \qquad \text{(Joules)}$$

Using the Bruce and Golde[56] model for the current surge of the return

$$i(t) = I_o\left(e^{-\alpha t} - e^{-\beta t}\right)$$

stroke and integrating the action integral with respect to time, the action integral can be approximated for the for the first strike as:

$$\Theta_R(T) \approx \frac{I_o^2 (1 - e^{-2\alpha T})}{2\alpha} \quad \beta >> \alpha$$

Subsequent strokes can be found by replacing I_o^2 with $I_o^2/4$. Again, according to Cianos and Pierce,[57] the action integral for intermediate current can be approximated as:

$$\Theta_I(T) \approx \begin{cases} I_i^2 (3.7 \times 10^{-4}) \left[1 - 1.4\, e^{-2\gamma T}\right] & \text{for } T > 1 \text{ ms} \\ I_i^2 (3.7 \times 10^{-4}) \left[1 - 1.4\, e^{-2\gamma T} + 0.5\, e^{-11\gamma T} - 0.1\, e^{-20\ T}\right] & \text{for } T \leq 1 \text{ ms} \end{cases}$$

Continuing current is constant, and is given as:

$$\Theta_C(T) = \begin{cases} I_C^2 T & \text{for } T < T_C \\ I_C^2 T_C & \text{for } T \geq T_C \end{cases}$$

Charge transfer is determined by integrating the current model with respect to time, and yields the following results:

$$Q_R \approx \begin{cases} I_o \left(\frac{\beta - \alpha}{\alpha\beta}\right) & \text{First stroke} \\ \frac{I_o}{2} \left(\frac{\beta - \alpha}{\alpha\beta}\right) & \text{Subsequent stroke} \end{cases}$$

$$Q_I \approx I_i \frac{\delta - \gamma}{\delta\gamma} \quad \text{Intermediate current}$$

$$Q_C \approx I_C T_C \quad \text{Continuing current}$$

Continuing Current

The continuing current phase of a lightning flash is important for direct effects because the lightning channel tends to dwell at one point on the vehicle and the energy is thus applied to a single point for a

longer time period. Figures 3-6 and 3-7 show statistical information from several researchers on the duration and amplitude of continuing currents.

Rise Time and Peak Amplitude

Rocket structural resonances due to changes in impedance at each interface occur in the low megahertz frequency range. Also, the cable transfer impedance increases as frequency increases, resulting in more efficient coupling at higher frequencies. The high frequency spectral content of a transient is a function of transient rise time and peak amplitude. Therefore, rise time and peak amplitude are significant waveform parameters that relate to electromagnetic coupling characteristics at high frequencies.

Fisher and Uman observed[60] that there is virtually no difference in the measured rise times for the first and subsequent strokes of the electric field radiated by a nearby flash. Taking this point one step further, Cianos and Pierce[61] defined rise time as the total rise time between the first detectable onset of the current surge and the time of peak current. They translated the relationship between electric field rise times and current rise times, assuming there are no ground propagation losses.

If i_t is the current at any instant t, L_t is the length of the channel being energized by i_t, and d is the distance, then the radiated field E_t at time t is given approximately by:

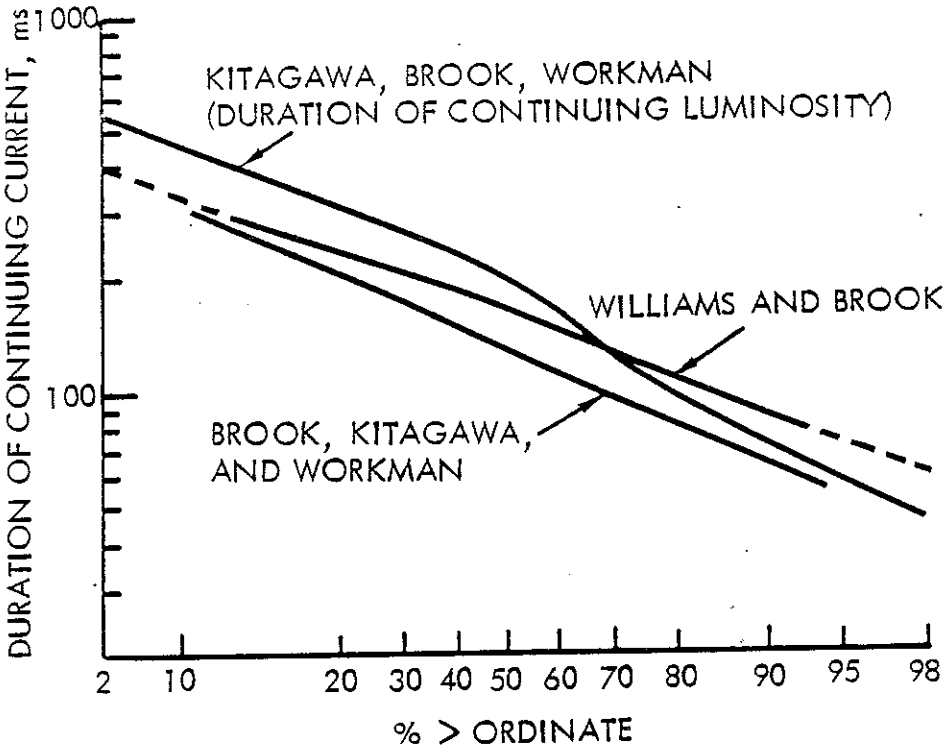

Figure 3-6. Duration of Continuing Currents [58]

$$E_t = \frac{1}{4\pi\epsilon_o}\left\{\int_o^t \frac{M_t dt}{d^3} + \frac{M_t}{cd^2} + \frac{(dM_t/dt)_t}{c^2 d}\right\}$$

where $M_t = 2i_t L_t$, and ϵ_o is the permittivity of free space.

The above equation indicates electric field rise times are slower (longer) than rise times for current (solid conductors have more C and L per unit length). Figure 3-8 shows statistics on the rate of current rise and Figure 3-9 gives statistics on time to peak current. Cianos and Pierce[62] deduced from these figures that peak currents and time of current rise are independent parameters. Table 3-4 lists rise

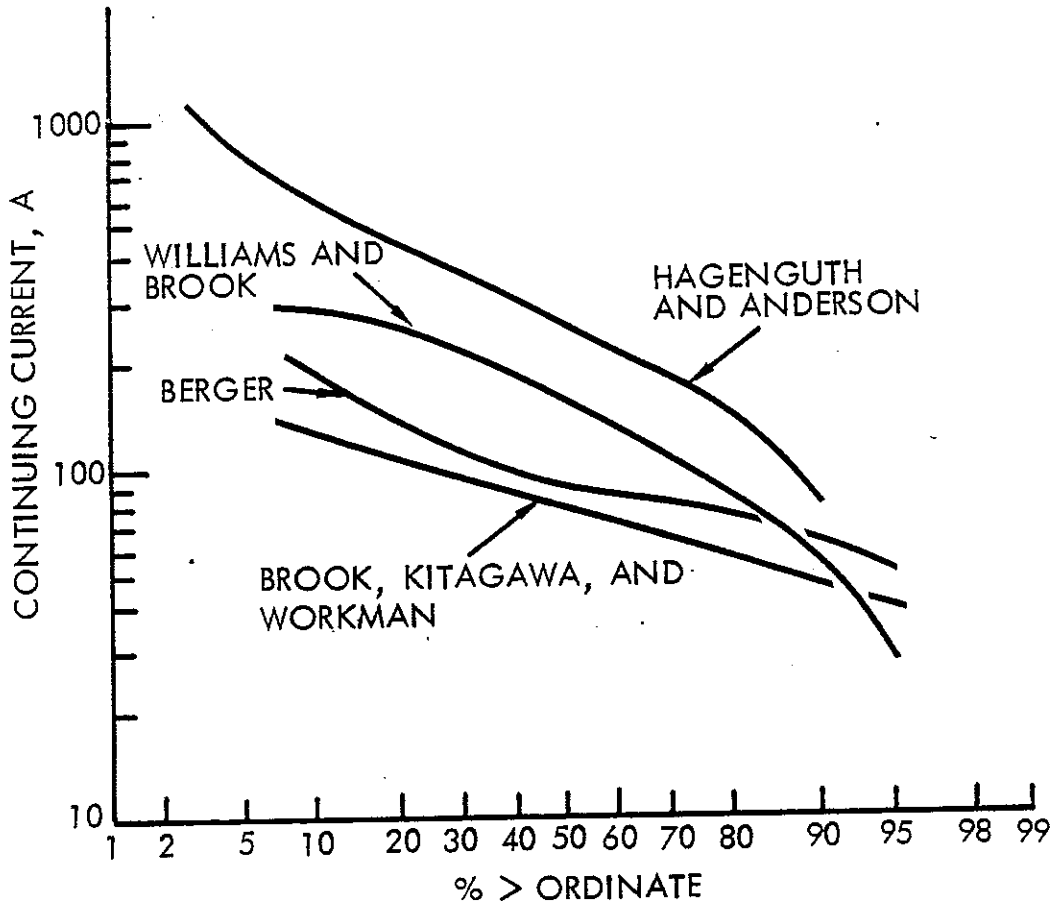

Figure 3-7. Amplitudes for Continuing Currents [59]

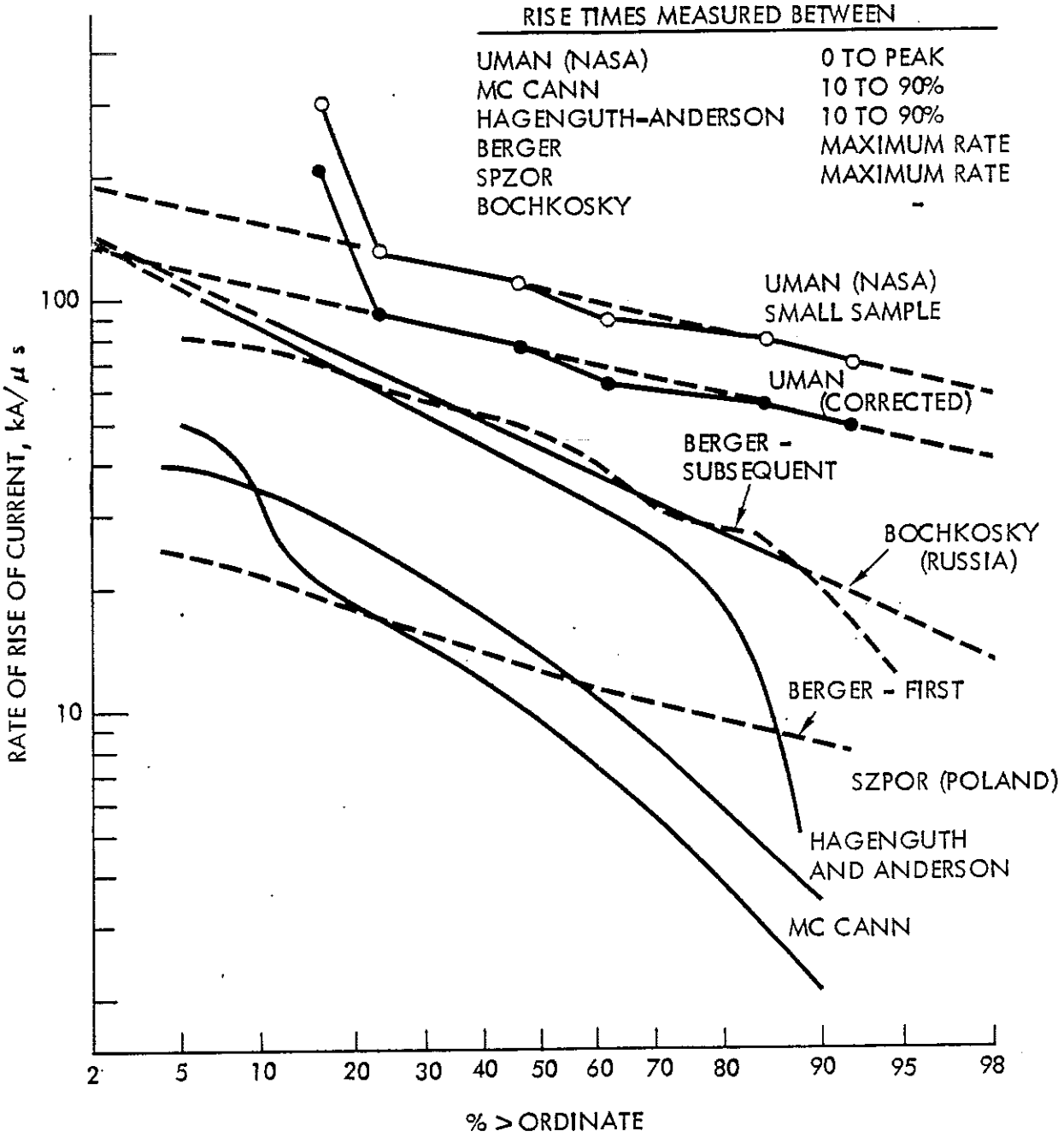

Figure 3-8. Rate of Current Rise [65]

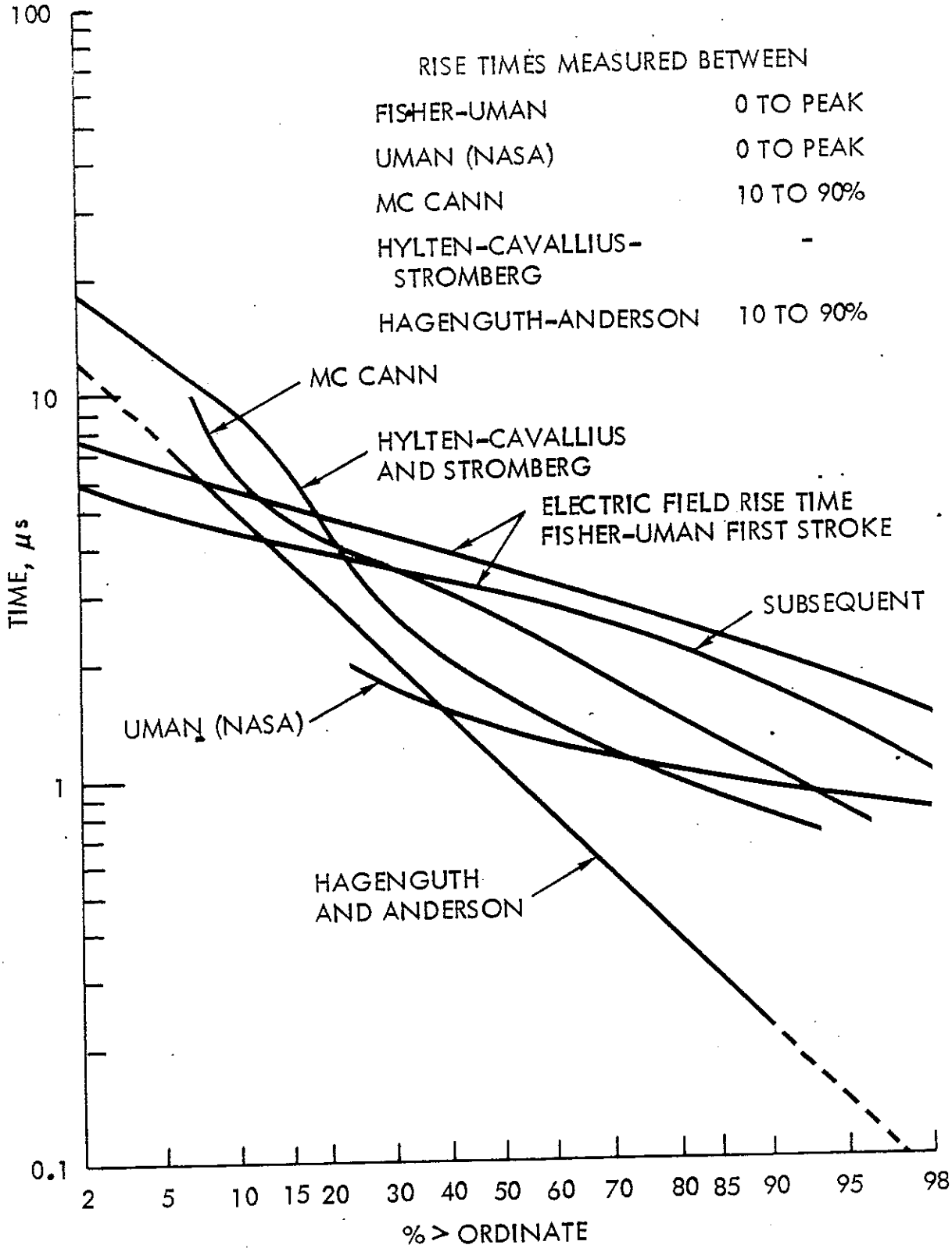

Figure 3-9. Time to Peak Current [66]

Table 3-4. Summary of Rise Time Data

Investigator(s)	Severity*	How Measured	Rise Time
AFSC DH 1-4	95%	Time to peak current, negative following strokes	220 ns
Cianos and Pierce	95%	Time to peak current	390 ns
Moore	Typical	On first return stroke	200-300 ns
Llewellyn	85%	Based on normal distribution with mean = 1.09 μs and standard deviation of 670 ns on over 2000 return strokes	200 ns
Severe Storm Lab (Oklahoma)	75%	Unknown	200 ns (all less than 1 μs)
Krider	Most	10-90% amplitude	200 ns (all less than 400 ns)
Berger	95%	Interval between 2 kA point and first peak	200 ns
Fieux	30%	10-90% amplitude	1 μs
Menko	Most	Time to peak current	2 μs

*Severity is defined here as the percentage of strokes where the rise time is greater than or equal to the value listed in this table.

times from nine different sources; Figure 3-10 presents a summary of peak amplitudes determined by various investigators.

Dr. Krider recently determined[63] that his original 200 ns value was instrumentation limited. He believes the correct value is closer to 90 ns with some as fast as 50 ns. As more sophisticated equipment becomes available, there should be data obtained suggesting much faster rise time.

Restrikes

The lightning flash for a representative model should contain at least one return stroke. According to Uman[64], 60% of all ground flashes

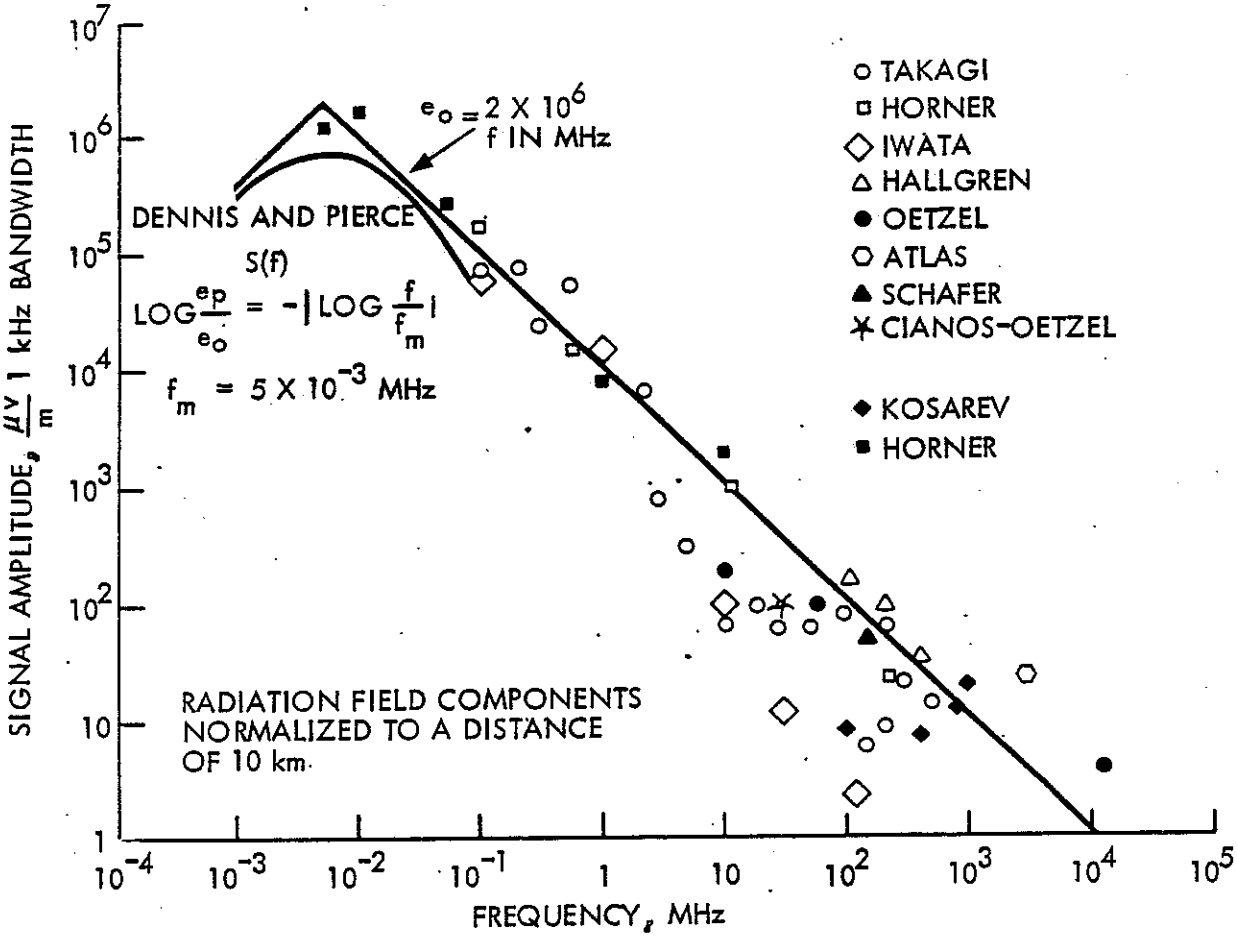

Figure 3-10. Peak Received Amplitude for Signals Radiated by Lightning [67]

contain at least one restrike. If the three previous assumptions are considered, the lightning channel remains stationary as the rocket moves through the channel, the first stroke has attachment points at nose and plume, and after the rocket has flown a distance equal to its length, any subsequent strokes attach only to the conductive plume, it is possible to assess the possiblility of a restrike occuring.

Figure 3-11 shows a nominal large rocket velocity profile for this example. Small rockets are normally much faster. Figure 3-12 shows the distribution of time interval between return strokes in a flash. Figures 3-11 and 3-12 were combined into Figure 3-13, which shows the distribution of flashes where the time interval between return strokes is short enough for a restrike to occur somewhere along the structure for this example. Figure 3-13 indicates that at one second after launch, the restrike component occurs fast enough to restrike this rocket in 99.9% of flashes containing restrikes. This figure also shows that restrikes can occur in times short enough to attach to any stage of a rocket.

Since restrikes occur in most lightning flashes, and since each restrike adds more energy into the flash, the possibility of at least one restrike hitting any size rocket while it is in the lightning channel must be assumed. The generic waveform diagram (Figure 3-5) shows a restrike occurring in a worst case situation, after a period of continuing current. Current data suggests that for positive flashes, restrikes do not occur.

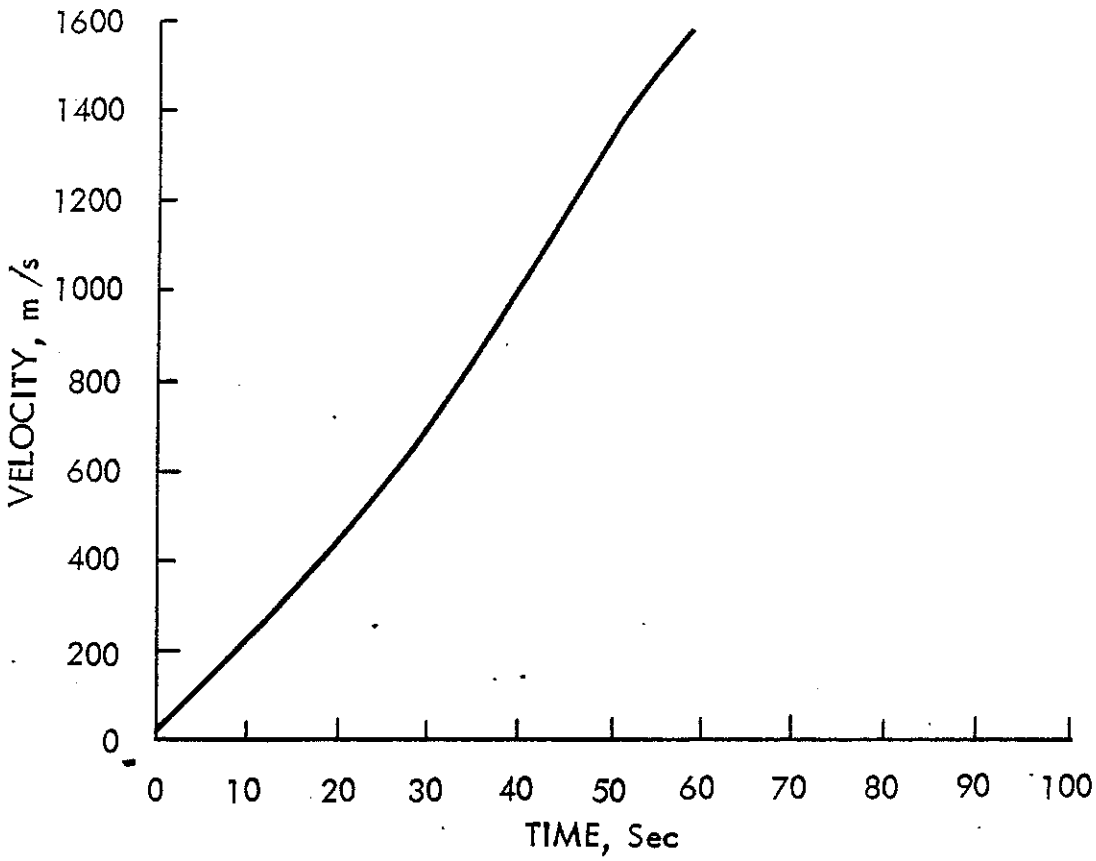

Figure 3-11. Nominal Rocket Velocity

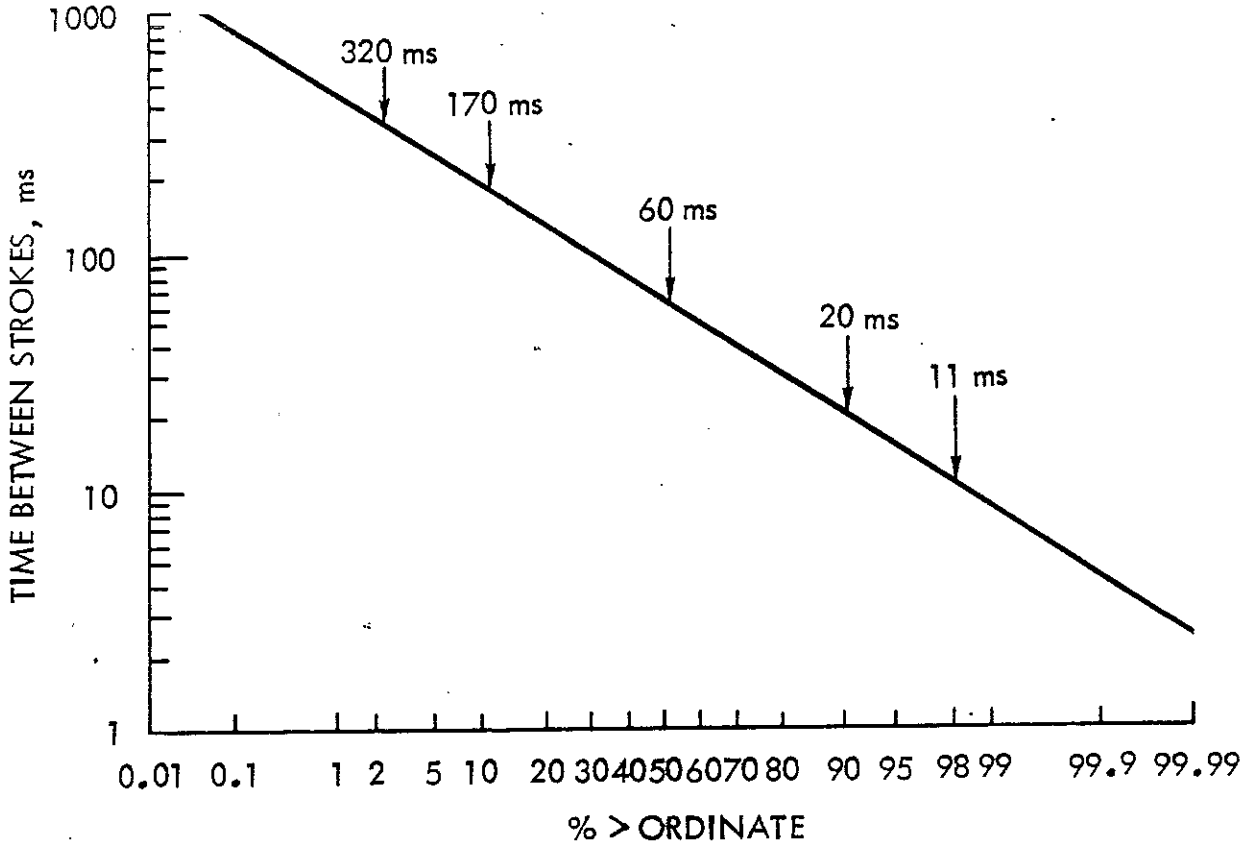

Figure 3-12. Distribution of Time Interval Between Strokes [68]

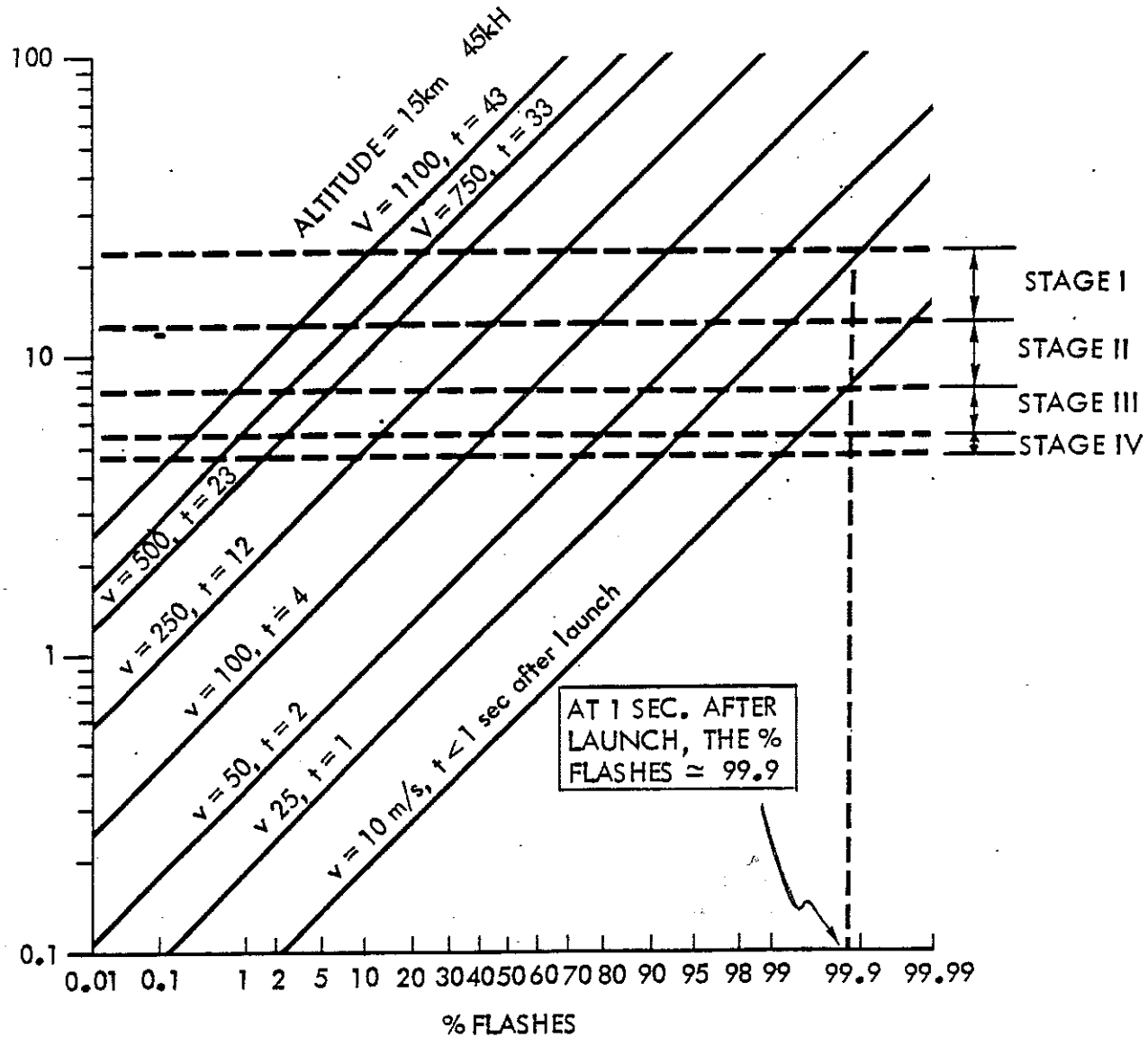

Figure 3-13. Flashes Where the Time Interval Between Strokes is Short Enough for a Restrike to Occur

In summary, the critical waveform parameters are the action integral, continuing current, rise time, peak amplitude, and restrike.

Severity

We wish to establish the requirement to be used in the design. The requirement used will be a compilation of parameters observed from the various studies presented at levels based on severity. Severity is defined as the percentage of strokes having the specified parameters less than or equal (in stress) to the stated levels.

For example, a lightning stroke is said to have a peak current of 95% severity when 95% of observed strokes have peak currents less than or equal to that value. On the other hand, a stroke is said to have a rise time of 95% severity when 95% of the observed strokes have rise times greater than or equal to that rise time. A lightning stroke can be hypothesized which has some number, n, of its critical waveform parameters at the 95% severity level. However, it should be emphasized that the probability of observing such a stroke is more like $(0.05)^n$ than it is like 0.05. If n is 4, taking the four critical waveform parameters (omit restrikes) to be statistically independent, the probability of observing such a waveform is about 10^{-5}.

The 95% level of severity appears to be the proper level to use for most applications. First, this permits the direct use of most of the data from known lightning studies because investigators have used this percentage in reporting results. Second, a rocket designed to these severity levels will have a high probability of success. Third, if an engineer considers the design consequences of using 99% severity levels, the expense would

be prohibitive. Consequently, 95% severity level is generally acceptable for most applications.

Waveform Recommendation

The Air Force Electromagnetic Handbook, AFSC DH 1-4,[69] provides basic lightning design guidelines that include a tabulation of lightning strike information for various severity levels which is shown in Table 3-5. Using the 95% severity level as our baseline, the preceding studies are compared in the significant lightning parameters. The waveform shown in Figure 3-14 represents the average of the 95% severity level for all studies examined.

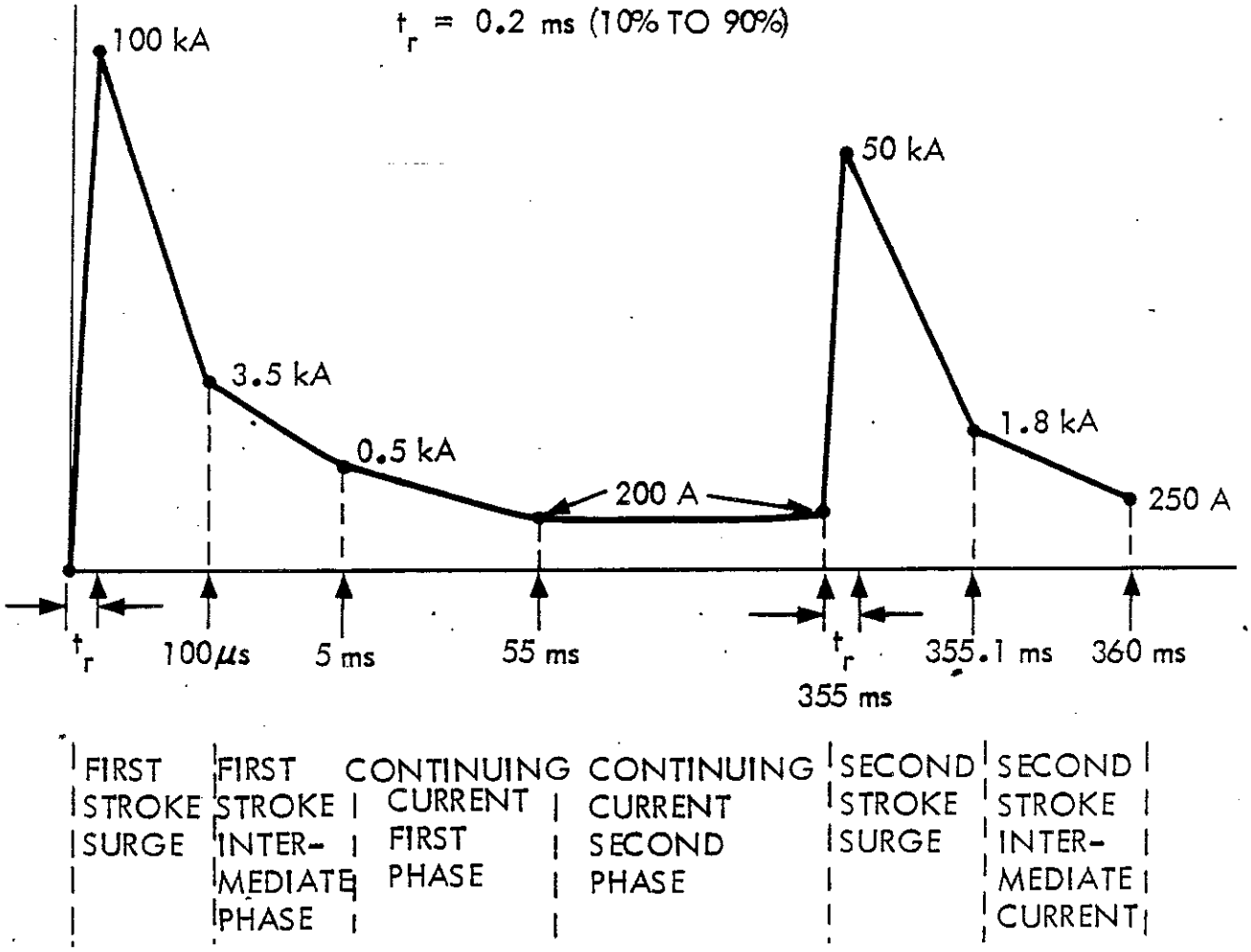

Figure 3-14. Lightning Model for Flight (Not to Scale)

Table 3-5. Review of Cloud-to-Ground Strokes From AFSC DH 1-4

Parameter	Percent of Lightning Strikes Exceeding Listed Value		
	95%	50%	5%
Peak Lightning Current (kA) (minimum 2 kA)			
Negative first strokes and flashes	14	30	150
Negative following strokes	4.6	12	30
Positive flashes (no following strokes)	4.6	35	250
Charge - Coulombs (C)			
Negative first strokes	1.1	5.2	24
Negative following strokes	0.2	1.4	11
Negative flashes	1.3	7.5	40
Positive flashes	20	80	350
Impulse Charge (C)			
Negative first strokes	1.1	4.5	20
Negative following strokes	0.22	0.95	4.0
Positive flashes (only one stroke)	2.0	16	150
Time to Peak Current (μs)			
Negative first strokes	1.8	5.5	18
Negative following strokes	0.22	1.1	4.5
Positive flashes	3.5	22	200
Maximum di/dt (kA/μs)			
Negative first strokes	5.5	12	32
Negative following strokes and flashes	12	40	120
Positive flashes	0.20	2.4	32
Time to Half-Value on Wavetail (μs)			
Negative first strokes	30	75	200
Negative following strokes	6.5	32	140
Positive flashes	25	230	2000
Integral (i^2dt) (ampere^2 second) (A^2s)			
Negative first stroke and flashes	5.0×10^3	5.5×10^4	5.5×10^5
Negative following strokes	5.5×10^2	6.0×10^3	5.2×10^4
Positive flashes	2.5×10^4	6.5×10^5	1.5×10^7
Time Intervals Between Negative Strokes (ms)	7	33	150
Duration of Flashes (ms)			
Negative (including single stroke flashes)	0.15	13	1100
Negative (including single stroke flashes)	31	180	900
Positive flashes	14	85	500

Time Domain to Frequency Domain Transform

Once the time domain current waveform has been established for the particular rocket being designed, the frequency domain characteristics must be determined. This section presents a direct transform anslysis.

Many computer programs are available to perform fast Fourier transforms of regular shaped straight line segments, or entire waveforms. Some programs require extensive hand manipulation in order to transform a waveform of this type to a usable form for rocket analysis.

Linear Equations

The lightning model is first expressed as a series of Ampere-time domain functions. Each function is labeled with an appropriate Roman numeral relating to the portion of the curve it represents. Straight line functions use the standard form Mx+b.

The Fourier transform actually expresses a function f(t) in terms of a continuous sum of exponential functions of the form $e^{j\omega t}$. The derivative of f(t) is, therefore, equal to the continuous sum of the derivatives of each exponential component. Since the derivative of $e^{j\omega t}$ is $j\omega e^{j\omega t}$, each differentiation of f(t) is the same as multiplying each exponential component by $j\omega$. This rationale leads to the time differentiation theorem in transform analysis.

$$\text{If} \quad f(t) \longleftrightarrow F(\omega)$$

$$\text{then} \quad \frac{df}{dt} \longleftrightarrow (j\omega) \cdot F(\omega)$$

$$\int_{-\infty}^{\infty} f(t) \, dt = 0$$

The time differentiation theorem is useful for the lightning waveform, but in itself it is not sufficient. Observing that shifting a function in the time domain has no effect on its frequency domain magnitude components, a shift of time t_o for some component of frequency ω is the same as a phase shift of $-\omega t_o$. In other words, shifting t_o in the time domain is equivalent to multiplying by $e^{-j\omega t_o}$ in the frequency domain. The Time Shift Theorem is shown below.

$$\text{If} \quad f(t) \longleftrightarrow F(\omega)$$

$$\text{then} \quad f(t - t_o) \longleftrightarrow F(\omega) \; e^{-j\omega t_o}$$

With these two theorems, the problem of transforming the lightning waveform can be addressed.

The time domain functions are differentiated twice to obtain a sequence of impulses. The transform of a unit impulse is 1. so using the time differentiation theorem on the series of impulses gives us $(j\omega)^2 \, F(\omega)$.

Applying the time shift theorem, and reorganizing using the identity

$$\pm \, \delta \, (t \pm t_n) = \pm \, e^{\pm \, j\omega t_n}$$

$e^{jx} + e^{-jx} = 2 \cos x$, gives an equation that can be resolved into a computable form.

In reality, the time waveform of the lightning current will smooth out due to diffusion time as it flows through the rocket structure. This approach will give worst case conditions since it assumes no smoothing of the waveform. The nose shroud lightning current penetration analysis performed later gives the equations necessary to modify the frequency content of the discontinuous waveform proposed due to diffusion time.

Energy Content

In order to use the frequency domain transform, and also as a check on the above transformation, the energy contained in the waveform can be calculated in the time and frequency domain. By Parseval's theorem, the energy in the frequency domain relates to the energy in the time domain by the following:

$$1\Omega \int_{-\infty}^{\infty} /f(t)/^2 dt = \frac{1\ \Omega}{2\ \pi} \int_{-\infty}^{\infty} /F(\omega)/^2 d\omega$$

Chapter 4

METHODOLOGY

Electronics Protection

Current flowing in the nose will cause current distribution at various locations on the hardware underneath. The magnitude of these currents needs to be calculated. All metal surfaces cause uniform current flow, creating the easiest problem for the engineer. Nonuniform current distribution on rockets containing composite material will cause the current to pinch at raceway or other structure attachment points, requiring unique magnetic field calculations. Once the waveform and amplitude of the coupled pulse at the pin level have been determined using transfer impedance techniques, interface protection circuitry can be applied. Shielding effectiveness evaluation for boxes is assessed so a determination can be made of the susceptibility of interior electronics to radiated fields.

Mechanical Protection and Shielding

Generally, there are two areas of concern relating to lightning in all rocket designs: the prevention of physical damage that could result in aerodynamic instability, structural failure, or excessive drag, and the protection of internal electronics from the effects of harmful lightning generated fields.

Depending on the rocket type, protection required, and threat involved, several techniques are available.

Shielding Insulators

The invention of lightweight, high-strength, and inexpensive thermoplastics and nonconductive composites provides a number of design options in addition to all metal construction. There are a number of alternatives available that can produce a continuous conductive surface on nonconductive parts:

- Silver reduction - a wet, multiple-step, silver-plating process in which a silver nitrate solution is sprayed onto the plastic substrate. The silver is reduced to pure elemental silver, which precipitates onto the part, while the nitrate is formed into a salt. The silver that does not make contact with the part can be reused.

- Conductive paints - including silver, copper, nickel, graphite, and copper graphite. Conventional spray equipment or paddle guns apply the paints to the molded parts.

- Vacuum metallizing - pure metal, usually aluminum, coats the plastic part, which generally has been primed with a base coat. The metal is boiled in a vacuum chamber and the condensing metal is deposited onto the surface of the parts in the chamber.

- Cathode sputtering - gas plasma discharge set up between a cathode, made of the material to be sputtered, and an anode, which serves as both an electrode and the support for the plastic substrates. Positively charged gas ions accelerate into the cathode, dislodging metal atoms that condense on the substrates forming a metal film.

- Flame and/or arc spray - molten metal, usually zinc, is deposited onto the substrate. With the arc spray pistol, two metal wires are melted in an electric arc and sprayed onto the part through a hand-held pistol. The flame spray gun atomizes a metal onto the part after the metal has been melted by contact with super-heated inert gas.

- Pressure-sensitive foils - applied with adhesive backing to the interior of an injection-molded part.

- Electroplating - numerous etching steps, including the application of a conductive surface before the actual plating process begins.

Shielding Material Selection

Choosing the correct shielding material requires a precise analysis of the problem. Once the degree of required shielding has been determined

alternatives can be considered in terms of cost, weight reliability, and conductivity. Only coatings used for shielding or increased ability to conduct current are addressed.

Unless a large number of parts, or the entire vehicle is to be coated, weight differences between various coatings are insignificant. If the outside surface, as is usually the case for lightning protection, of the rocket is to be coated, environmental effects for each material are a factor. Since significant vibration is encountered during launch, only materials that give a very good adhesive bond should be considered. Further, since the rocket encounters severe aerodynamic heating of the outside shell, and is effected by erosion due to atmospheric dust particles, only materials with high melting temperatures should be considered for this application. Less severe temperature and environmental problems are encountered on interior coatings, but in addition to the exterior damage caused by a strike attachment, vibration is still a major problem. Generally, coating costs are calculated on a per-square-foot basis. Many coatings are deposited with conventional spray equipment, thus overspray and the cost of masking materials may affect the cost of the coating.

Vacuum metallizing, electroplating, and cathode sputtering methods of shielding require large capital investments for equipment and highly trained employees. Spread over a relatively small number of units, these costs become a concern.

Compatibility of the coating with the substrate is very important.

Adhesion, abrasion resistance, impact properties, flexibility, environment and chemical resistance, and thermal coefficient of expansion must all be considered as they relate to the material being coated.

The part shape or contour and size effects the choice of a coating. For example, metallic foils are difficult to apply to contoured surfaces and large parts may be too bulky for vacuum metallizing.

The choice of a coating to provide effective radio frequency interference shielding and conductivity should be one that is relatively inexpensive, easy to apply, capable of an acceptable level of attenuation or conduction, compatible with the substrate material, and meet all applicable requirements. Table 4-1 is a comparison of the various coating type materials available.

Magnetic Shielding

Magnetic shielding reduces fields within a region by flux diversion. A low reluctance path is provided to divert the flux around the region requiring the reduced field strength. The amount of flux flowing into the shield is proportional to the intensity of the magnetic field, the cross section available to conduct the flux, and the flux capturing area. In the case of a rectangular box, the largest flux capturing area is the broadside of the enclosure. Where possible, arranging to have this side perpendicular to the H field will cause maximum flux to be intercepted by the largest area, and thus will minimize the induced field. Flux density in the shield material is dependent on the available paths and the total cross sectional area of the flux paths. For example, consider

Table 4–1. Comparisons of Shielding Materials

Comparisons of shielding materials

	Advantages	Disadvantages
1. Silver reduction		
	• Good conductivity • Low capital investment	• Tendency to oxidize • Masking difficult • Multiple-step process
2. Conductive paints		
Silver	• Good conductivity • Conventional equipment • Resistant to flaking • Conductive oxide • Ease of application	• Expensive
Nickel	• Conventional equipment • Good conductivity • Good resistance to oxidation	
Graphite	• Conventional equipment • Ease of application	• Not very effective — electrostatic discharge only • Pits with exposure
Copper/graphite	• Conventional equipment	• Two-step application
Copper	• Ease of application	• Copper oxidation reduces conductivity
3. Vacuum metallizing		
	• Can be put on any plastic • Good conductivity • Not limited to simple designs • Familiar technology	• Vacuum chamber limiting factor • Base coat needed • Expensive special equipment needed
4. Cathode sputtering		
	• Good conductivity • Good adhesion	• Expensive equipment • Microscopic cracking • Heat of application could cause distortion • New technology • High power requirements
5. Flame and/or arc spray		
	• Good conductivity • Hard, dense coating • Effective over wide frequency range	• Special equipment • Separation from substrate due to difference in thermal expansion coefficient • Improper use — flame spray may distort or warp thermoplastic housing
6. Pressure-sensitive foils		
	• Die-cut to part shape • Good for experimental work • Good conductivity	• Complex parts difficult to coat • Labor intensive
7. Electroplating		
	• Decorative • Excellent electrical parameters • Good conductivity • Resistant to chipping	• Limited to certain thermoplastics • Expert knowledge of plating • High equipment costs • Needs scratch-resistant coating to protect surfaces • Low current density • Deep side walls difficult to plate

a box oriented perpendicular to the flux lines. The flux paths available to the entering flux are the four side panels as shown in Figure 4-1. If the shape of the enclosure is fixed, the flux density of the material is primarily controlled by material thickness and orientation. An appropriate material thickness and shield material must be selected to prevent material saturation and provide the shielding attenuation required at the lowest significant field frequency.

The residual field in the interior of the shield enclosure will be at a level that is required to satisfy the boundary conditions for a given flux density in the shield (Magnetic Ohm's Law). This level of field residual is primarily dependent on the magnetization characteristics of the material at the operating flux density. To achieve low residual field (high attenuation), the material must have high permeability.

Since magnetic flux lines are continuous, and the total flux intercepted by the shielded box must equal the flux through the four side panels of the enclosure, in the worst case orientation the flux density "B" in the material is given by the equation of Figure 4-1. The factor of 2 in the effective flux capture area is introduced to approximate the probable field distortion due to the presence of other physical bodies near and within the enclosure. It is assumed the distorted field will increase the flux concentration, but the actual distortion is nearly impossible to predict. The 2 factor makes the equation nearly exact for this application.

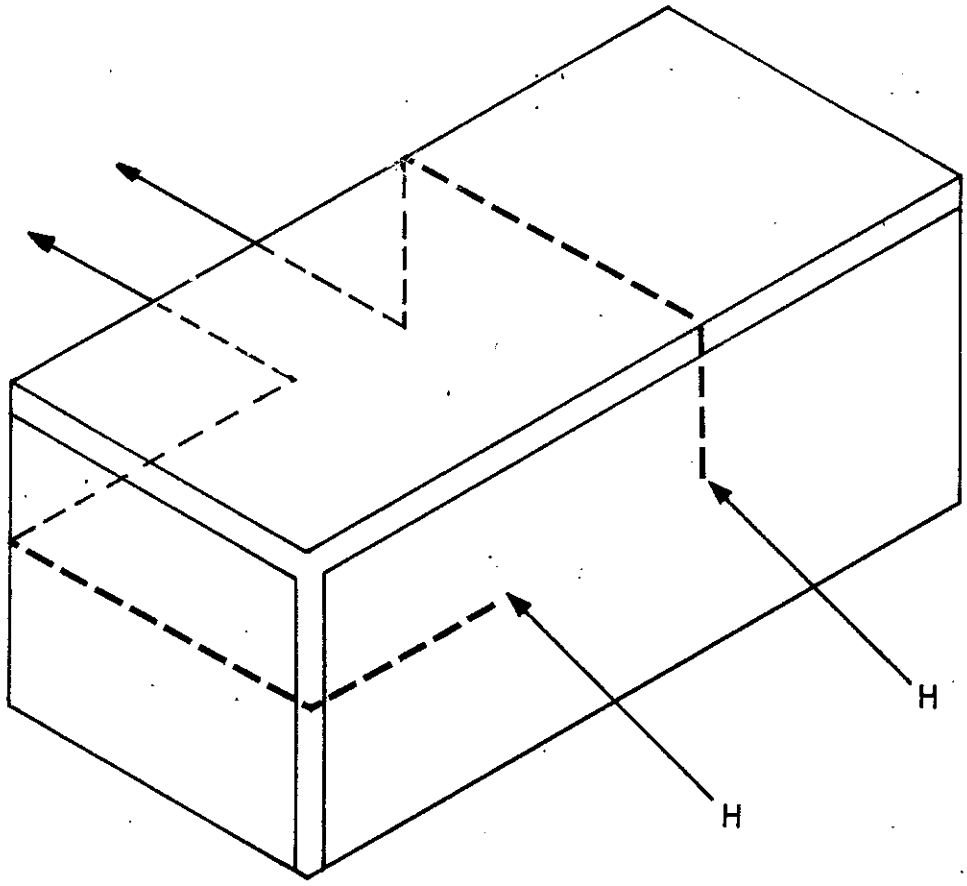

Figure 4-1. Flux Paths Available

$$B = \frac{\mu_o H_o A_e}{a_T} = \frac{\mu_o H_o A_e}{4\Delta(h+\ell)}$$

where

μ_o = permeability of air ($4\pi 10^{-7}$)

H_o = H field exterior of enclosure (oersted)

A_e = effective flux capture area ($A_e = 2A$)

a_T = total cross-sectional area of four panels

Δ = material thickness

h = enclosure height

ℓ = enclosure length

B = flux density (gauss)

A = physical flux intercept cross-section area of enclosure perpendicular to magnetic flux lines (four side panels)

External Shielding

Since lightning will strike the nose first, where the primary control equipment is normally located, this portion must be shielded. Further, to insure that internal cabling and wires do not become the primary conductive path for lightning current, some large conductive surface must extend the entire rocket length. Since all metal surface construction is simple to protect, the case of modern lightweight nonconductive surface designs will be addressed. When using mostly graphite construction, a raceway, or conductive cylinder protecting all downstage cables must be designed with interface provisions to insure separation as each stage disconnects.

A standard design allows a discharge path for lightning and provides flexibility to severe weight limitations. Since the nose is the primary attachment point, the nose itself must be of sufficient strength to withstand the entire lightning strike. Should a reattachment occur, it will be of lesser amplitude (½ amplitude for a restrike), and will attach at some lower position. A strike scenario would be current attachment to the nose, nonuniform conduction to the raceway, uniform conduction down the raceway, and finally reattachment to the conductive plume at the exhaust port.

As an option, should a more uniform current distribution be required to reduce the value of the diffusing magnetic field everywhere in the upper stage, conductive strips can be placed along the rocket skin at intervals between the upper and lower stages. Since magnetic field

strength falls off reciprocally with distance, another option is to locate memories or other sensitive devices as far horizontally from the raceway as possible.

Memory Shielding

The major area of concern at the box level from magnetic fields is the threat to susceptible computer memories. A plated wire memory for example, will be altered or erased after exposure to a transient magnetic field of just over 3 oersteds. If this level is exceeded during a strike, electronics would continue to function normally, but preprogrammed information would be altered drastically. High frequency lightning energy usually will not hamper memories located inside a completely sealed conductor, but diffusion penetration of low frequency components poses a threat. Searing[71] has concluded the low frequency range of concern for plated wire memories is between 3,000 Hz and direct current from a 100 kA strike. General Electric[72] has determined that core memories can withstand a transient magnetic field pulse of up to 23 oersteds without significant degredation. To protect memories, the level of field strength capable of being tolerated by the memory must be determined and shielding must be provided by the proposed design. Since shield attenuation is difficult to predict at corners and since the stray magnetic fields inside a shield near edges could greatly exceed memory limits, it is recommended as a safety factor that the maximum tolerable interior field used for calculations contain at least 1 gauss safety margin.

Rough Estimates Of Flux Density Due To Current Flow

The field strength at any location on a particular design depends on the rockets structural design and the orientation of the susceptible circuits.

If current is constrained to a relatively small area, or if an estimate of the current can be predicted, Ampere's circuital law can be used as a rough estimate to find the magnetic induction at a distance r from an assumed infinitely long current wire (Biot-Savart Formula).

$$\oint B \cdot d\bar{\ell} = \mu_o I \qquad B(2\pi r) = \mu_o I \qquad B = \frac{\mu_o}{2\pi} \sum I/r$$

closed loop

vector sum

For current flowing over a larger area, and for fields within the shroud itself, an estimate can be made either by using the results of Goulette and Felske[73], or by using the techniques presented in the following sections of this document.

Shielding Configuration

---Determining the shield configuration is important in memory design. The edges and corners of a square box create fringing effects due to non-uniform current flow on the surface of the box. The preferred shape, space permitting, is a hollow sphere. If this is impractical the next best shield is a smooth, gently curving, hollow spheriod. A few mils of gold leaf could be wrapped around a permeable spheroid producing a double layer shield that further guarantees high frequency protection.

Interior Memory H-Field Determination

To evaluate the actual field environment that impinges on a memory, two analysis techniques are necessary. First, the convolution method is used to predict the maximum field level (H) and the field buildup rate

within the enclosure. The method is a time domain input/output response analysis. Second, a frequency domain response analysis, based on a transfer function is used to predict the frequency content of the field within the enclosure.

H-field interior to the memory enclosure results from two components, the diffused field due to the current flow on the outside of the enclosure and the diffused field due to current flow on the exterior of the vehicle skin.

The diffusion process of the exterior magnetic field through cavity walls into an enclosure, and the filtering effects of the enclosure cavity on the exterior field is discussed extensively in other sources.[74,75] The impulse and frequency response of enclosures are derived by these same sources. They are functions of the enclosure geometry $\xi = \sqrt{g}\, K$, and the conductivity (σ) of the enclosure material. The parameter $K = (\mu o/\mu)\,(a/\Delta)$ in terms of ξ , is given by $\xi = (\mu o/\mu)\,(V/S)\,(1/\Delta)$. Where μ = permeability of the material, μo = permeability of free space, Δ = material thickness, a = half width or radius of enclosure, g = shape factor, V = enclosure volume, and S = enclosure surface area. From antenna theory, the effective radius of any object is the square root of the quantity found by dividing the surface area by π .

Since there is a fast decay of the higher order terms in this application, the approximate impulse response is given below. High frequency components associated with the fast rise time are filtered by the outer rocket skin.

$$\frac{H_i}{H_o} = \left(\frac{1}{\xi t_d}\right) \quad e^{-\left(\frac{t}{\xi t_d}\right)}$$

where

H_i = interior H field of enclosure

H_o = exterior H field impinged on enclosure

$t_d = \mu\sigma\Delta^2$ (diffusion time of enclosure wall)

The enclosure holding the memory has a geometry factor of 12 based on a parallel plate cavity model at $\mu/\mu_o = 1$, ($K = a/\Delta$). This ξ factor is for an H field environment where the magnetic flux lines flow in the direction perpendicular to, and through the broadside dimension of the enclosure. Thus it is a worst case for maximum coupling. The enclosure time constraint is ξt_d, and the first corner frequency of the enclosure filtering bandwidth response can be found by setting $\omega\xi t_d=1$.

If the current split between the outer stage shell and the inner enclosure wall can be determined, the following convolution calculation will yield the interior enclosure H-field.

$$H_i(t) = F_1 * F_2 = \int_o^t F_1(\tau) \cdot F_2(t-\tau)\, d\tau$$

$F_1 = H_{ext}(t)$, exterior H field

$$F_2 = \left(\frac{1}{\xi t_d}\right) \quad e^{-t/\xi t_d}$$

$H_i^S = F_1^S * F_2^S$ S = outer shell

$H_i^{S/M} = (F_1 * F_2)^S * F_2^M$ M = Memory Enclosure

$H_i^M = F_1^M * F_2^M$

where

$H_i(t)$ = interior H field of enclosure

F_1 = $H_{ext}(t)$, exterior H field

F_2 = impulse response of enclosure

Superscript = enclosure involved or origin of H_{ext}

Once the interior field strength has been calculated, the amount of shielding necessary to protect the memory can be determined.

Shielding Effectiveness

Shielding is measured in terms of an attenuation level known as shielding effectiveness. When an electromagnetic wave impinges on a shield (see Figure 4-2) some of its energy is reflected at the first surface of the shield, some is absorbed by the shield, and some is transmitted through the shield. Energy may also be reflected at the second surface of the shield.

Denoting the incident intensities and power by E_1, H_1, and P_1, and the transmitted intensities and power by E_2, H_2, and P_2, the attenuation or shielding effectiveness, S, may be expressed (in dB) as any one of the following three ratios:

a) Electric field shielding effectiveness, $S_E = 20 \log E_1/E_2$ dB, where E_1 and E_2 are measured in the same units of electric field strength, such as volts/meter.

b) Magnetic field shielding effectiveness, $S_H = 20 \log H_1/H_2$ dB, where H_1 and H_2 are measured in the same units of magnetic field strength, such as amperes/meter.

c) Total electromagnetic shielding effectiveness, $S = 10 \log P_1/P_2$ dB, where P_1 and P_2 are measured in the same units of power, such as watts/meter^2.

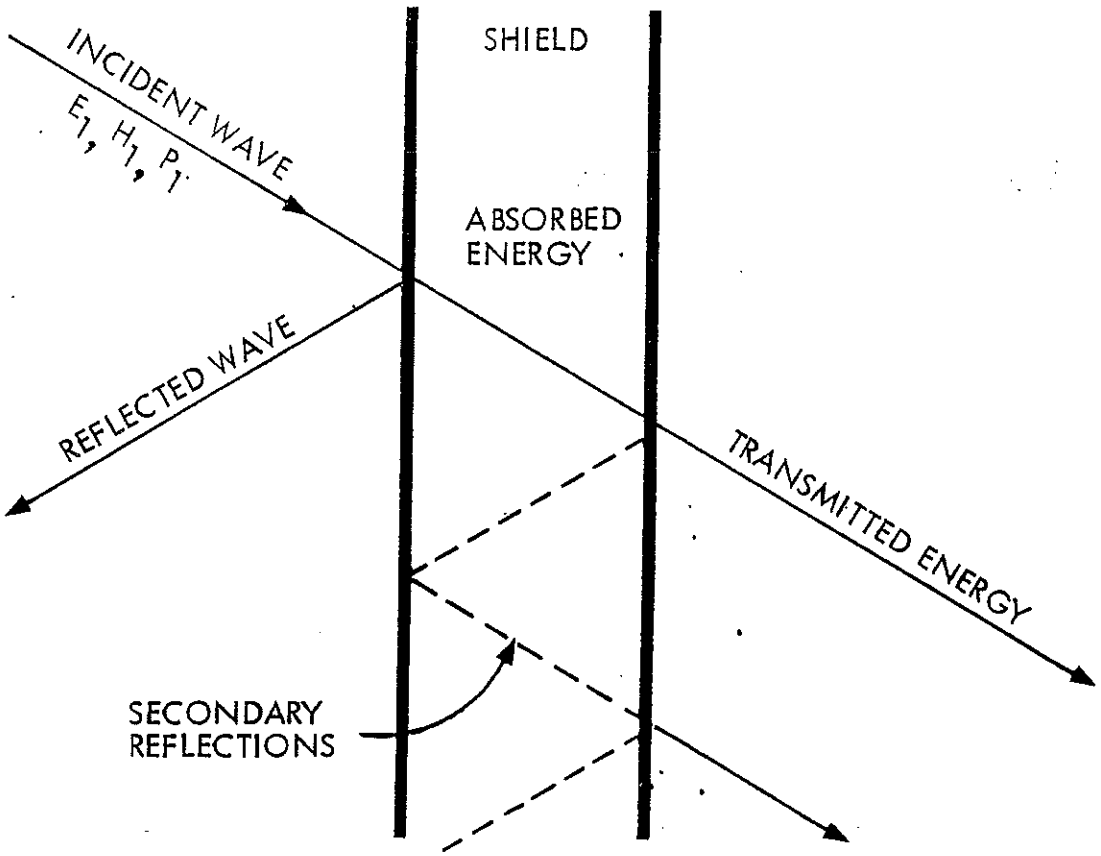

Figure 4-2. Attenuation of EMI By a Shield

If the electromagnetic wave is planar and impinges at right angles to the surface of a single-layer shield, and if the area of the shield is infinite, the total single-layer shielding effectiveness, S, may be expressed as the sum:

$$S = (A + R + B), \text{ dB}$$

Where A is the absorption (or penetration) attenuation (or loss) in dB, R is the reflection attenuation in dB, and B represents additional attenuation caused by successive internal reflections. B is only considered when the absorption is low enough that the losses due to such internal reflections are significant.

The term B, common to all fields, is given by:

$$B = 20 \log_{10} \left[1 - \left\{ \frac{Z_s - Z_w}{Z_s + Z_w} \right\}^2 \times \frac{1}{10^{A/10}} \left\{ \cos 7.68 \times 10^{-4} \, t \sqrt{f\mu G} - j \sin 7.68 \times 10^{-4} \, t \sqrt{f\mu G} \right\} \right]$$

where: Z_s is the intrinsic impedance of the shield in vector form, and

Z_w is the incident wave impedance in vector form.

B can be neglected when $A > 10$. If not, then B must be computed. The terms in the previous equation can be defined by the equations,

$$Z_s = (1+j) \sqrt{\frac{\mu f}{2G}} \times 3.69 \times 10^{-7} \text{ ohms (vector form)}$$

and Z_w for each of the three wave types is

$$Z_{we} = -j \frac{0.71 \times 10^{12}}{f r_1} \text{ ohms (electric)}$$

$$Z_{wm} = j \, 0.2 \times 10^{-6} \, f r_1 \text{ ohms (magnetic)}$$

and

$$Z_{wp} = 377 \text{ ohms}$$

Therefore, depending on the magnetic absorption characteristics of the shielding material, the value of B may or may not be necessary to determine shielding effectiveness.

The absorption attenuation, A, is defined as:

$$A = 3.3t \sqrt{\mu f G} \text{ dB}$$

where

t = shield thickness in mils (thousandths of an inch)

μ = shield relative permeability

f = frequency in MHz

G = shield conductivity in mhos/meter

It can been seen by the above equation that doubling the shield thickness will double the absorption to 6dB, but doubling either the shield permeability or conductivity will increase dB absorption by only 3 dB.

The reflection attenuation, R, is:

$$R = 20 \log \frac{(k + 1)^2}{4k}$$

where k is the ratio Z_w/Z_s of the wave impedance (Z_w) at the first surface of the shield, to the intrinsic impedance (Z_s) of the shield. As is normally the case, the above equation can be simplified if $Z_w/Z_s >> 1$, then $k + 1 \simeq k$ and the equation becomes:

$$R = 20 \log \left(\frac{Z_w}{4Z_s} \right), \text{ dB}$$

where

Z_w = wave impedance at the shield in ohms

Z_s = intrinsic impedance of the shield in ohms

The shield intrinsic impedance is given by:

$$Z_S = \sqrt{2\pi\mu f/G} \text{ ohms}$$

where

μ = relative permeability of shield

f = frequency in Hz

G = conductivity of shield in mhos/meter

Substituting back into the reflection attenuation gives:

$$R = 20 \log \left[\frac{Z_w}{4} \sqrt{\frac{G}{2\pi\mu f}} \right] , dB$$

These equations show that the reflection loss R is dependent on the wave impedance of the incident wave as well as on the properties of the shield. This fact is useful in determining near fields, where Z_w varies rapidly with distance from the source; high impedance fields ($E/H > 377$) decreasing to 377, and low impedance fields ($E/H < 377$) increasing to 377. In general, the intrinsic shield impedance is $Z_s << Z_w$, so that shields used in high impedance fields should be placed as close as possible to the source, for greatest mismatch (Z_w/Z_s); while shields used in low impedance fields should be placed as far as possible from the source, for greatest mismatch.

Plots of reflection and absorption losses for iron and copper are shown in Figure 4-3. This illustration gives a physical representation of the behavior of the component parts of an electromagnetic wave, and illustrates the difference between magnetic field and electric field shielding, and why it is more difficult to shield magnetic fields.

Magnetic Coupling

A usual problem generated by allowing currents to flow in a grounding device or ground plane is the undesirable effect this current may have on conductors running adjacent to it. Inductive coupling can introduce a voltage in the adjacent conductors, weather inside a cable or on a circuit card inside a box. This voltage can be very difficult to remove,

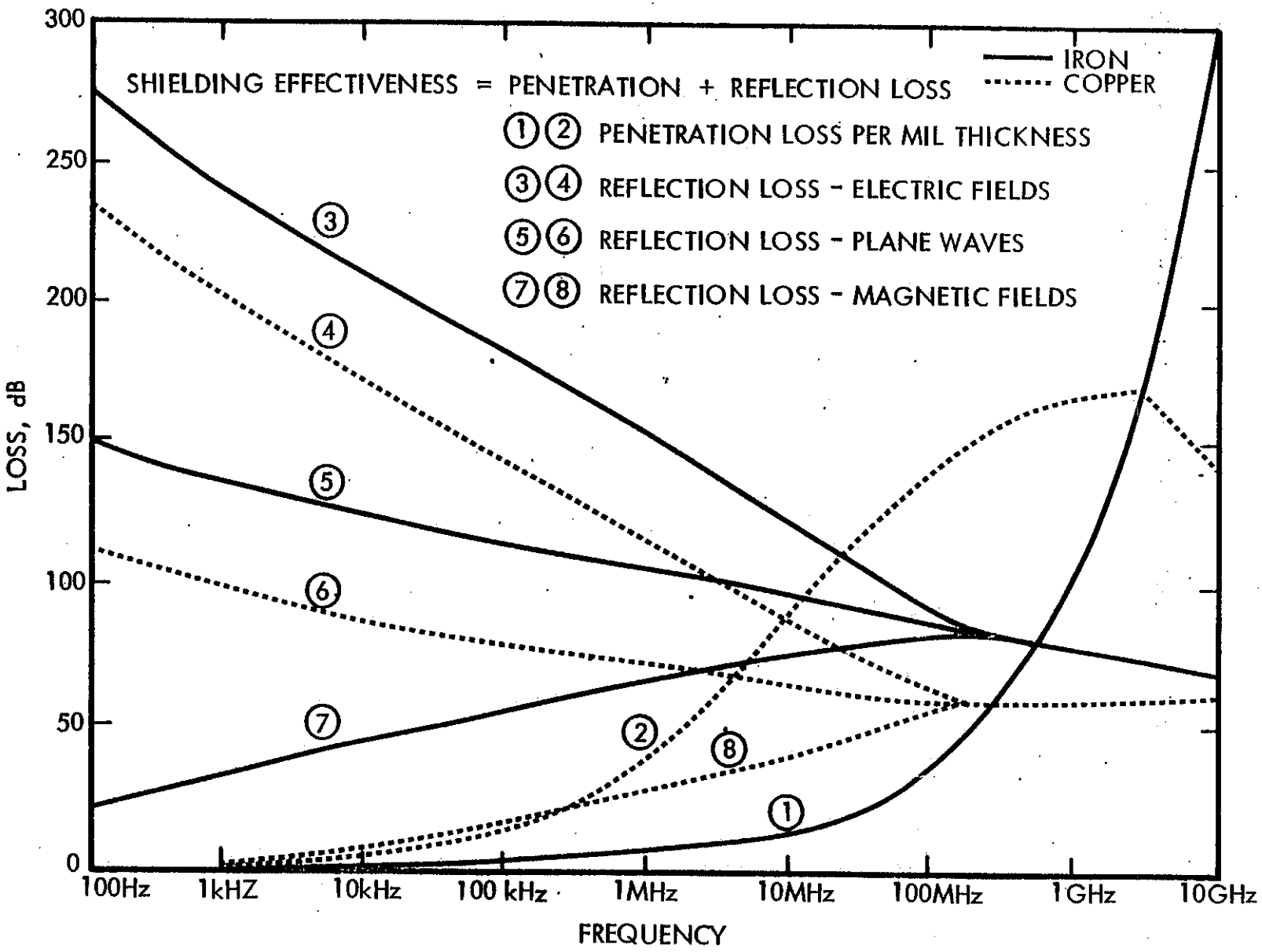

Figure 4-3. Shielding Effectiveness of Metal Barriers[76]

particularly when induced in low impedance circuits.

The electromagnetically coupled voltage between two parallel lines under closed circuit conditions will increase linearly with an increase in current, and will decrease with an increase in the spacing between the conductors by decreasing the mutal inductance.

As previously discussed, magnetic fields can be reduced external to the box or shielded cable. Once the rocket skin internal field or box level internal field has been determined, the internal induced voltage must be evaluated. The internal induced voltage on a circuit is the combination of the diffused field and the field produced by current flow on the external surface of the box or cable.

The reduction of magnetically induced voltages can be accomplished in several ways. Basically, the induced voltage is produced by a change in flux linkages within a loop of finite area. The amount of voltage appearing on a wire due to a magnetic field can be found precisely from:

$$\phi = \int \vec{B} \circ dS$$

ϕ is know as the flux of $\vec{B}$ over the surface S. Voltage, V, is then found by:

$$V = \frac{d\phi}{dt}$$

Box Level Protection

When evaluating coupled noise on internal circuit cards, any change in circuit configuration or parameters, which will change the flux linkages, will change the induced voltage. The separation of the circuits

will reduce the induced voltage by reducing the flux density in the pickup loop. The voltage can also be reduced if the area of the pickup loop is reduced, since this is a method of reducing flux linkages. In addition, circuits can be made less sinsitive to magnetic fields by providing single point circuit grounds when possible.

In general, the power transferred through magnetic coupling will be decreased as the signal circuit impedance is increased. However, susceptibility to electrostatic coupling will be increased. The optimum value of impedance will be the lowest value for which the magnetically coupled power is made small. Since the optimum value is a function of the circuit wiring, and it is not always possible to calculate or to measure the effective pickup loop internal impedance, the commonly used values of 300 - 600 ohms for low impedance signals represents a good average circuit impedance level for general use, and will result in minimum magnetic and electrostatic coupling.

Since it is difficult to determine induced circuit voltage based on the particular configuration and layout of a circuit mounted inside an electronics box, the usual approximation is to assume all transmitted energy through the shield from the largest side can couple to an individual worse case wire loop. This approximation also assumes a worse case orientation, and simplifies the mathematics involved when complex electronic modules are being examined. The induced voltage (at the diffused lightning waveform frequencies) can then be applied directly against threshold levels of individual circuits. It should be pointed out that this analysis considers only the case of energy

from an external field coupled inside individual boxes, not the case of induced voltages on interconnect cables damaging interface ports.

Shielded Cable Protection

A few methods are available which will reduce magnetic induced voltages in cable wires. It is sometimes possible to design circuit configurations in which equal and opposite self cancelling voltages are induced in the circuit. This is the principle by which magnetic coupling is reduced using twisted-pair wiring. At frequencies below 5 KHz, a twisted-pair will provide over 20 dB of magnetic coupling reduction, while copper braid shielding will provide pracitcally none. The effectiveness of conventional copper braid shielding for magnetic field reduction will increase as the frequency is increased above 5 KHz. Ferrous shielding is required for reduction below 5 KHz. For optimum effective magnetic decoupling throughout the lightning spectrum, twisted pair conductors enclosed by conventional copper braid shield is usually employed.

In practice, several conditions may occure which can cause incomplete cancellation of voltages. For instance, if the magnetic field is distorted, such as would be caused by placing magnetic material near the wire, the flux density in one loop would be different from that in the adjacent loop and an imbalance current would flow in the closed circuit. Another condition contributing to incomplete cancellation would be nonuniformity in the twist which can result in adjacent loops of different areas, so cancellation from loop to loop would not occur. If a twisted-pair does not cross a current carrying wire, the effects of the pair being immersed

in a nonuniform field producing a net induced voltage are decreased.

The effectiveness of twisted-pair wires depends to a large extent on the uniformness and tightness of the twist employed. A shielded twisted-pair with the shield terminated at one end is usually used to protect agianst low frequency interference. However, open shields are susceptible to arcing from the high current levels associated with lightning. Therefore, in this application, a twisted-pair with the shield grounded at each end is the preferred wiring for reduction of magnetic and electrostatic coupling.

The optimum circuit configuration from the standpoint of reducing magnetic coupling for a single conductor shielded wire is that in which the signal return is through the shield as in coaxial cable, and the shield is grounded to the ground plane at one point. The principle involved is to have the shield loop area less than or equal to the circuit loop area in order to minimize shield flux linkages. This circuit offers somewhat better magnetic protection than does an unshielded twisted-pair of 6 turns/foot grounded at one point. The approach is valid only when considering double-ended or ungrounded circuits. If single-ended or grounded circuits are being used, the shield would be effectively grounded at each end and a complete loop would exist.

Shielding Effectiveness of Double Overbraid Cables

The magnetic shielding effectiveness of the double overbraid cable can be determined if the assumption is made that cables are similar to

a double cylinder enclosure. Shielding effectiveness is defined below.

$$S.E. = 20 \text{ Log } \frac{H \text{ outer}}{H \text{ inner}}$$

For a double overbraid shield of Ni-clad copper wire, the shielding configuration is similar to concentric cylinders in the topological order of Ni-Cu-Ni-Ni-Cu-Ni from outer shell to inner shell. In general, nesting of shields produces more attenuation than the sum of the individual shields. Therefore, all the nickel can be combined into the inner cylinder and the copper into the outer cylinder such that a double cylinder is formed. Now we have two infinitely long coaxial cylinder shields with the properties as defined in Table 4-2.

Table 4-2. Properties of the Double Cylinder Enclosure

	Material	Thickness (M)	Effective Conductivity	Permeability (H/M)
Inner	Nickel	$d_1=9.334\times10^{-5}$	$\sigma_1=1.086\times10^{7}$ mho/m	$\mu_1=1.257\times10^{-4}$
Outer	Copper	$d_1=2.739\times10^{-4}$	$\sigma_2=3.23\times10^{7}$ mho/m	$\mu_2=1.257\times10^{-6}$

Lee and Bedrosian[77] have shown cylindrical shells provide less shielding for the axial external field than the transverse external field. Rizk[78] has shown that for the case where the sum of the internal radius (a) and shield thickness (d) equals the internal radius of the outer shield (b), the outer to inner ratio of the field strength is given as:

$$\frac{Ho}{Hi} = \left[\cosh\ \gamma_1 d_1 + \frac{j\omega\mu_o\ \sigma_1 a}{2\gamma_1}\ \sinh\ \gamma_1 d_1\right]\ \cosh\ \gamma_2 d_2$$

$$+ \left[\sinh\ \gamma_1 d_1 + \frac{j\omega\mu_o\ \sigma_1 a}{2\gamma_1}\ \cosh\ \gamma_1 d_1\right]\ \sinh\ \gamma_2 d_2$$

where $\gamma = \sqrt{j\omega\mu\sigma}$

Therefore, a worst case shielding effectiveness to low frequency axial magnetic fields for a double cylinder enclosure can be calculated.

Analysis Using Transfer Impedance

Transfer impedance is a method used to determine voltages appearing on internal wires as a result of external shield currents. The concept was proposed by Schelkunoff in 1934 and has gained support through the work of Edward Vance and others. Transfer impedance is now accepted and used in electromagnetic pulse engineering but it has little support in some other electronics disciplines because of its departure from classical transmission line theory when dealing with real life applications. The following discussion provides an understanding of the method used for transfer impedance calculations. Some key areas of disagreement with the technique are pointed out. This technique is used to determine expected pin voltage levels in subsequent sections of this document.

For current to appear on a cable shield, it can be induced by an incident wave, or result from some distribution along a path between point sources. When a lightning stepped leader attaches to the missile nosecap and a subsequent channel is formed with an opposite charge potential on the ground, current flows between the two charge centers. If the rocket is an integral part of the lightning channel, current will flow via some distributive mechanism through the conductive structure of the rocket.[79] Since there is also an electromagnetic field associated with the lightning strike, only a thorough analysis of the combination of the distributive current effects and the incident field coupling effects can provide an accurate number for shield currents. According to Vance,[80] shield current

propagating with velocity c, regardless of how the current is induced, can still be analyzed using transfer impedance techniques. A structural ground return path is not apparent in the case of lightning current distribution, but is a key element of the coaxial cable model proposed by Vance.

Coupling Through Cable Shields

When lightning current flows in a cable shield via any mechanism, a voltage V and current I will appear on the internal conductors. This is due to external electric and magnetic fields which penetrate the cavity. This internal voltage and current can be calculated with the equations for a transmission line with a distributed source current. If the shield contains apertures (braided wire holes, etc.), the transmission line will contain a distributed shunt-current source, as well as a distributed series-voltage source. The distributed-source voltage is a function of the properties of the shield and the shield current. The distributed-source current is determined from the shield properties and the voltage between the shield and the structure that serves as the shield current return path. Since the current source depends on the charge density on the outside surface of the shield, for shields that can be represented as transmission lines, the charge density and shield voltage are related through the external capacitance per unit length of the shield. Figure 4-4 illustrates the shield/voltage current relationship. The shield current I is flowing from end 1 toward end 2, and the voltage V is measured with respect to the shield-current return path.

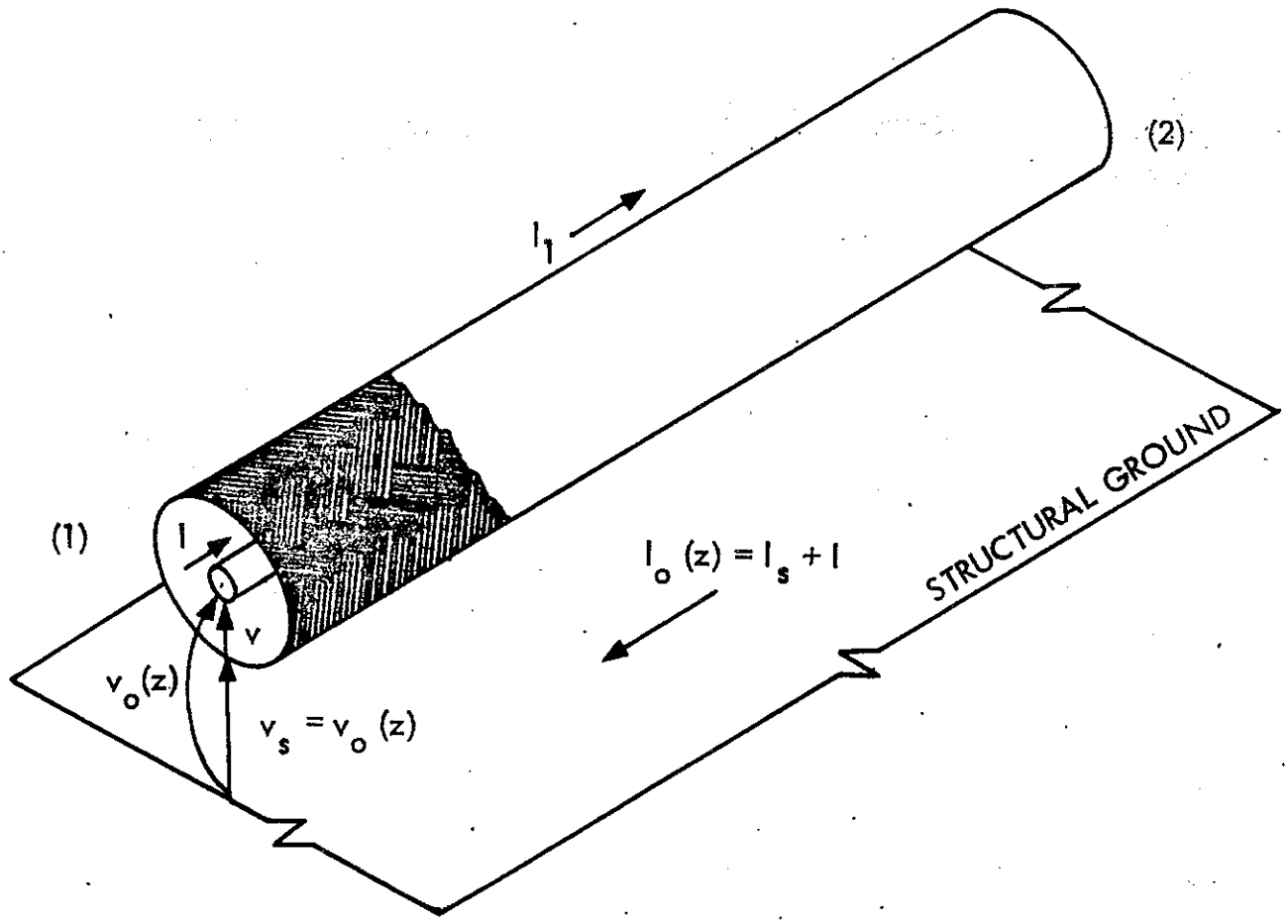

Figure 4-4. Voltages and Currents Associated With Shielded Cable Analysis[81]

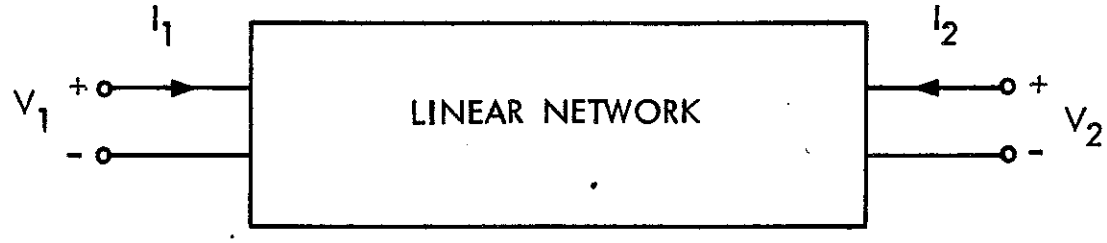

Figure 4-5. Two Port Network

Transfer Impedance

Consider the two port network as it is shown in Figure 4-5. The voltage and current at the input terminals are V_1 and I_1. V_2 and I_2 are specified at the output port. The directions of I_1 and I_2 are both customarily selected as into the network at the upper conductors (and out at the lower conductors). For a network which is linear and contains no independent sources within,

$$V_1 = Z_{11} I_1 + Z_{12} I_2$$

$$V_2 = Z_{21} I_1 + Z_{22} I_2$$

or in the matrix form:

$$\begin{bmatrix} V_1 \\ V_2 \end{bmatrix} = \begin{bmatrix} Z_{11} & Z_{12} \\ Z_{21} & Z_{22} \end{bmatrix} \begin{bmatrix} I_1 \\ I_2 \end{bmatrix}$$

The Z parameters, called open circuit impedances, may now be described as voltage-current ratios with either $I_1 = 0$ (the input terminals open-circuited) or $I_2 = 0$ (the output terminals open-circuited).

$$Z_{11} = \left. \frac{V_1}{I_1} \right|_{I_2 = 0}$$

$$Z_{12} = \left. \frac{V_1}{I_2} \right|_{I_1 = 0}$$

$$Z_{21} = \left. \frac{V_2}{I_1} \right|_{I_2 = 0}$$

$$Z_{22} = \left. \frac{V_2}{I_2} \right|_{I_1 = 0}$$

The specific name of Z_{11} is the open-circuit input impedance, Z_{22} is the open-circuit output impedance, and Z_{12} and Z_{21} are the open-circuit transfer impedances. Usually Y = 1/Z for a particular element. Here, Y_{ij} is the $(i,j)^{th}$ entry of the admittance matrix, and can not be related to the reciprocal of the $(i,j)^{th}$ entry of the impedance matrix. Therefore, the following equation for transfer admittance must be noted.

$$Y_{ij} \neq \frac{1}{Z_{ij}} \quad \text{where } i = 1,2 \quad j = 1,2$$

Transfer Impedance Definition

Using the previous relationships for the lumped parameter case, the transfer impedance of a shield can be defined in the general form below.

$$Z_T = \frac{1}{I_o} \frac{dV}{dz} \Bigg|_{I=0}$$

where I_o is the total current flowing in the cable, and dV/dz is the voltage between the conductors and the shield per unit length (dz) generated by this current.

According to Vance,[82] the transfer impedance always contains a diffusion component that relates the shield current to the longitudinal electrical field inside the shield. This is because the electric field inside a current-carrying shield is never zero. In addition, for leaky shields such as tape-wound or braided-wire shields, the transfer impedance will contain a mutual inductance term that accounts for coupling through

apertures in the shield.

The transfer admittance of a shield is dependent on the external surroundings of the cable, as well as the properties of the shield. The general definition of the transfer admittance is:

$$Y_T = - \frac{1}{V_o} \frac{dI}{dz} \Bigg|_{V=0}$$

where V_o is the voltage between the internal conductors and the external structure, and dI/dz is the current per unit length flowing into the internal conductor from the external structure. The transfer admittance gives the short-circuit current induced in the internal conductor. The transfer admittance of metal tubular shields with no apertures is negligible, but for shields containing apertures, the transfer admittance contains a mutual-capacitance term that accounts for capacitive coupling between the internal conductors and the external structure that serves as the shield current return path.

It should be noted that for the case of lightning currents, the return path is not in the structure, and it is not readily apparent that the condition $I_o Z_T \ll V_o Y_T Z_{12}$ is necessarily satisfied. In his book, Vance[83] claims the transfer admittance term can be neglected if shield voltage V_o is negligible (low impedance external circuit), or if the load impedances Z_1 and Z_2 are small (low impedance internal circuit). With no structural return path, and high impedance line receivers, the justification for neglecting the admittance term in this application appears invalid.

Transfer Impedance Transmission Line Model

An element of transmission line of differential length dz that contains a distributed voltage source $E_z(z) = Z_T I_o(z)$, where $I_o(z)$ is the current in the shield, and a distributed current source $J(z) = Y_T V_o(z)$, where $V_o(z)$ is the external voltage of the shield, is shown in Figure 4-6. An input impedance Z_1 and an output impedance Z_2 are assumed and must be used to calculate reflection coefficients. The properties of the shield are incorporated in the transfer impedance Z_T, and those of the shield and external structure (of questionable applicability for lightning) are incorporated in the transfer admittance Y_T.

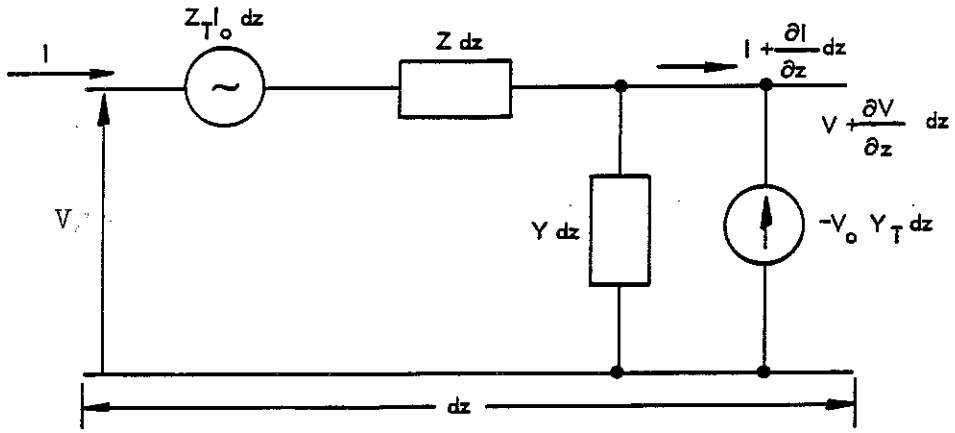

Figure 4-6. Equivalent Circuit for Internal Circuit When Both Transfer Impedance and Transfer Admittance are Included

The differential equations for the internal voltage V and current I are:

$$\frac{dV}{dz} + ZI = E_z(z)$$

$$\frac{dI}{dz} + YV = J(z)$$

where Z is the series impedance per unit length, Y is the shunt admittance per unit length of the transmission line formed by the internal conductors, the shield, $E_z(z)$ is the source voltage per unit length, and J(z) is the source current per unit length produced by the external current and voltage of the shield. The characteristic impedance of the transmission line model, Z_o, is obtained from the impedance per unit length, Z, and the admittance per unit length, Y.

$$Z_o = \sqrt{Z/Y}$$

The above equation is in reality the square root of the ratio of $j\omega L/j\omega C$, since inductance and capacitance are the dominant terms.

Reflection Coefficients and SWR

The reflection coefficient, ρ, is an important parameter in the understanding of power transfer. That is, the reflection coefficient governs the transfer of voltage and current from the sending end to the receiving end of a transmission line. This concept is best understood by examining the standing wave. As the name implies, the standing wave is the interference between a forward traveling wave and the wave reflected at the terminating interface.

The forward traveling wave, whether on a two wire line, coaxial line, or waveguide, can be represented at its input as:

$$V_D(\text{at } D = 0) = V_f e^{j\omega t}$$

where f represents the forward direction, and D represents location. The corresponding forward traveling wave at a later time and position can be represented as:

$$V_D = V_f e^{j\omega(t - (z_o/v_o))} \quad (1)$$

where z_o is the line impedance, v_o is the velocity of light, and $\omega = 2\pi f$. Similarly, a backward (b) traveling or reflected wave at position D can be represented as:

$$V_D = V_b \, e^{j\omega(t+(z_o/v_o))} \qquad (2)$$

Combining (1) and (2) gives an expression for a conductor with two traveling waves moving in opposite directions.

$$V_D = e^{j\omega t} \left[V_f \, e^{-j(\omega z_o/v_o)} + V_b \, e^{j(\omega z_o/v_o)} \right] \qquad (3)$$

Calculating the corresponding current at position D gives the following expression.

$$I_D = \frac{e^{j\omega t}}{z_o} \left[V_f \, e^{-j(\omega z_o/v_o)} - V_b e^{j(\omega z_o/v_o)} \right] \qquad (4)$$

The negative sign is due to a backward propagating wave, while current, by convention, always flows in the forward direction. A phase constant can be defined as $\beta = \frac{\omega}{v} = \frac{2\pi}{\lambda}$. Using this relationship, (3) and (4) can be simplified as follows.

$$V_D = V_f \, e^{-j\beta z_o} + V_b \, e^{j\beta z_o} \qquad (5)$$

$$I_D = \frac{1}{z_o} \left[V_f \, e^{-j\beta z_o} - V_b \, e^{j\beta z_o} \right] \qquad (6)$$

Refering back to figure 4-6, and letting dz equal to some finite length ℓ, the reflection coefficients can now be determined for the input and output. In this case $Z_o = z_o$.

$$\rho_1 = \frac{Z_1 - Z_o}{Z_1 + Z_o} \qquad \rho_2 = \frac{Z_2 - Z_o}{Z_2 + Z_o} \qquad (7)$$

It can be seen that if the cables are infinitely long, or if the cables are terminated in their characteristic impedances, then $Z_1 = Z_2 = Z_o$, and

ρ_1 and ρ_2 go to zero. Vance recognized these relationships in his SRI report on buried shielded cables.[84] Reflection coefficients represent the primary weakness of using transfer impedance methods on commonly used cables. Most noncoaxial shielded cables are not terminated in their characteristic impedance, making the problem considerably more complex.

The input impedance can be derived in terms of its reflection coefficient from (5) and (6) if the input boundary is defined at $-\ell$, or $z = -\ell$.

$$Z_1 = Z_o \left[\frac{e^{j\beta\ell} + \rho_2 e^{-j\beta\ell}}{e^{j\beta\ell} - \rho_2 e^{-j\beta\ell}} \right] \tag{8}$$

Using (8) and writing the input impedance in terms of the reflected wave from the load end (Z_2) gives the following useful expression in transmission line theory.

$$Z_1 = Z_o \left[\frac{Z_2 \, \mathrm{Cos}\beta\ell + jZ_o \, \mathrm{Sin}\beta\ell}{Z_o \, \mathrm{Cos}\beta\ell + jZ_2 \, \mathrm{Sin}\beta\ell} \right] \tag{9}$$

If the two traveling waves in (5) are examined, it appears that the first term becomes more negative while the second term becomes more positive in phase as Z_o increases. At some value Z_o, the two terms will be in phase and the voltages will add, giving a maximum voltage.

$$V_{max} = |V_f| + |V_b| \tag{10}$$

At a distance of one quarter wavelength, the voltages will be out of phase and will subtract, giving a minimum voltage (V_{min}).

The voltage standing wave ratio is defined in terms of the maximum and minimum voltage values.

$$V_{SWR} = \frac{V_{max}}{V_{min}} = \frac{|V_f| + |V_b|}{|V_f| - |V_b|} \qquad (11)$$

The reflection coefficient is defined as $\rho = \frac{V_b}{V_f}$, and is always less then 1. Therefore, the voltage standing wave ratio can be written in terms of the reflection coefficient in the following important equation.

$$V_{SWR} = \frac{1 + \rho}{1 - \rho} \qquad (12)$$

An example of reflection calculations is given in Appendix B.

For the case of a cable with matched terminations at its ends, the reflected voltage will have the same magnitude and shape at both ends, but the polarity is opposite. Also, if one end of the shield is shorted to the core, the open-circuit voltage at the opposite shield end will double, but retain the same waveform.

For an electrically short cable (length L short compared to a wavelength) terminated in impedance Z_1 at one end and Z_2 at the opposite end, the induced currents through the voltages across the terminations are, according to Vance[85], as follows:

$$I_1 \approx I_o Z_T L \frac{1}{Z_1 + Z_2} + V_o Y_T L \frac{L_2}{Z_1 + Z_2} ; \quad (L \ll \lambda)$$

$$V_1 \approx -I_1 Z_1$$

$$I_2 \approx I_o Z_T L \frac{1}{Z_1 + Z_2} - V_o Y_T L \frac{L_2}{Z_1 + Z_2} , \quad (L \ll \lambda)$$

$$V_2 \approx I_2 Z_2$$

For the frequency range of interest in this lightning analysis (below 10 MHz), transfer impedance calculations are useful in approximating the lightning induced pin voltages. However, as has been pointed out, more precise predictions for pin voltages can not be determined with this technique.

Shielding Effectiveness and Shielding Attenuation

There is a tendency to improperly relate classical shielding effectiveness (SE_{DB}) with the shielding attenuation term used in transfer impedance calculations. The relationship between the two terms will be addressed here. Shielding effectiveness is defined by IEEE and elsewhere in terms of a power ratio.

$$SE_{DB} = 10 \text{ Log } \left[\frac{P_s}{P_c}\right]$$

where: P_s = power incident on the cable shielding from lightning, and P_c = power transmitted to the cable conductor. Assuming the contribution of $\overline{I_c}$ by $\overline{V_s}$ is very small, the following equations can be written:

$$P_s = V_s I_s \text{ Cos } \theta_{ss} = I_s^2 Z_{ss} \text{ Cos } \theta_{ss}$$

$$P_c = V_c I_c \text{ Cos } \theta_{cc} = I_c^2 Z_{cc} \text{ Cos } \theta_{cc}$$

where:

$$\bar{Z}_{ss} = Z_{ss} \angle \theta_{ss}$$

$$\bar{Z}_{cc} = Z_{cc} \angle \theta_{cc}$$

Therefore, expressing the classical shielding effectiveness term in an expanded form yields the following equation.

$$SE_{DB} = 10 \text{ Log } \left[\frac{I_s^2 \ Z_{ss} \text{ Cos } \theta_{ss}}{I_c^2 \ Z_{cc} \text{ Cos } \theta_{cc}}\right]$$

$$SE_{DB} = 10 \left\{ \text{Log} \left[\frac{I_s^2}{I_c^2} \right] + \text{Log} \left[\frac{Z_{ss}}{Z_{cc}} \right] + \text{Log} \left[\frac{\text{Cos } \theta_{ss}}{\text{Cos } \theta_{cc}} \right] \right\}$$

The above equation is the key to relating shielding effectiveness and shielding attenuation. For transfer impedance analysis to be exactly valid, $Z_1 = Z_2 = Z_o$ and the reflection coefficients are equal to zero. For a reactive network, if $R_{ss} + X_{ss}$ is the cable shield reactance, and $R_{cc} + X_{cc}$ is the cable conductor reactance, the following assumptions can be made:

$$Z_{ss} \cong Z_{cc}; \quad \text{Log} \left[\frac{Z_{ss}}{Z_{cc}} \right] \cong 0$$

and

$$\theta_{ss} \cong \theta_{cc}; \quad \text{Log} \left[\frac{\text{Cos } \theta_{ss}}{\text{Cos } \theta_{cc}} \right] \cong 0$$

The shielding effectiveness term will then equal the shielding attenuation term:

$$SE = 20 \text{ Log} \left[\frac{I_s}{I_c} \right]$$

This relationship is for the case of coaxial cables terminated in their characteristic impedance.

Cable and Nose Skin Analysis

Since lightning attaches to the nose portion of a rocket first, the magnitude and phase values of the lightning current determined earlier are directly applicable to all cable runs within the rocket. The objective is to determine the possibility of malfunction due to a lightning strike

on the nose shroud. Frequency domain values are preferred since many of the responses of coupling the lightning energy to conductors are frequency dependent. The magnitude and phase provide the driver function for a series of transfer functions as outlined in Figure 4-7.

The transfer impedance for a braided wire shield times the current flowing on the shield or conductor characterize the frequency dependent voltage shouce in the transmission line model.

F(s) of Figure 4-7, represents the filter on a wire. The inverse Laplace transform of $Z_T(s)$ $I_t(s)$ F(s) will give the voltage transient due to lightning at a circuit level. $Z_T(s)$ is dependent on shield parameters. The current flowing on a shield, $I_t(s)$, is composed of both direct current and current due to coupling from the magnetic field. Current can be represented by I(s) D(s), where D(s) is the current division transfer function. Straight current division between various conductors under the nose skin is used to calculate current down to the cable shield level.

A common cable assembly will consist of a number of twisted shielded pairs (TSPs) in a cable bundle. The bundle is often wrapped with tape, a double overbraid is woven on, and a jacket put over that. The pertinent feature is that it is then a multiconductor cable assembly with two levels of shielding, a double overbraid and an inner cable braid. It is also important in the analysis to factor in the twisted pair response for differential balanced loads.

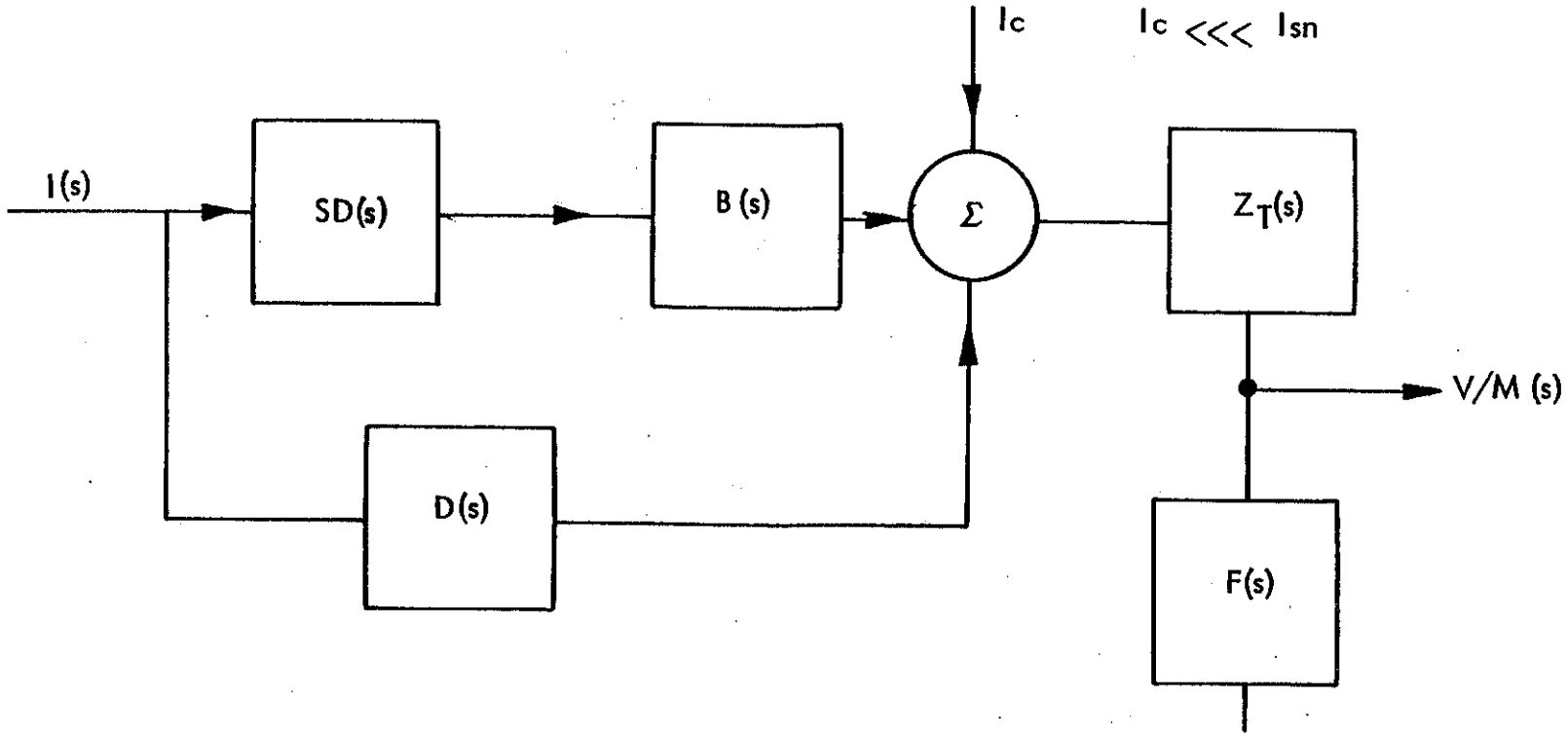

Figure 4-7. Transfer Function Outline

The current source on the overbraid will produce a current on the inner shield. The open circuit voltage between the outer shield and inner shield is given by the outer shield transfer impedance multiplied by the shield current. The impedance this voltage is driving is the resistance of the inner shield with the coaxial inductance in series. A 360 degree termination of the cable or conductor shield will provide low cable termination resistance and negligable inductance, and also eliminates the differential coupling to the conductors caused by inherent unequal magnetic field distribution resulting from pigtails. Inductance is calculated assuming a coaxial geometry as:

$$L = \mu_o/2\pi \ \ln (b/a) \ H/m$$

where b = outer shield radius and a = inner shield radius.

The transfer impedance of a typical Raychem TSP has been measured. For tin flashed braid, the transfer impedance is approximately 20 milliohms/m + $j\omega 0.6$ nH/m. A total transfer function between the current flowing on the outer shield and the open circuit common mode voltage inside the shield can be obtained from:

$$\frac{V_{cm}}{I_s} = \frac{I_{is} \ Z_{is}}{I_s} = \frac{Z_{Tos} \ Z_{Tis}}{Z_{is-os}}$$

where

Z_{Tos} = transfer impedance outer shield

Z_{Tis} = transfer impedance inner shield

Z_{is-os} = impedance between inner shield and outer shield

Depending on the safety margin to be used and the shield involved, a transfer impedance/shielding attenuation curve can be drawn and used with a common mode voltage equivalent circuit as shown in Figure 4-8.

Inner Surface Energy

The percent of current on the inner surface of the rocket nose is calculated from:

$$\text{percent on inner surface} = e^{-t\sqrt{\pi f \mu \sigma}}$$

where

t is the thickness in millimeters

μ is the permeability

σ is the conductivity

It is easy to see that at best, a rocket nose would adequately attenuate only the high frequency components of lightning. The low frequency components will flow on the inner nose surface.

Using the percent of current on the inner nose surface plus the attenuation due to skin effects, a determination can be made of the amount of energy on the inner nose surface. Energy is determined by first determining the current on the inner skin. The nose can be modeled as a low pass filter. The percent of attenuation as a function of frequency due to skin effect is shown in Figure 4-9 for typical skin material.

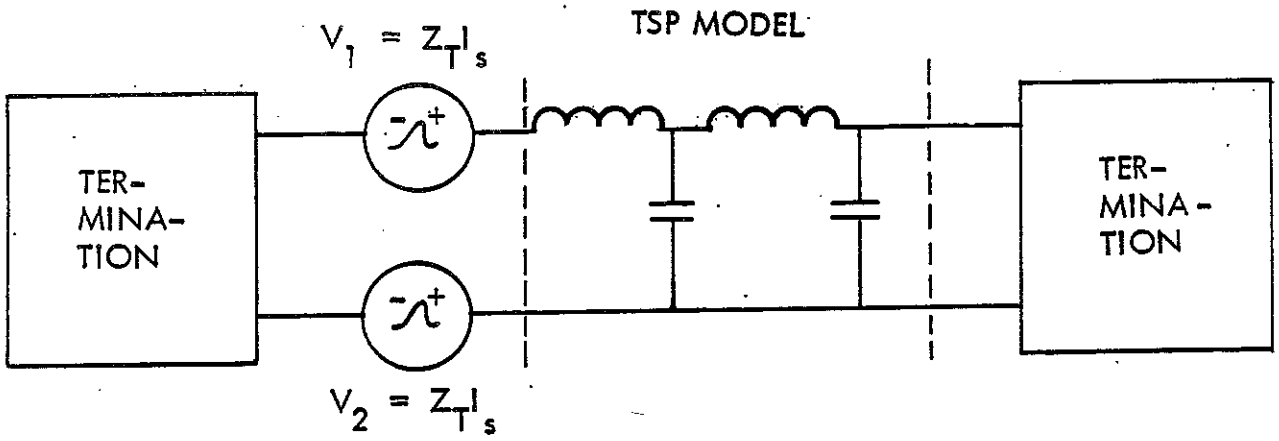

Figure 4-8. Common Mode Voltage Circuit

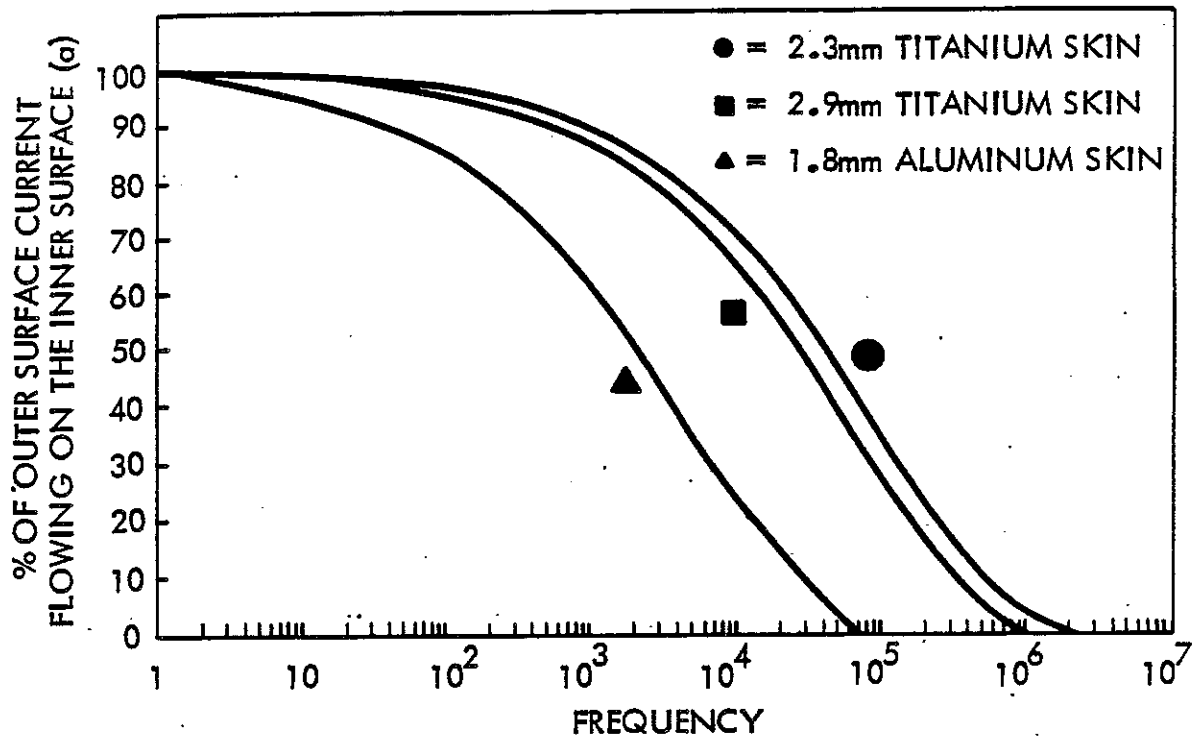

Figure 4-9. Attenuation Due to Skin Effect

The peak current calculated using current division can now be used as a cable current driver. Transfer impedance values for cables are determined using the methods of the previous section. By multiplying the transfer impedance of the cable shield times the shield current, a Thevenin voltage source (the pin driver) can be determined. This voltage, and the in-band frequency range of the receiving device, specify the protection circuitry or filtering required at the pin livel.

Interface Protection From Lightning Pulses

Several devices are on the market which provide fast enough response times and are powerful enough to suppress the induced lightning current pulse on an input pin. The curves shown in Figure 4-10 are typical characteristics for a PN silicon transient voltage suppressor. Diodes designed for transient suppression are normally much faster than standard zener diodes used for voltage regulations, and also have higher power capabilities. Since rockets are susceptible to multiple strikes, gas discharge devices should be avoided since they can ionize after one strike.

General Semiconductor of Tempe, Arizona manufactures such a device which they call a transorb. The term has gained widespread usage by interface designers to signify any solid state surge suppression diode of this type.

Since lightning current can be either positive or negative in a particular strike, two bipolar diodes are required to suppress a pulse of either polarity.

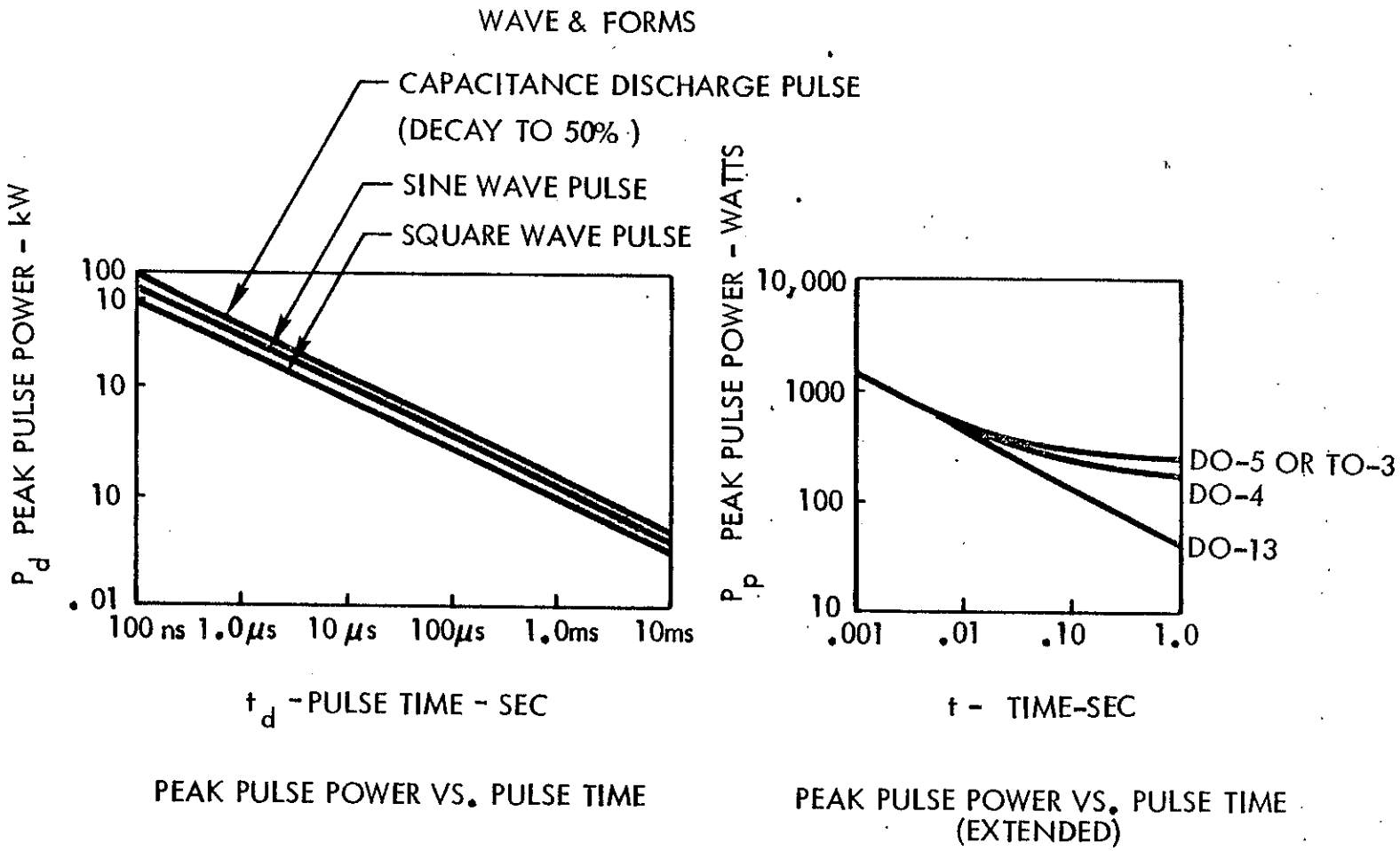

Figure 4-10. Typical Voltage Suppressor Characteristics

The larger the diode, the greater its capacitance, and the slower its turn on time. Therefore, particularly on low impedance ordnance and power lines, some high frequency filtering is required. The in-band sensitivity levels are compared against the high frequency components of the lightning waveform for each driver or receiver device to determine the particular filter required. If the impedance of a monitor or signal line is sufficiently high that it is not susceptible to high coupled current pulses, only a filter may be required for protection. Figure 4-11 shows typical interface protection circuits.

Filter Configurations

Power lines are usually considered low impedance; therefore, the line side of the filter should present high impedance. Filter configurations are shown in Figures 4-12 through 4-15. Load equipment can be any impedance; if high, the load side of the filters should show low impedance, which means inductance in series with the line, and a capacitor from the load side to ground ("L" circuit).

The "C" is a low impedance filter used where both source and load impedance are high. Volumetrically, it is very efficient in low voltage circuits requiring medium range attenuation (20-40 dB) at medium range RF (150 kHz).

Figure 4-12. "C" Feed Through Capacitor

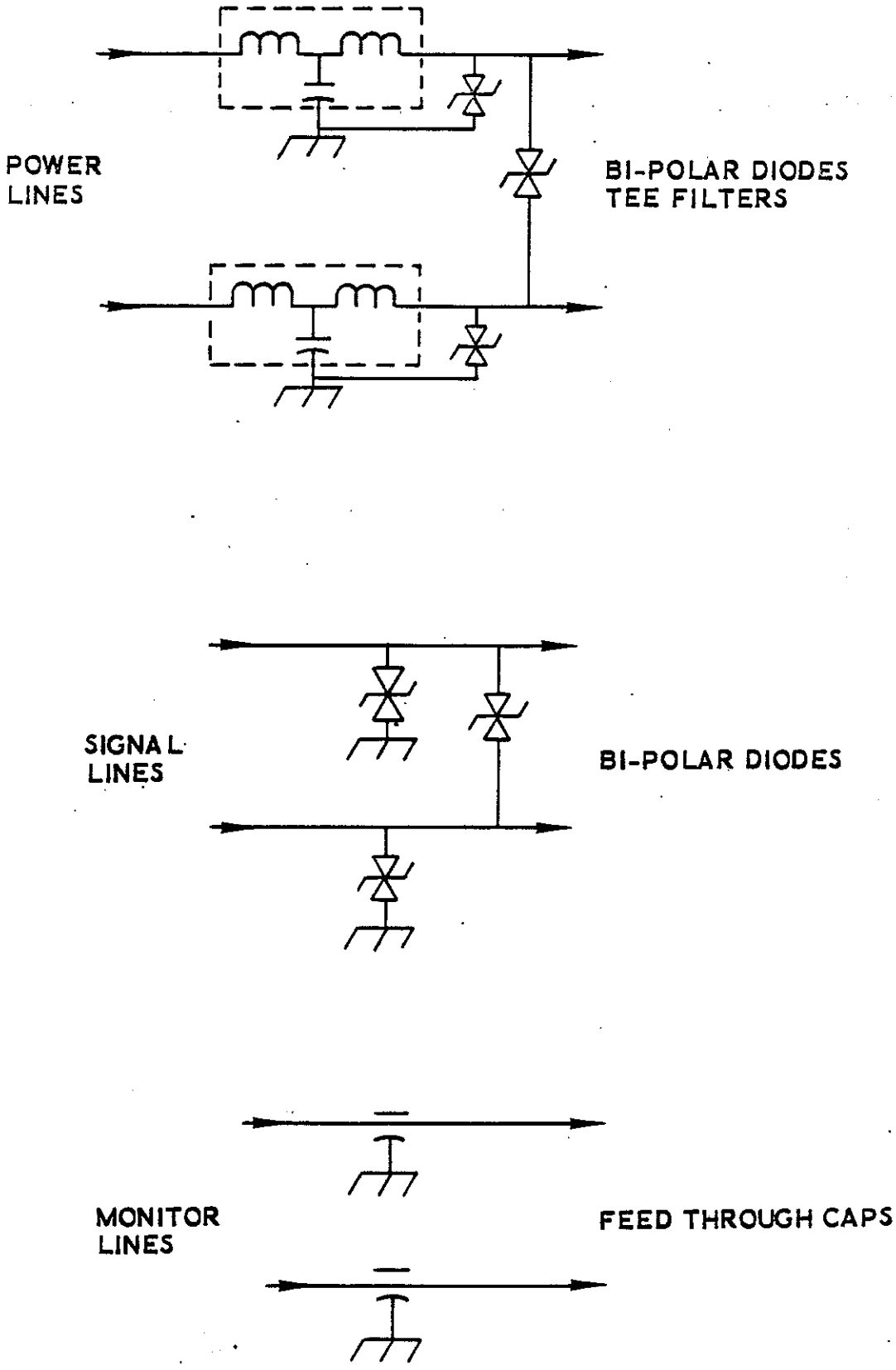

Figure 4-11. Interface Lightning Protection Devices

The "Pi" section low impedance filter is used where both source and load impedances are high. Volumetrically, it is the most efficient filter for any value voltage circuit and any value insertion loss requirement. It is used on oscillatory voltages and random noise voltages. The "Pi", being a tank circuit, will ring at the natural resonant frequency of the filter more under shock excitation than "L" or "T" circuits, reducing its usefulness for lightning protection.

Figure 4-13. "Pi" Section

In general, the "L" section is used on high impedance noise sources and low impedance lines. This configuration will resonate when shocked with transients at selected frequencies, producing dips in the resonance curve. Therefore, it is not useful in lightning protection applications.

Figure 4-14. "L" Section

The "T" section is used in circuits where both source and load impedances are low. It is especially recommended for circuit interrupting devices such as relays, in that it eliminates "ringing" since current impulses are reduced by the low shunt capacitance and high series inductance. It is very effective in reducing transient type interference such as lightning pulses.

Figure 4-15. "T" Section

Figure 4-16 shows the interface protection design for a typical differential driver/receiver circuit. Note that the surge suppressors are located before the feedthrough capacitors.

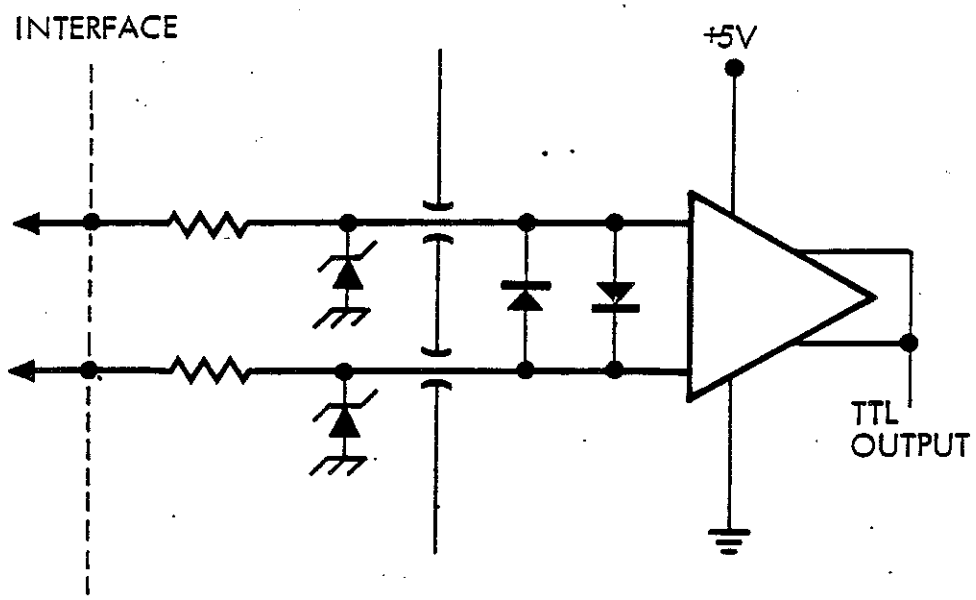

Figure 4-16. Interface Circuit Model

Integrated Circuit Susceptibility

McDonnell Douglas published a report for the Navy in August 1978 titled "Integrated Circuit Electromagnetic Susceptibility Hanbook."[86] Figures 4-17 and 4-18 are from this report. It can be determined how much protection is needed for a particular IC based on the information from these graphs, and the expected threat determined by the previous methods discussed.

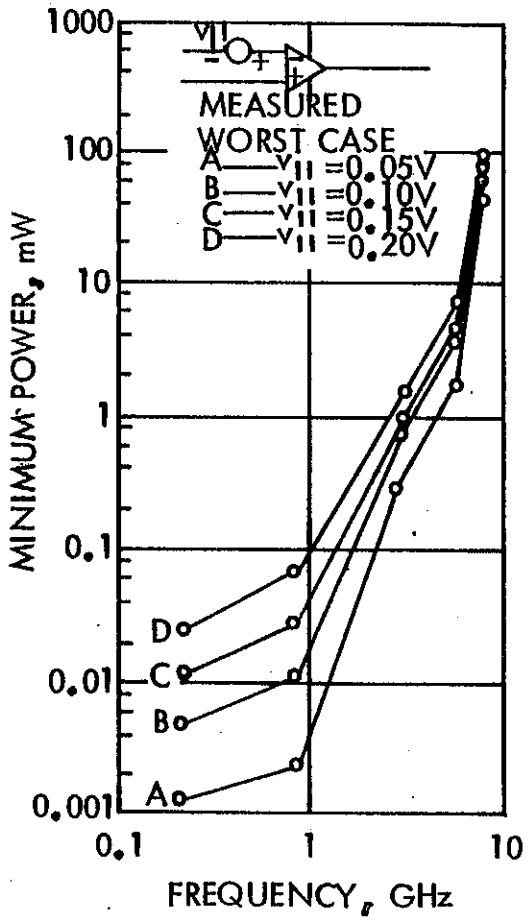

Figure 4-17. Worst Case Susceptibility Values for OP amps

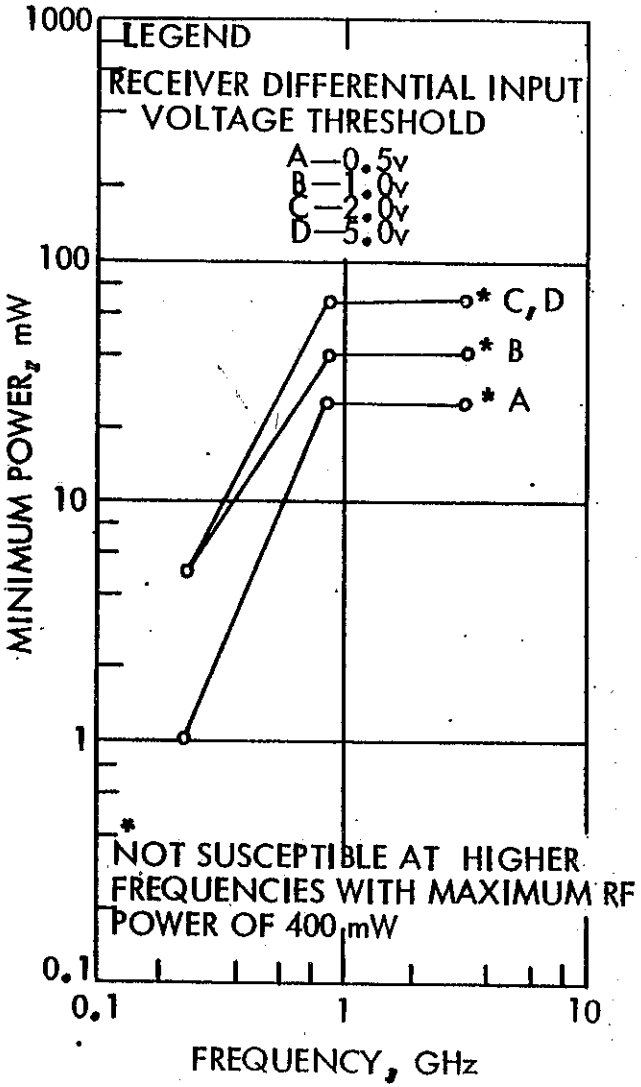

Figure 4-18. Worst Case Susceptibility Values for Line Drivers and Receivers

Squib Protection

Ordnance devices are generally used at various locations inside a rocket. These electroexplosive devices (EEDs) may be either the hot bridgewire (HBW) or the exploding bridgewire (EBW) type.

Two failure modes due to lightning are possible for EEDs: pin-to-pin supplied energy (where energy is provided directly to the bridgewire by the current flowing through it); or pin-to-case arcing (in this case a high voltage measured in the thousands of volts applied between a pin and case causes an arc which initiates ordnance). According to MIL-STD-1512, HBWs are considerably more susceptible than EBWs to both effects. Early EED designs, according to Franklin Institute,[87] had post-burn and nonuniform wire terminations which could, through pin-to-case voltages, cause arcing when subjected to potentials near 8,000 volts. Modern squib designs attempt to eliminate this problem by imposing proper quality control standards.

We can dispense with the pin-to-case concern by noting that only low voltages will be seen between the case and a grounded input pin prior to arming since MIL-STD-1512 requires an A/D device be located in series with the line.

For the pin-to-pin case threat, further analysis is required. The bridgewire itself is surrounded by a nonconductive explosive compound, and is completely enclosed in a stainless steel case similar to a BNC connector jack. The case is usually buried inside a second case containing the ordnance. Transfer impedance for the small diameter cable can be used

to determine the induced pin voltage. Since the pin-to-pin induced voltage is about the same for both EBWs and HBWs, the threat to the more susceptible HBWs will be examined.

To understand how HBWs can inadvertently be initiated, the minimum fire level must first be determined. Specifications usually list all fire and no fire levels required. The susceptibility threat from the lightning induced energy must be compared to the no fire level if a safety margin is the design objective. To establish the minimum energy level required to fire an HBW, its internal parameters must be examined.

Rosenthal developed the classical lumped parameter model used to analyze a modern bridgewire device. The model is given below.

$$C_p + \gamma\theta = P_t$$

where:

C_p = heat capacity of the bridgewire

γ = combination of all possible heat losses

θ = temperature rise

P_t = power to the wire as a function of time

The thermal time constant $\tau = C_p/\gamma$ gives the time it takes for a wire to reach two-thirds of the bridgewire's stable temperature no matter what current is input to the device. The NASA standard initiator uses a mix of $Z_r/KCLO_4$, and has a τ = 0.1 ms. The mix reaches the fire temperature of 700^{o}C in 0.1 ms, with about 0.029 joules applied. This value is

compared against the lightning induced energy applied over an equal time period to determine if the bridgewire is susceptible. Less energy over the same period of time, or more energy over a longer period may not fire the device. Over longer time periods, the γ coefficient takes over and the temperature cannot be reached.

Assuming a NASA standard initiator, it it a simple matter to estimate if enough energy is coupled due to a lightning strike to fire the device. Calculate the transfer impedance for the ordnance cable used and determine an equivalent circuit similar to that shown in Figure 4-19. Use the action integral equation to determine the delivered lightning energy in joules appearing at the HBW for a time period equal to the duration of the lightning induced pulse at the pin level.

To compare the lightning induced energy level with the energy level required to fire the HBW, the lightning energy must be normalized to an equivalent time period. This means, assume the lightning energy is applied in a pulse of even magnitude, and compare this energy to the energy required over the τ period necessary to fire the initiator being used.

Transmission System Protection

The previous sections examined interface driver/receiver circuits and ordnance squibs. Two other devices requiring examination are the antennas and sensitive receiver inputs. Since most sensitive receivers employ JFET inputs, the following analysis will concentrate on this type of antenna receiver interface.

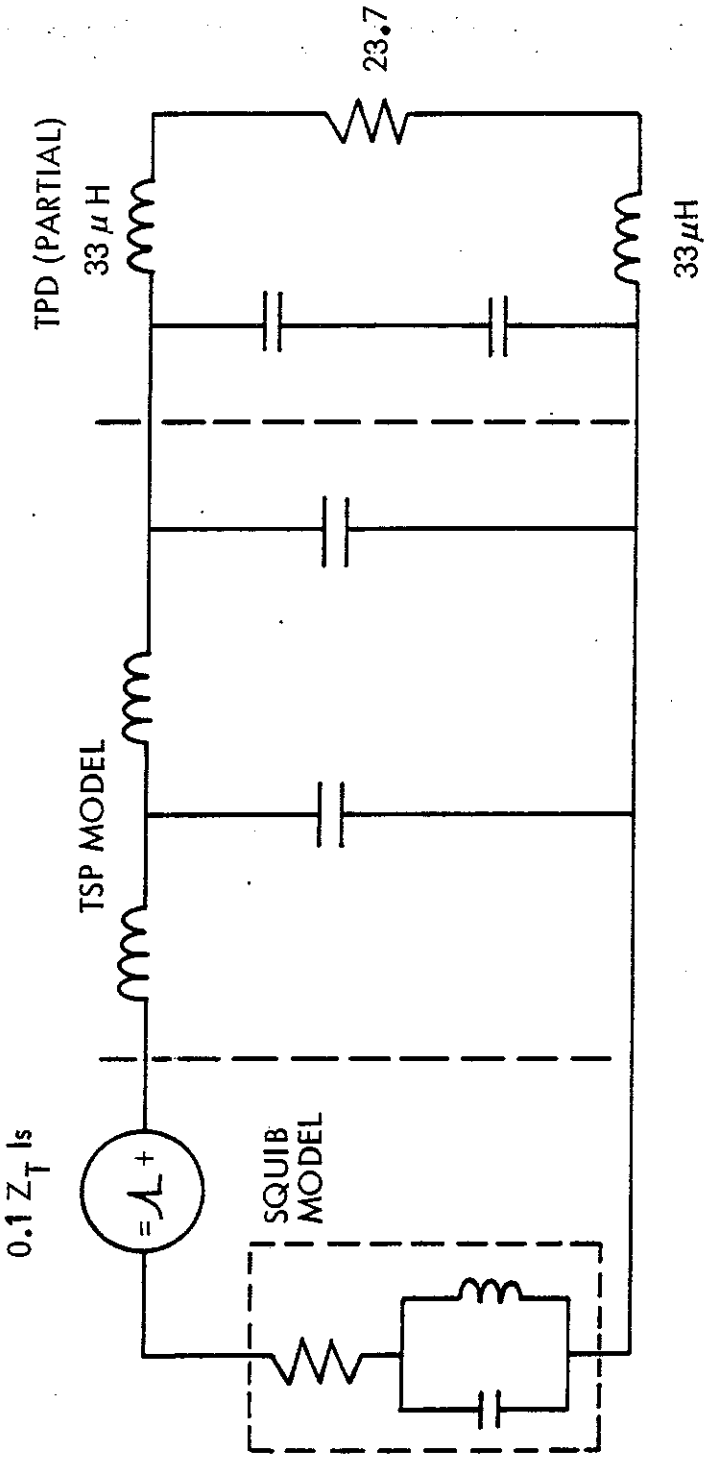

Figure 4-19. Circuit Model to Analyze Squib Problem

Patch antennas consist of a radome, radiating element, substrate, and an aluminum backing plate, usually secured to the rockets surface by a rectangular mounting plate. Pointed screw heads are normally used. This design assures lightning will not penetrate the small space between the screws because the dielectric strength of the antenna window is much greater than the voltage drops between the screw heads. The geometric center of the radiation element is normally connected to the rocket by a low inductance stub. The antenna delivers power to the transmission line by another stub located a short distance off center. Normally, the long axis of the rocket lies in the plane formed by the two stubs.

Signals from the antenna are provided and fed to a receiver by an RF coupler. RF couplers are normally constructed from two rectangular wires separated by about 0.38 mm and running parallel for one quarter-wavelength. The voltage from one wire to ground that can be handled by a coupler is estimated to be in excess of 1000 volts. RG 393/U coaxial cable can withstand 1900 volts dc.

The first stage of a JFET input receiver front end is shown schematically in Figure 4-20. This example uses a JFET (2N5397) in a grounded gate configuration. The breakdown voltage of this JFET is 25 volts. Failure modes of JFETs do not always follow the Kt^{-B} thermal model, therefore, it is assumed that any pulse exceeding 25 volts will damage the device. A low inductance (2 nH) connection from the input to ground effectively shunts low frequency currents.

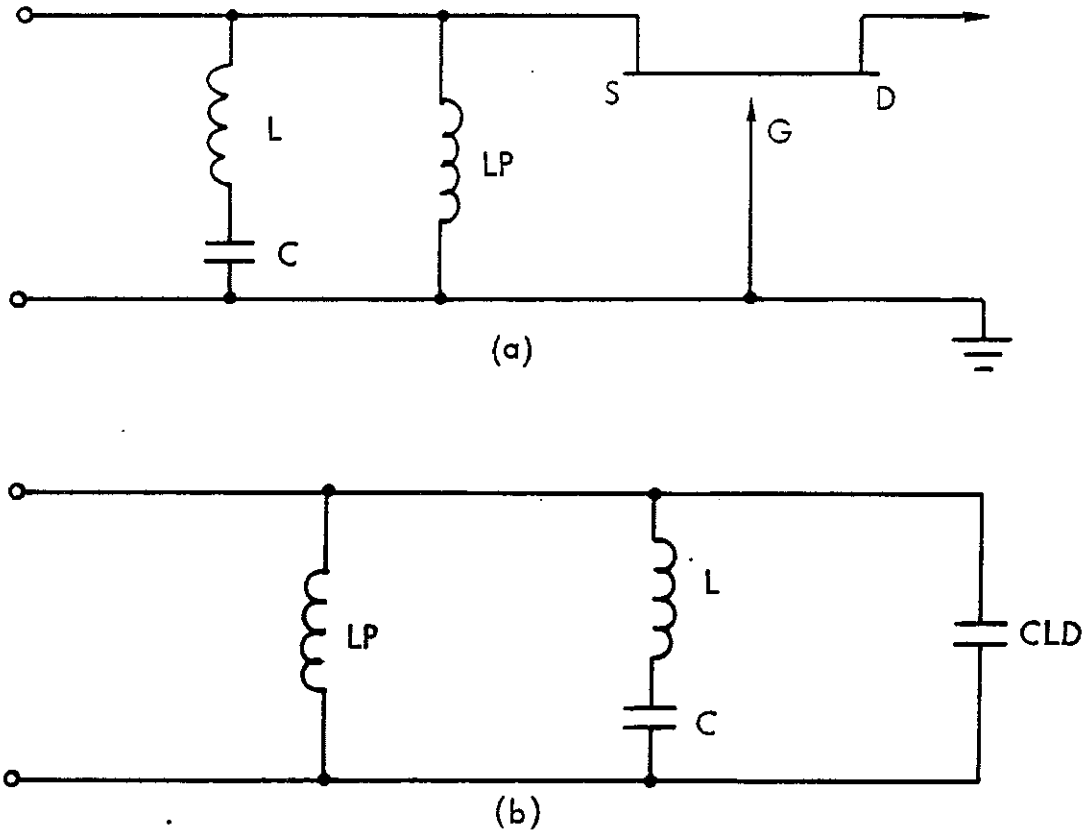

Figure 4-20. Receiver RF Input and Circuit Used to Model Input

Antenna Susceptibility to Lightning

When the stepped leader attaches to the rocket, large changes occur in the surface electric E field. The antenna is susceptible and responds to dJ_s/dt, where J_s is the surface current. To obtain an approximation to the effects, we assume that either:

a) Attachments occur on the nose and plume and current distributes fairly uniformly over the diameter of the rocket, or

b) A first return stroke attaches near the antenna, as shown in Figure 4-21, and current flows down the raceway for a composite design and out the plume.

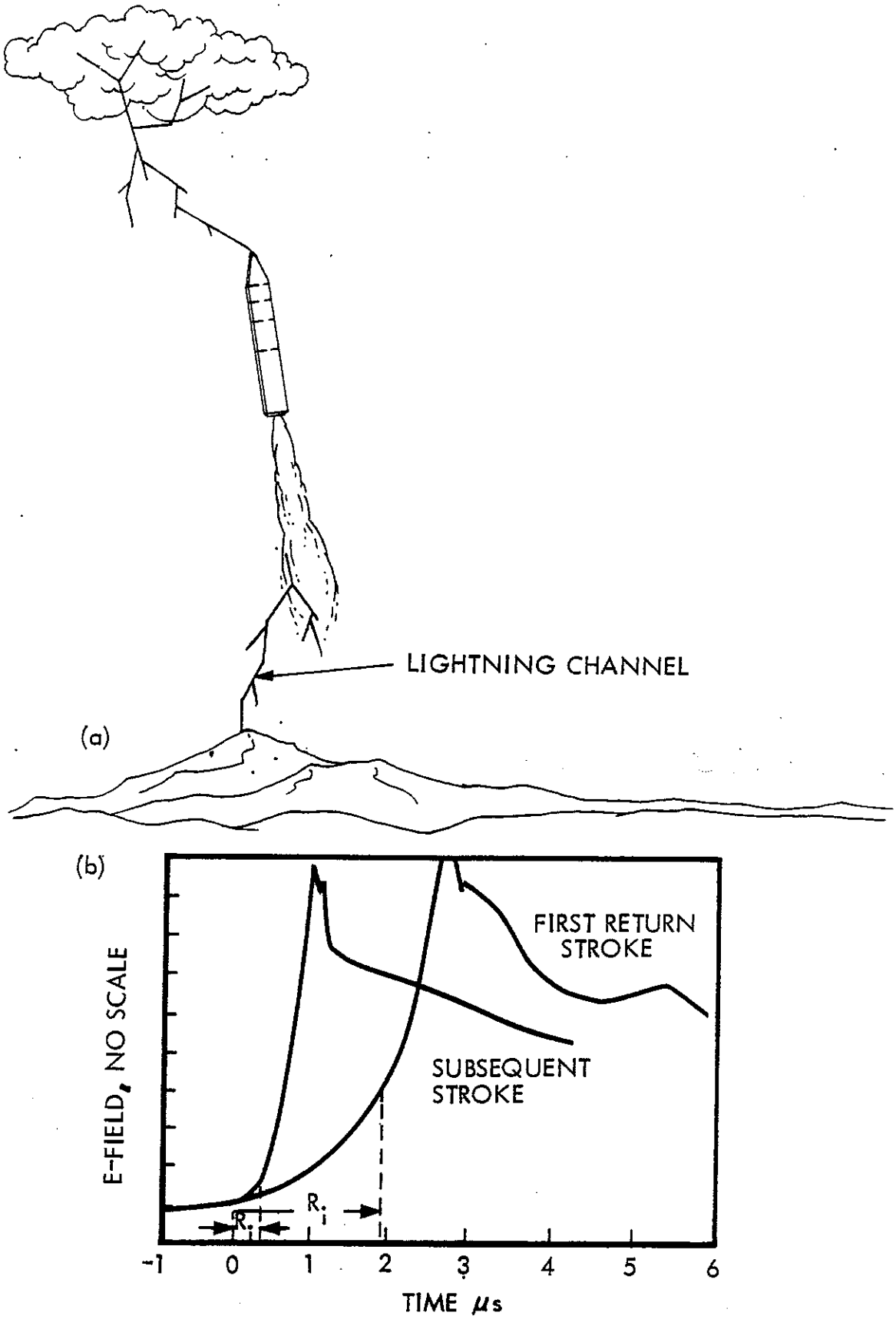

Figure 4-21. **(a) Lightning Attachment**
(b) Time Dependence of Lightning Fields

Receiver Susceptibility to Lightning

The major threat to the receiver comes from magnetic field coupling to the antenna that produces an induced voltage proportional to the time derivative of the lightning current. For the lightning waveform of Figure 3-14, the time derivative is a sequence of square wave pulse functions, the first being the most significant threat to the receiver. To simplify the analysis, the current waveform of Figure 4-22 is used. This waveform is scaled so that the effect on the circuit will be approximately the same as the first segment of the lightning waveform.

As the rocket climbs, a lightning arc channel may be swept over the antenna, as shown in Figure 4-23. The radome must be able to withstand a potential difference, ΔV, equal to L di/dt. L is the effective inductance of the channel, about 1 μH per meter. For the lightning waveform of this example, di/dt is 4×10^{11} amps/sec. For an antenna distance D of about 0.10 m, a voltage ΔV as large as 40 kV can develop across the radome.

Fields generated by near-miss flashes are not considered, since they will be less than fields induced by an attached stroke.

Direct Strike Antenna Effects

If a strike attaches directly to the antenna, the radiating element will be damaged. Using the values of $\int i^2\,dt = (5 \times 10^6 \text{ amp}^2\text{-sec})$ for the waveform of this example, it can be shown that a direct attachment to the copper radiating element of a standard antenna would melt the plating over

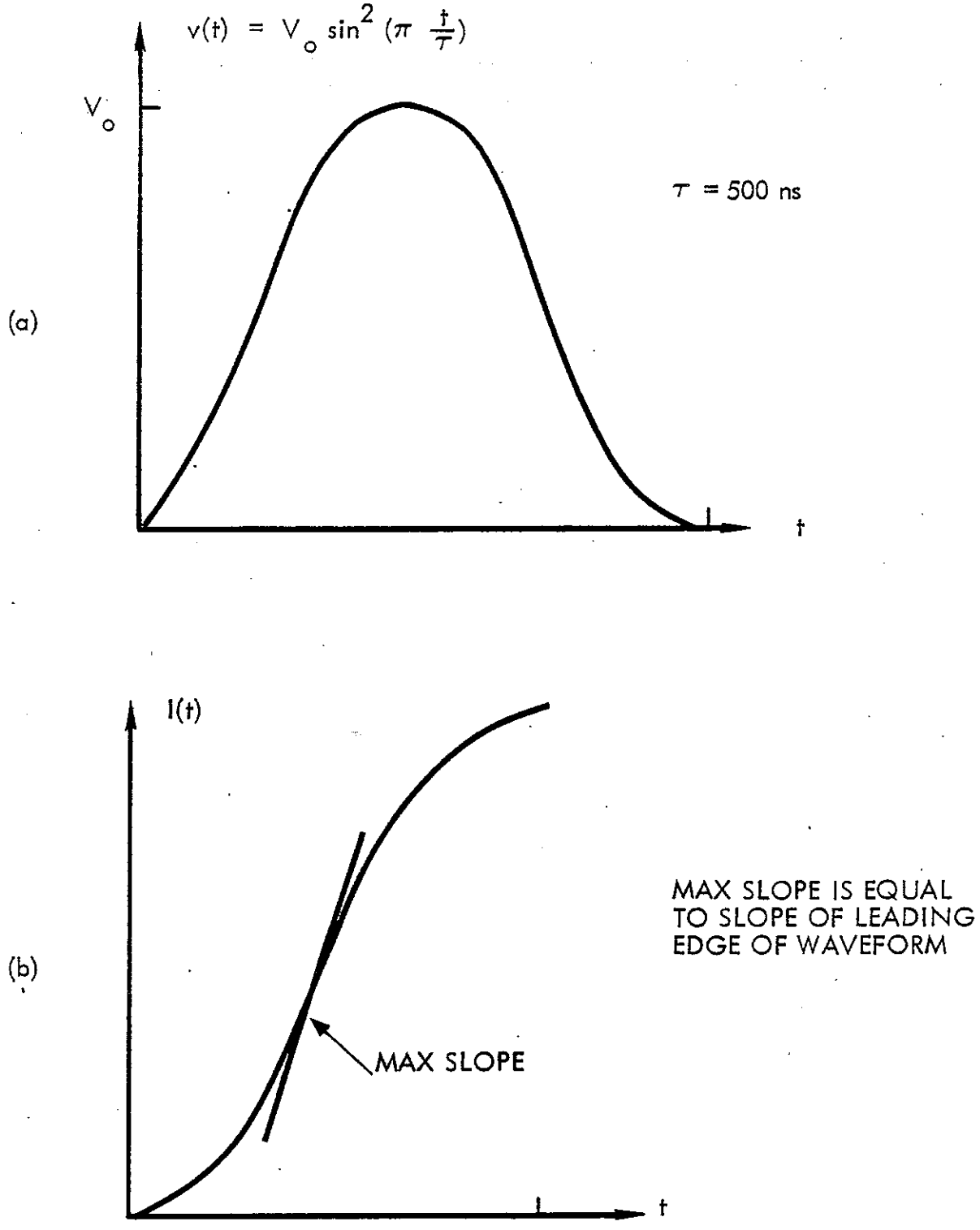

Figure 4-22. (a) Induced Voltage of Functional Form Sine Squared, (b) Waveform From Which it is Derived

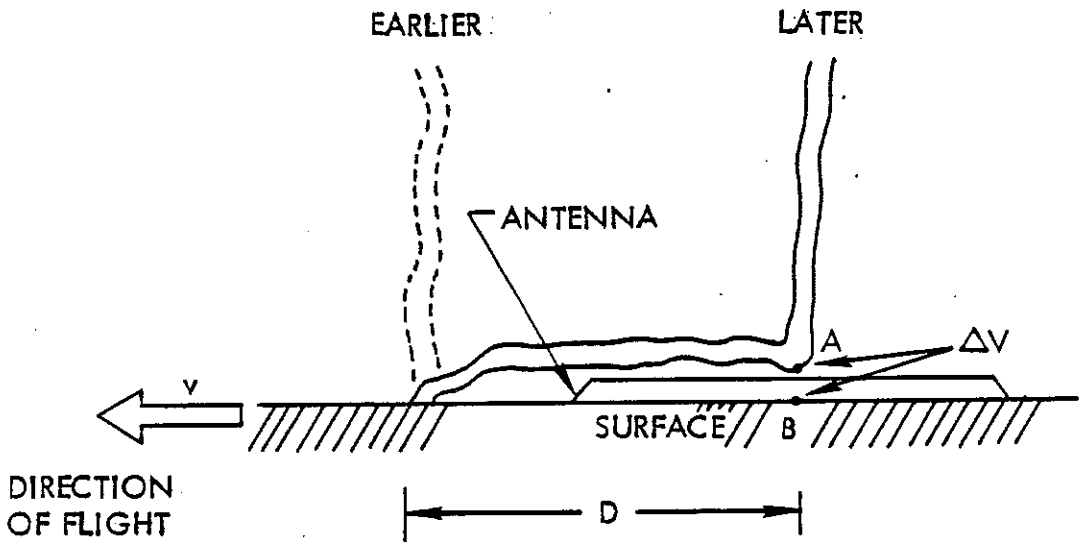

Figure 4-23. Lightning Channel Sweeping Across Radome

a significant radius for both the exit and entrance points rendering the antenna inoperable. However, an attachment to the antenna can occur only if the radome punctures. Radomes are manufactured usually from teflon and fiberglass which has a dielectric strength on the order of 104 Vdc/mm. Impulsive withstand voltages has been found to be twice the minimum[88], so a radome can actually withstand twice the impulse calculated. This is adequate for the estimated 40 kV threat, so direct attachment is not usually a problem with side mounted antennas. Impulsive loading on antenna cavaties due to the shockwave associated with a strike is addressed later in this document.

Antenna Coupling of Indirect Effects

Either changing electric fields (dE/dt) or changing magnetic fields (dB/dt) at the surface of the rocket can couple energy into the antenna. The changing electric fields cause displacement currents, and changing magnetic fields induce voltages. The displacement current depends on the capacitance of the antenna, its height, and on dE/dt. Figure 4-24 shows an equivalent circuit of the antenna for a dE/dt threat. The source current, IS(t), it given by:

$$I(t) = h \times C \times dE/dt$$

where h is the height of the antenna element from the ground plane, and C is the capacitance of the radiating element. C can be approximated by the following equation:

$$C = K \frac{\epsilon_o A}{h}$$

K is the dielectric constant of the substrate, and A is the area of the antenna element. The inductance L represents the shorting stub in this example that connects the radiating element to ground. Its value can be estimated from calculations using formulae developed by Sandia.[89]

To determine the induced voltage in the antenna, the effective height of the antenna, h_{eff}, has been calculated from the effective area, A_{eff}, as follows:

$$h_{eff} = (A_{eff}\ 50/377)^{1/2}$$

A survey of various kinds of antennas showed that effective areas are on the order of 0.32 or less.

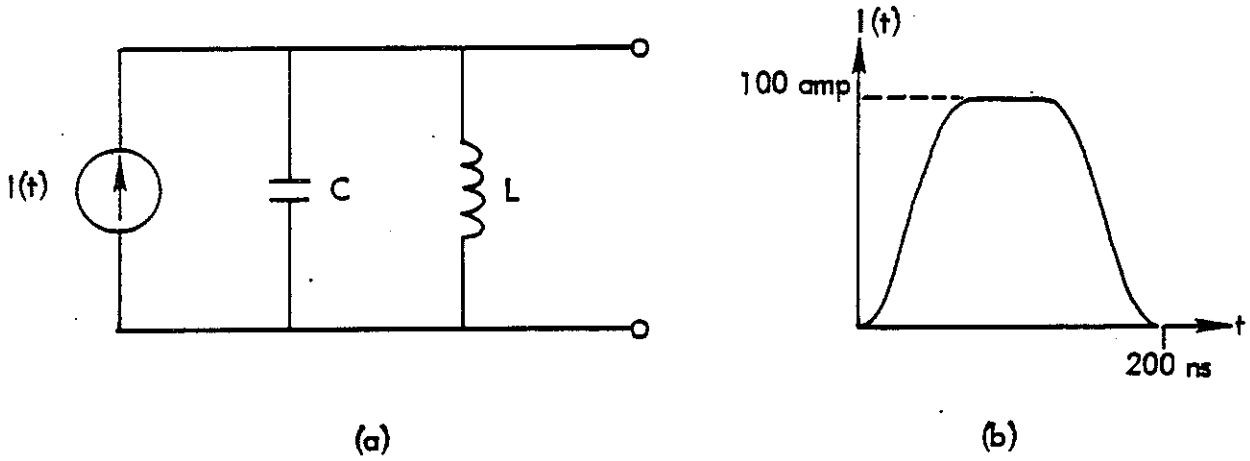

Figure 4-24. (a) Equivalent Circuit for Antenna, (b) Given a dE/dt Threat

A changing magnetic field (dB/dt) induces an EMF in the shaded area, ABCD, which represents an antenna loop, shown in Figure 4-25(a). The EMF, V, is found from the equation below:

$$\left| V \right| = \frac{d\phi_B}{dt} = \mu_o A \left| \frac{dJ_s}{dt} \right|$$

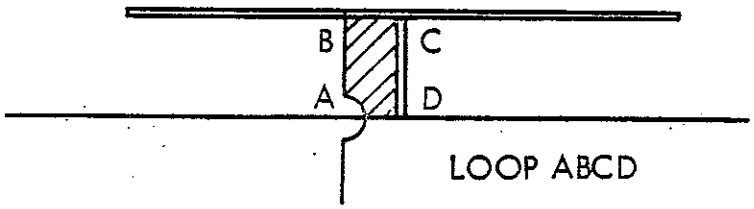

(a)

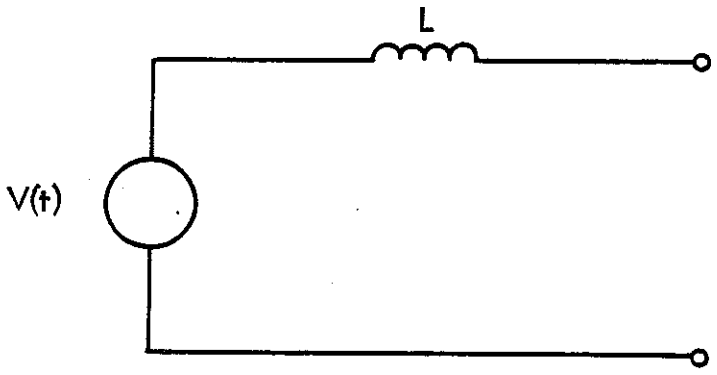

(b)

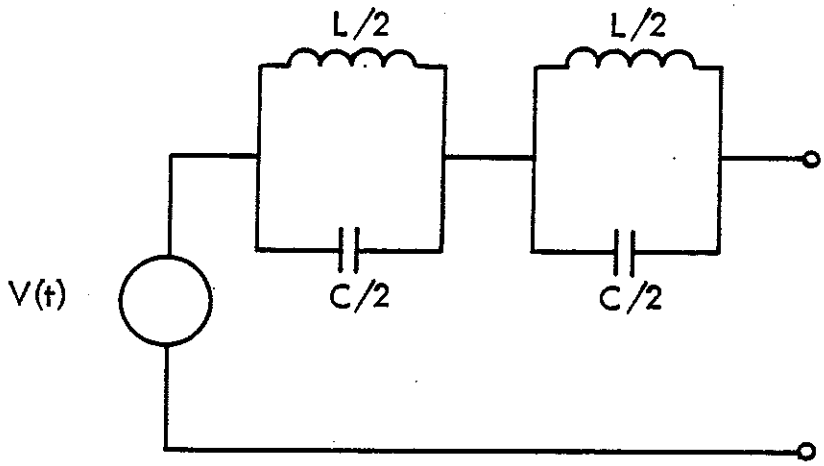

(c)

Figure 4-25. (a) Loop Area for dB/dt Threat,
(b) and (c) Equivalent Circuits for Antenna Given a dB/dt Threat

ϕ_B is the flux of B, A is the area of the loop ABCD, and dJ_s/dt is the rate of change of the component of surface current parallel to ABCD. By calculating a loop area of a proposed design, V can be calculated for the cases of rocket design considered.

Positioning antennas opposite raceways or as far removed as possible, and orienting the loop areas ABCD (Figure 4-25(a)) to minimize the intercepted flux reduces the induced voltage when using a composite designed vehicle. ABCD should be oriented perpendicular to the rockets long axis, which is generally the direction of current flow. However, for positions 90^o from a raceway the optimal orientation is not significant.

The parameters of the worst case source voltage are taken to be a sine-squared voltage pulse of 350 volts with a rise time from zero to maximum of 125 ns. (see Figure 4-22.)

Two models of source impedance shown in Figure 4-25 can be used in the calculations. A simple model (Figure 4-25(b)), used for dB/dt inputs, includes only the inductance of the loop ABCD. The model in Figure 4-25(c), used for dE/dt inputs, includes some of the distributed capacitance of a real antenna. Although responses by an antenna are not exactly represented by these simple circuit models, use of 350 volts amplitude ensures worse case answers.

RF Coupler, Transmission Lines, and Receiver Analysis

Figure 4-26 and 4-27 show the complete models which can be used to

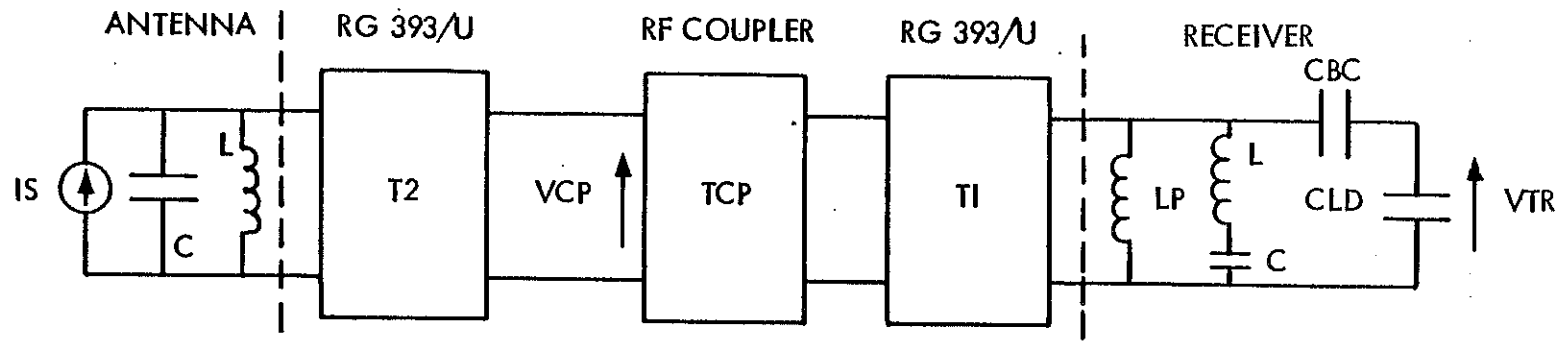

Figure 4–26. Complete Circuit for dE/dt Threat

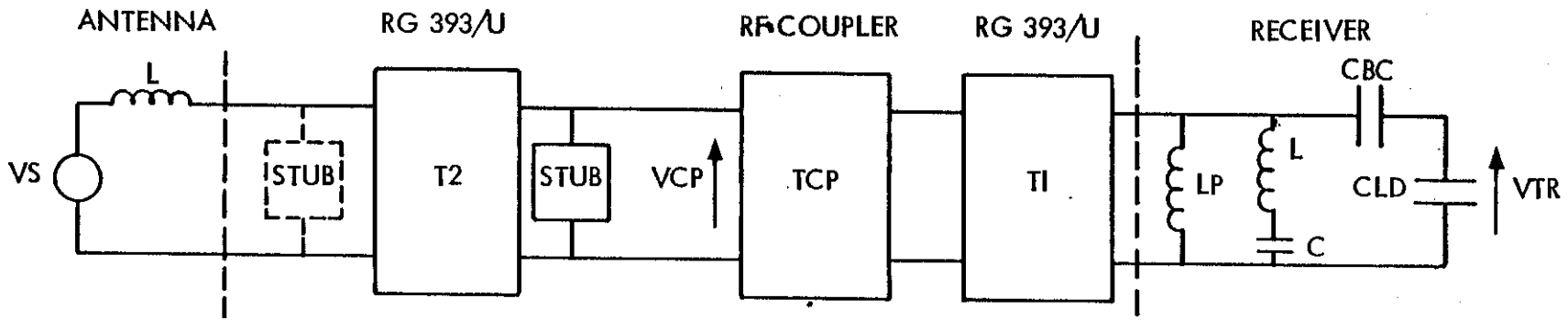

Figure 4–27. Complete Circuit for dB/dt Threat

determine the dE/dt and dB/dt induced transients for a standard receiver system. Two methods of reducing lightning effects are shown. The blocking capacitors, CBC, are shown in both casses. A quarter-wavelength stub is shown for the dB/dt threat. VCP is calculated transient voltage across the input of the coupler, and VTR is the voltage calculated across the source gate junction of the JFET.

Both the low frequency (below 30 MHz) transient levels appearing at the JFET and coupler, and the in-band power delivered to the receiver can be determined. This frequency range includes resonant frequencies of the transmission lines, as well as the major part of the lightning current spectrum. The part of the spectrum denoted as in-band is the band centered on the receiver operating frequency. Figure 4-28 shows the spectral density of a lightning strike.

Raceway Analysis For Composite Designed Rockets

For a mostly composite rocket to survive a direct lightning strike, a recaway of conductive material must be incorporated along the length of the structure to safely shunt lightning current into the exhaust plume. This lightning rod provides electromagnetic shielding and mechanical protection for the major electrical cables running the length of the vehicle.

Of fundamental concern is how the current will distribute between the raceway and the cable shields underneath. Since isolation between the inner control wires and the current floating in the shields varies with

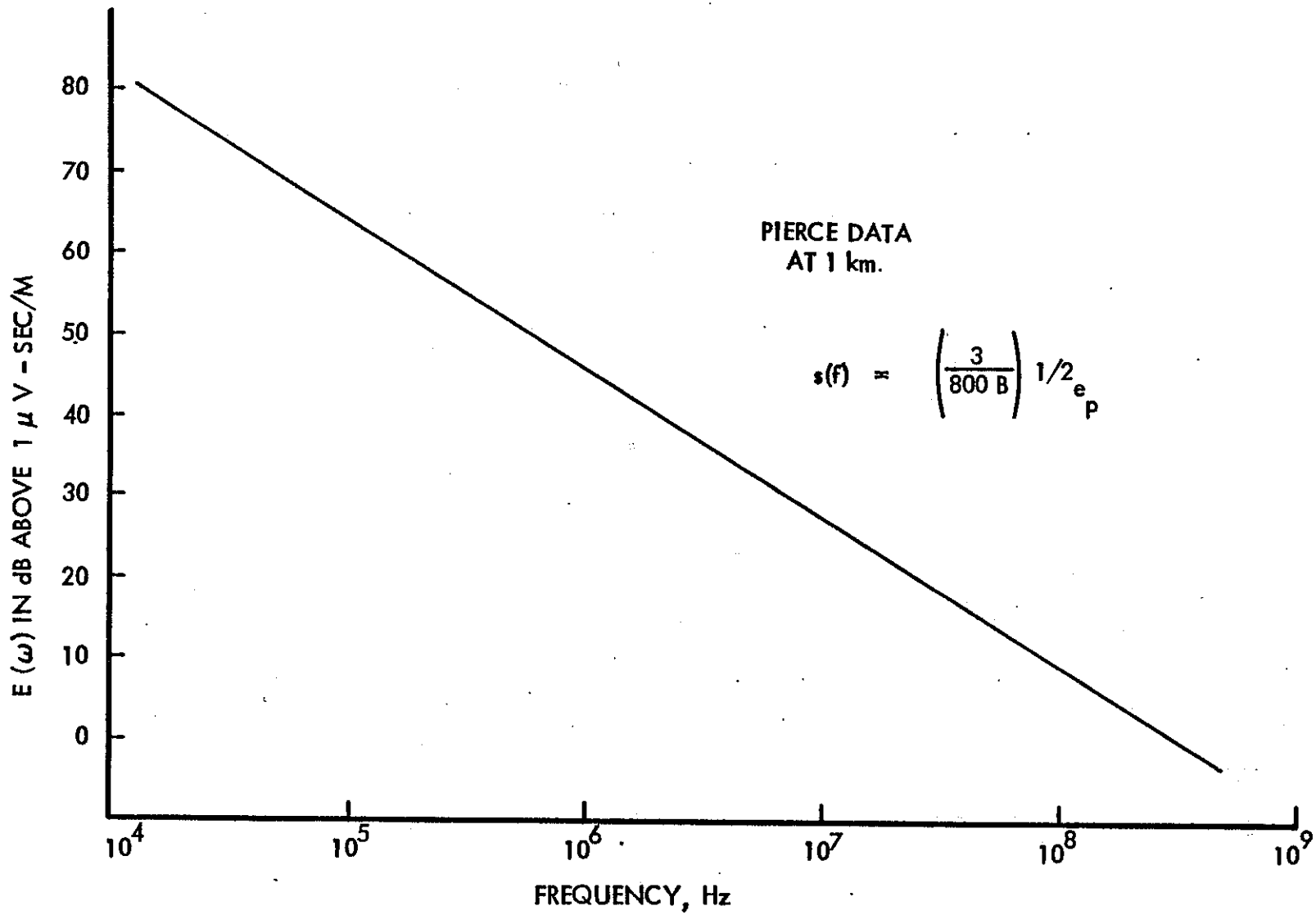

Figure 4-28. Spectral Density of Electric Field Strength Normalized to 1 km[90]

frequency, it is necessary to determine the actual frequency distribution before any affects on control signals can be analyzed. At very low frequencies, the metal resistance and contact resistance between metal parts are the important parameters affecting current division. At high frequencies the raceway inductance will be the major factor in current distribution.

Current Analysis

The raceway is designed to incorporate sections, both for ease in installation and handling, and to allow staging if required. The raceway must also allow for elongation and expansion of each stage as they are pressurized. A major problem occures in designing joints necessary to maintain good conductivity during the flight mode so arcing will not occur. Cover plates can be made electrically continuous by welding flexible bus straps across the bend joints. Base plates are often designed as a single sheet of metal, and preformed to provide a metal conduit around the inner cables. The seam between the base plate and cover plate can be closed by screws spaced evenly apart along each seam.

Another concern is the design of a low inductance current path from the raceway into the exhaust plume to provide a smooth transition for the cables and raceway currents through the aft skirt into the engine compartment. To do this, the cables and raceway should both be grounded through a low inductance, high current flexible aluminum strap to the aft polar boss. The lightning current will jump from the polar boss through the nozzle into the exhaust plume. This design philosophy makes the strap the only path lightning current will follow after flowing down the raceway.

The low frequency equivalent circuit for the entire assembly can be found by calculating the electrical resistance of each current path. When current flow is uniform, the resistances are found from the cross sectional areas of the various conducting members. At the bend joints and at aft transistions, the current flow is highly nonuniform. To estimate the resistance at transitions, the current flow can be modeled with resistance paper (teledeldos paper). The change in resistance of a uniform flow caused by the transition to a strap or bolt can then be estimated.

After the resistances of all transitions, joints, and contacts are estimated, they can be used to determine the current distribution in the major branches of the cable and raceway or other structural network. The currents and voltages can be determined using the SPICE-B general purpose circuit simulation computer program or an equivalent. The program can be eventually expanded to include the high frequency information (by adding inductances and capacitances), and information on each stage for multistage rockets until the entire rocket has been modeled.

To determine the short circuit currents or open circuit voltages induced into the control wires, it is necessary that the transfer impedance of the cables be specified as a function of frequency. The expanded SPICE model, which includes reactive values, supplies not only transfer impedance information, but can be used to examine the vehicles oscillatory response.

Oscillatory Response to The Lightning Waveform

When a lightning flash strikes the rocket structure, an oscillatory current proportional to the physical dimensions and mechanical characteristics of the vehicle occurs. The rocket will ring as a shock excited dipole rediator, heavily excited by the rapidly changing electromagnetic fields.

According to Fisher,[91] when an aircraft is struck by a lightning flash, the superimposed oscillation will be less intense because of two factors, the damping presented by the lightning channel, and the finite front time of the lightning current. This section will explain lightning induced oscillations in rockets, and a method whereby these oscillations may be determined. The exact values are not important here, but the analysis does point out one significant fact: many substantial high frequency harmonics can exist on the rocket over and above those resulting directly from the initial lightning waveform.

Surge Propagation

Consider the conductor of some finite length shown above a ground plane in Figure 4-29. The conductor has an inductance, L, per unit length, and a capacitance, C. If the conductor is sufficiently high (h) above the ground plane, L and C will have little frequency or waveshape dependence.

Surge impedance, Z, is defined as the ratio of the voltage amplitude to the current amplitude. The magnitude of the surge impedance is found from the magnitudes of the inductance and capacitance per unit length.

For most conductors, surge impedance is between 300 and 500 ohms.

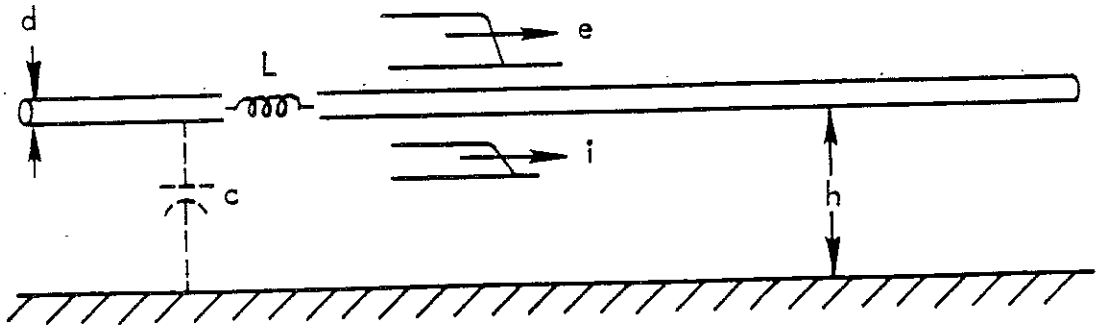

$$z = \sqrt{\frac{L}{C}} = \frac{e}{i} = 60 \ln \frac{4h}{d}$$

$$v = \frac{1}{\sqrt{LC}} = 3 \times 10^8 \text{ M/sec} \sim 1 \text{ ft/ns}$$

Figure 4-29. Conductor Voltage and Current Propagation [92]

Propagation velocity along the conductor is determined from the inductance and capacitance. For a conductor in the air, the velocity of propagation along its surface is the speed of light, about 1 foot per ns; diffused current is somewhat slower.

Consider a lightning wave that strikes a conductor similar to the nose of the rocket. The wave will travel down a conductor of one diameter (the nose) until it meets a conductor of a different diameter (a uniform cylinder), where there will be a reflection at the point of discontinuity. Figure 4-30 outlines the condition described. Figure 4-30(a) shows a single transition point in which an incident voltage E_i travels down a conductor of surge impedance Z_1 until it meets a conductor of surge

a) A SINGLE TRANSITION POINT

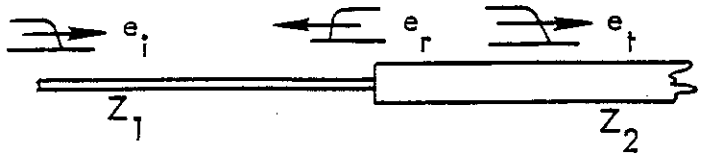

$$e_t = \alpha e_i \qquad i_t = \gamma i_1$$

$$e_r = \beta e_i \qquad i_r = \delta i_1$$

$$\alpha = \frac{2Z_2}{Z_1 + Z_2} \qquad \gamma = \frac{2Z_1}{Z_1 + Z_2}$$

$$\beta = \frac{Z_2 - Z_1}{Z_1 + Z_2} \qquad \delta = \frac{Z_1 - Z_2}{Z_1 + Z_2}$$

b) TWO TRANSITION POINTS

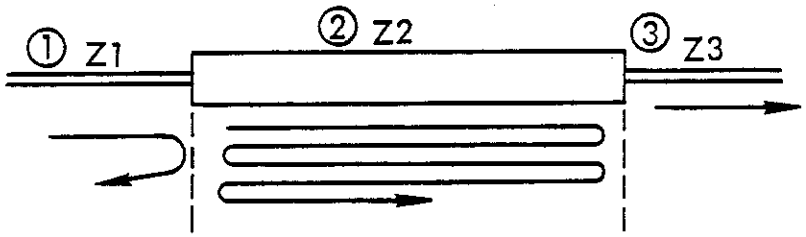

c) WAVESHAPES

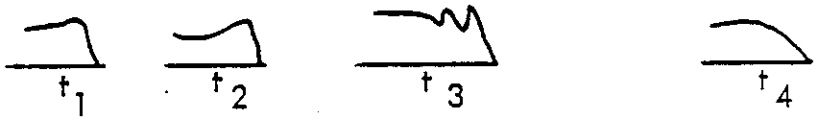

Figure 4-30. Surge Propagation at Junction Points [93]

impedance Z_2. At that point of discontinuity, a voltage wave is reflected, E_r, which travels back along the original path. A transmitted voltage, E_t, penetrates onto the conductor of surge impedance Z_2 and continues onward. Associated with each of these voltage waves is a corresponding current wave.

Each reflected or transmitted wave will have a magnitude proportional to the surge impedance magnitude of the other two conductors. Assume that the rocket receway on each stage is the same outer dimension, with only some type of a stage connector forming any discontinuities along the individual stage lengths. α, β, γ, and δ will be the transmission or reflection operators.

Figure 4-30(b) shows the condition where there is a surge impedance Z_1 coupled to a length of impedance Z_2, and then coupled to still another impedance Z_3. If there is a wave incident on this conductor system from left to right, there will be a reflection at the junction on conductors 1 and 2 with a surge transmitted onto conductor 2. This surge propagates from left to right until it meets the transition of conductors 2 and 3, where a second reflection occurs. The reflected wave travels right to left along conductor 2 until it meets the transition of conductors 1 and 2 again, where still another reflection occurs. The resulting system involves a wave oscillating back and forth along conductor 2 suffering new reflections at each end. This oscillatory wave decreases in amplitude with each new transmission and reflection, depending on the conductor surge impedance. Each additional conductor in the chain will add a new set of oscillations to each other conductor. The technique used to solve

lattice diagrams is detailed in Appendix B.

The previous description is for the case of step function voltages. We can assume the percentage of overshoot will be slightly less for the proposed lightning waveform since it is in reality a reversed sawtooth with a 240 ns time to peak pulse, and then a long fall time.

Impedance of the Lightning Channel

Knowing the surge impedances of each rocket stage is not sufficient to completely explain the oscillation phenomena. Both Fisher[94] and Wagner[95] concur that surge impedance of a lightning flash is in the order of 3,000 ohms for a return stroke of 100 kA. This value is large compared to a simple conductor in air, but reasonable considering that a lightning return stroke has a high inductance and capacitance. Solid conductors have high capacitance but low inductance per unit length.

Golde[96] determined analytically that channel surge impedance should be between 390 and 450 ohms. It can be assumed, therefore, that channel surge impedance is not a critical factor in a rocket coupling analysis.

Vehicle Transmission Line Model

Having examined the raceway current distribution and the fundamentals of oscillatory responses, a rocket can now be modeled to represent the raceway, stage rings, interstage conductive references, and nose assembly. The rocket motor plasma exhaust is modeled as a conductive rod coupled inductively and capacitively to the raceway. The analysis model of the

previous section is to be expanded to include all stages and the shroud, along with all reactive values.

As with the dc analysis, the values of the reactive components are determined by geometry. The burning rocket plasma is modeled as a conductive rod, but the exterior plume is not considered. The plume is conductive, but plume conductivity is insignificant compared to other values in this model. Self-inductances, L, and capacitances, C, for the burning plasma are determined assuming a surge impedance Z_0:

$$Z_0 \simeq \left[60 \ \ln \left(\frac{2\ell}{a}\right) - 1 \right] \text{ -ohms}$$

Propagation velocity, v, is approximately 3×10^8 m/sec. ℓ is the length, and a is the equivalent radius of the object of interest. The values of L and C are then:

$$L = Z_0/v = H/m \qquad C = 1/Z_0 v = F/m$$

For the stand-alone geometry, the inductance of each individual section of a rocket can be estimated by the rough straight-wire formula:

$$L_{wire} = 0.00508\ell \left[\ln \left(\frac{4d}{\ell} \right) - \frac{3}{4} \right] \ \mu H,$$

where ℓ is the length of the section in inches and d is the diameter in inches. The inductance of a raceway section is obtained by averaging the inductance for a straight rectangular bar:

$$L_{bar} = 0.00508\ell \left\{ \ln \left[\frac{2\ell}{b+c} \right] + 0.5 + 0.2235 \left[\frac{b+c}{\ell} \right] \right\} \mu H,$$

where ℓ is the length of the section in inches, b is the width in inches, and c is the thickness in inches. Upon finding the inductance, the

capacitance of each section can be determined from:

$$C = \left[\ell/\upsilon \right]^2 / L'$$

where L is the inductance, ℓ is the length of the section, and υ is the speed of light.

For the coaxial geometry, the capacitance and inductance per unit length are given by:

$$C_{\ell} = \frac{2\pi\epsilon_o}{\ln(b/a)}$$

and

$$L = \frac{\mu \ln(b/a)}{2\pi}$$

Where b is the radius of the outer return path conductor and a is the radius of the rocket. The inductance and capacitance of the raceway are obtained by computing the inductance and capacitance of a round wire offset in a circular cylinder. The center of the wire is offset the radius of the rocket.

The affect of impedance discontinuities at the attachment points causes reflections resulting in a transient resonant response at times greater than or equal to 1.5 μs, following the lightning current waveform. The magnitude of the transient response is dependent on the zero-to-peak rise time. For rise times greater than 500 ns, the transient response becomes unimportant, and the rocket response could be specified as following the lightning current waveform.

Physical Damage From Shockwaves

There are two primary modes whereby physical damage to the rocket structure will occur, shockwaves or dielectric breakdown. The shockwave associated with a strike will occur after the current channel is in close proximity to, but not attached to the vehicle surface. The worst case condition could take place if a strike did not attach to the nose, but bounced and attached further down. The shockwave would hit when the portion of the channel parallel to the rocket surface collapsed. The overpressure condition is similar, except it occurs when the channel is formed.

The area of concern is the effect of the shockwave or overpressure condition on external covers or sensors, and on the nosecone structure itself. Since the maximum pressure condition occurs during the transient associated with the first stroke surge, the problem is to reduce the amperage versus time (100 microseconds) plot to a value of energy per unit length of the parallel portion of the channel.

Energy per meter in the lightning channel is based in this case on the first stroke surge, and the breakdown strength of air. Figure 2-5 shows the field at which the breakdown of air occurs as a function of altitude. Since the field strength reduces significantly with altitude, the example will consider the case below 10,000 meters altitude. Troutman[97] has shown the energy per meter of channel length can be calculated as:

$$W = V \int_0^{100\ \mu s} Idt = 3 \times 10^6 (5.15) = 15.45 \times 10^6 \text{ joules/meter}$$

Assuming a 30 to 60 millimeter channel diameter, the value of the impulse and overpressure response can be calculated in Figure 4-31 and 4-32 as a function of distance from the rocket surface. As discussed previously, under swept stroke phenomena, the distance is a complex function of local geometry, nature of the surface, speed of the rocket, and lightning waveform at the time of occurrence. The relationship of Figures 4-31 and 4-32 can be expressed by the following equation.

$$I = 15585d^{-1.341}$$

where I is the Impulse (Taps) and d is the distance from the lightning channel center.

A schematic of impulsive loading on a typical cross section of a nosecone due to lightning is shown in Figure 4-33. The impulse level generated increases as the channel distance decreases, but only to a limiting distance of about 6 cm. Closer then this distance attachment will usually occur. Impulsive loading is also limited to the surface area between tangent points since shock front overpressure decreases rapidly beyond this area. The average tangent point angle for a nose section can be found from the following equation.

$$\theta_{(TP)} = \cos^{-1}\left(\frac{\bar{R}}{\bar{R} + C}\right)$$

where $\bar{R}$ is the average radius of the nosecone section and C is the perpendicular distance to the surface.

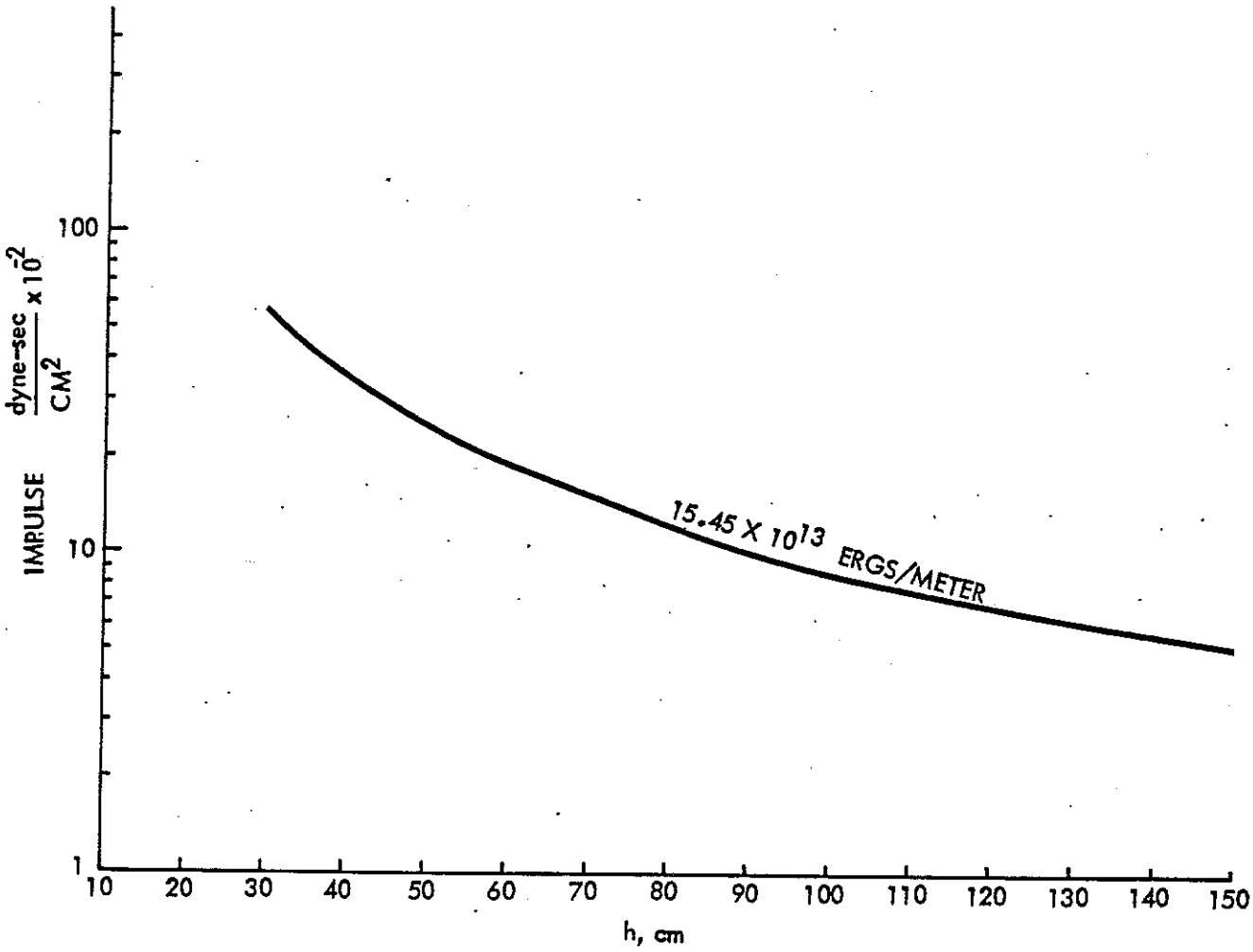

Figure 4-31. Impulse Response

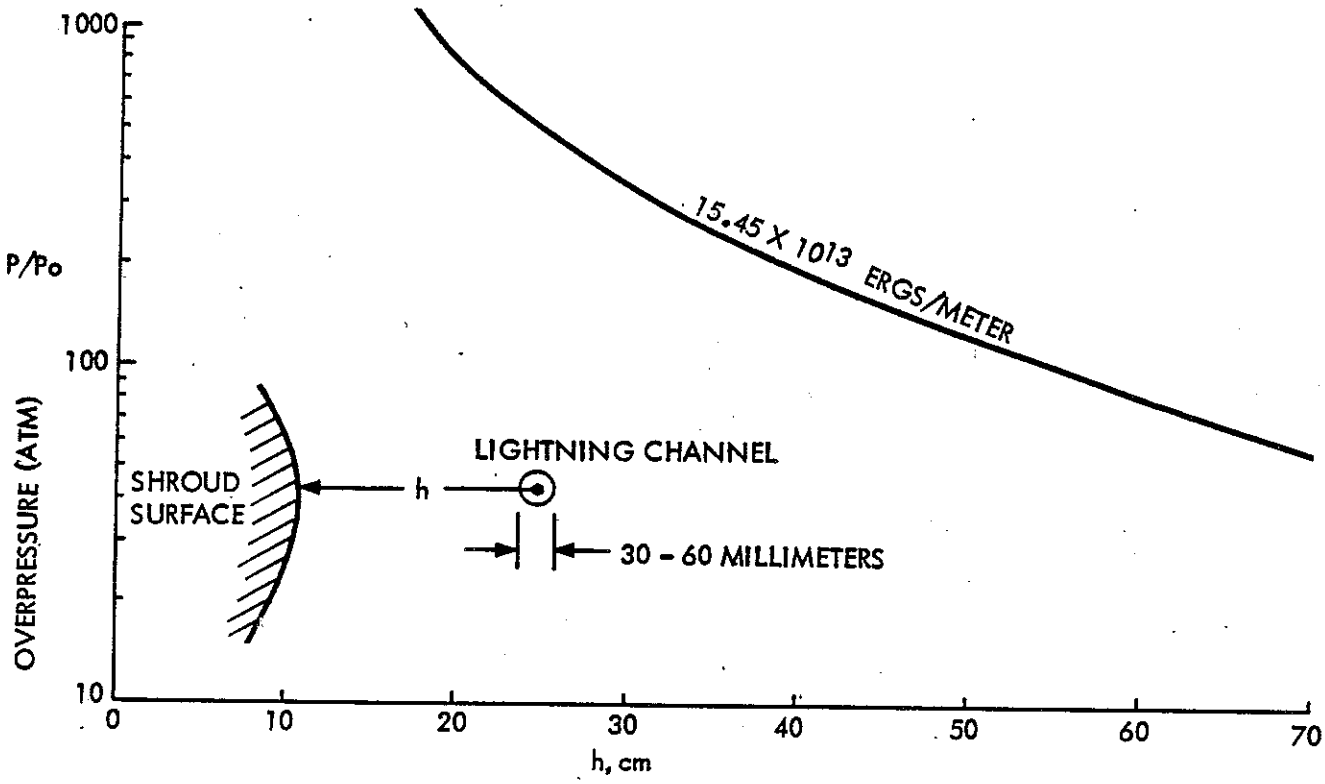

Figure 4-32. Overpressure Response

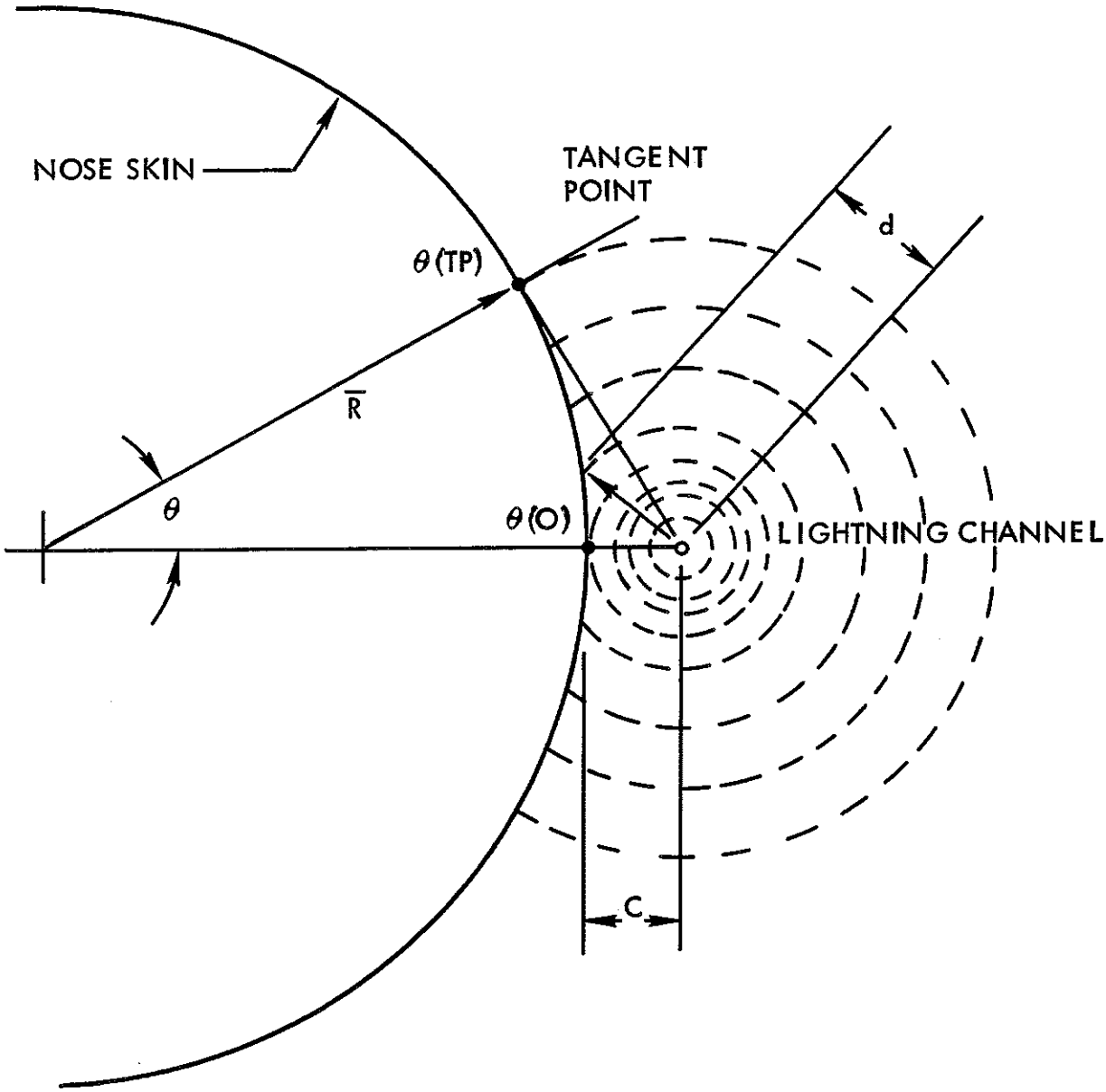

IMPULSIVE LOADING ON NOSE

Figure 4-33.

By noting the distance from the lightning channel center to any point on the nosecone surface between tangent points:

$$d = \frac{C + R(1 - \text{Cos } \theta)}{\text{Cos } \theta}$$

the equation for impulse level as a function of θ can be written as follows for this example.

$$I_{(\theta)} = 15585 \left[\frac{C + \bar{R} (1 - \text{Cos } \theta)}{\text{Cos } \theta}\right]^{-1.341}$$

Since impulsive loading due to lightning acts on a small portion of the nosecone, overall structural response is usually not a problem. However, the ability of covers or sensors located near the shockwave must still be considered. The local ability of a shell to withstand impulsive loading can be determined by the following Martin equation.[98]

$$I_{(CR)} = 2.0 \sqrt{E/\rho} \ \rho\bar{R} \ (t/\bar{R})^2$$

where $I_{(CR)}$ = Critical Impulse

E = Modulus of Elasticity

ρ = Material density

$\bar{R}$ = Average shell radius

t = Wall thickness

Bonding

The high current levels associated with a lightning discharge require

structure bonds to maintain very low impedance values. Since environmental degredation is common shen the rocket structure is exposed, some effort is required to insure good long term bonding.

The most common types of corrosion which can effect electrical bonds are the oxidation of metal surfaces, galvanic corrosion at the contact of two dissimilar metals, and the degredation by the materials used for shielding, such as acid in the adhesive.

For good long term shielding, several variables should be considered. First, it is important to use the most suitable corrosion resistant form of the metal required. The preferred electrical bond is bare metal to metal contact in most applications. If wieght is a dominant factor, such as is the case for rockets, a light metal like aluminum is required. Since metals are available in various grades, the type used should be the one most resistant to deterioration by oxidization or other probable environments in the particular application.

It is important to provide corrosion protection for the metal chosen. A large selection of surface finishes are available for most metals. If the bond surface requires contact with a Monel metal or tin-coated steel r-f gasket, tin or cadmium plated surfaces offer the best finishes. If the resistance path is critical, chromate type film treatment is often specified. Most modern films, if thin, have low resistance values immediately after application, but some increase their resistance after standing.

Dissimilar metals should not contact each other. When dissimilar metals are in contact and exposed to a corrosive atmosphere, galvanic action destroys the electromagnetic shielding and bonding characteristics. Access doors, bolt holes, and joints should be sealed by conductive gaskets or other materials of closer galvanic properties. Since an atmosphere with moisture is usually necessary for galvanic action to occure, gaskets often combine environmental and conductive characteristics. A sealant will prevent moisture from transporting the ions of the corrosion mechanism.

It is important to realize that graphite acts like a metal in promoting galvanic corrosion. Graphite is nearly as active as gold, and should definitely not be used in contact with aluminum or magnesium. The need to direct lightning current into a graphite structure via a bolt connected into the fiber's conductive orientation is often necessary. Care should be taken to select an appropriate bolt material. Also, graphite often encloses a conducting metal added to greatly increase its conductivity. Adding powdered metal to the graphite itself greatly decreases its strength. A treated metal braid is the best approach when the need for increased conductivity exists.

Lightning Effects on Conposites

In rocket design, strength, weight, and costs are major design drivers, and this has led to increased composite usage. Several candidate materials can be evaluated based on their electrical characteristics as well as other properties. The following discussion stressed the lightning related characteristics of such materials. It should be noted, however, that

electrical characteristics are often not considered a driver in graphite selection.

Nominal lightning strikes at the 95% level can contain currents as high as 100,000 amps. Streamers can have values of 100 amps, while static discharges range from 10^{-3} to 10^{-6} amps. The 100,000 amp current will penetrate a 10-ply graphite/epoxy panel, producing severe damage between the composite material and any interior conductors. A high modulus graphite/epoxy 10-ply panel can withstand this same current with no appreciable damage and can easily dissipate the static charges produced by ice, sand, or any other particles striking the rocket skin while causing no p-static interference effects. Therefore, all other requirements being equal, high modulus panels are considered prime candidates for rocket applications where the ability to conduct current is important.

Dielectric Strength For Composites and Insulating Materials

Data on dielectric strength for several nonconductive composites were compared, as was the resistivity of several conductive materials. Values ranging from 580 to 15,400 micro-ohms per centimeter were found for several fabric materials containing carbon and graphite phenolic composites.

Typical dielectric strengths for composites and insulating materials are as follows:

a) Kevlar/epoxy style 120 fabric, 48% fiber, 30 mils thick

Frequency = 10^6 Hz, dielectric constant = 4.12
Dielectric strength = 957 V/mil

Dielectric strength = 634 V/mil for 40% fiber and 125 mils thick

Dielectric constant 3.25 perpendicular and 3.67 parallel to E at 77°F and 4.05 parallel to E at 315°F

b) Fiberglass/epoxy filament wound cylinder, 30 to 80% fiber, 1.7 to 2.2 specific gravity, and 350 to 400°F heat distortion temperature

Dielectric strength = 130 to 400 V/mil

c) Molded glass phenolic composite with a 1.7 to 1.9 specific gravity range

Dielectric strength = 130 to 300 V/mil

d) Typical dielectric strength for insulating materials:

Nylon	Sp.Gr. = 1.14, D.S. = 300-400 V/mil
Polypropylene	Sp.Gr. = 0.9, D.S. = 500-600 V/mil
Nomex Aramid Paper Type 412	Sp.Gr. = 1.0, D.S. = 560 V/mil

Electrical Resistance of Panels

High modulus graphite/epoxy panels, 6-ply, 33-mil thick layups with 2-inch wide by 6-inch long gage sections were examined. Resistivity values for the basic fiber ranged from 0.8 to 5.5 x 10^{-3} ohm cm. For the high modulus graphite fibers, various industrial sources indicate values of 1.0 x 10^{-3} ohm cm for HMX and 0.7 x 10^{-3} for GY70. Values for the threshold current carrying capability of graphite/epoxy composites ranged between 37 and 64 KA/cm^2. It was also found that for antenna radiation effects above 100 MHz, graphite/epoxy performs like a metal. Table 4-3 gives tho orientation effects of graphite/epoxy panels 2"x6"x6-ply thick.

Joints and Interfaces

Rivets and metal screw fasteners will have little effect on the overall resistance of graphite/epoxy panels. Plasma spray Ni over the

Table 4-3. Orientation Effect of Graphite/Epoxy Panels

Layup	Resistance Range ohm	Current kA Range
$(\pm 45, 90)_{2S}$	0.4 to 0.35	1 to 5
$(\pm 90, 0)_{2S}$	0.35 to 0.32	1 to 5
$(90 \pm 45)_{2S}$	0.37 to 0.31	1 to 10
$(0 \pm 45)_{2S}$	0.21 to 0.18	1 to 13
$(\pm 45, 0)_{2S}$	0.25 to 0.19	1 to 7
$(0, 0, 90)_{2S}$	0.25 to 0.2	1 to 3

panel ends at interfaces will reduce or eliminate any arcing activity at jioning locations. A 2-mil Kapton film should be adequate for electrically isolating graphite/epoxy joint interfaces. Co-cured graphite/epoxy-to-graphite/epoxy joints have been able to transfer normal lightning currents without damage. However, lightning currents will arc around or through nonconducting adhesive joints. The addition of Ag or Al powder to the joint material will insure conductivity, but the adhesive bond strength is reduced, and possible corrosive action may result.

Conductivity of Composites at High Frequencies

The conductivity of graphite/epoxy composites in the fiber axis direction is ten times greater that conductivity perpendicular to the axis. Over the range from 12.5 GHz to 18 GHz, conductivity values are estimated as between 3 and 4 x 10^5 mho/m parallel, and between 0.3 and 0.4 x 10^5 mho/m perpendicular to the fiber axis. Shielding effectiveness

for graphite/epoxy cross-ply symmetric laminates were measured with the following results:

Thickness, mils	dB Loss at 1 GHz	13 GHz
40	110	200
80	190	380

Electrical Resistance for Carbon Yarns, Fabrics, and Composites

Fabrics are woven from yarns, and composites are made by either laying up fabric layers for 2D materials, or they are assembled from yarns as in 3D materials. Electrical resistance data is presented in Tables 4-4 through 4-8 for carbon and graphite yarns and fabrics, and the composites made from these yarns and fabrics.

Tables 4-7 and 4-8 list the resistance for rayon precursor graphite fabrics, and the resistance for Pitch and Pan based fabrics.

Dielectric Punch-Thru

Assuming a composite material is used in the forward portion of a rocket, the charge flow must be examined to determine if dielectric breakdown will occur. The E-field on the charged surface can be determined from the following equation.

$$E = \frac{Ps}{2\epsilon} = \frac{Q/A}{2\epsilon} \quad V/m$$

where

Ps = charge density in coul/m^2
Q = charge (coul max on surface before corona)
A = area in m^2
ϵ = dielectric constant ($\epsilon \simeq 4$ for Kevlar)

Table 4-4. Carbon and Graphite Information

Yarn	Precursor	Resistivity, ohm-cm	Modulus, Million psi
VYB	Rayon	7700	6
T-300	PAN	1700	4
AS	PAN	2000	31
HMS	PAN	1000	55
GY70	PAN	700	88

Table 4-5. Electrical Resistance for Carbon or Graphite Materials

Yarn	Precursor	Carbon or Graphite	Resistance ohm/cm
GY70	PAN	Graphite	640-1700
AU&AS	PAN	Carbon	3950-4900
HMS	PAN	Carbon	1700-2500
VYB105	Rayon	Carbon	10740-14700
GY2-1	Rayon	Graphite	7690
HM	PAN	Graphite	1490
HT	PAN	Carbon	1570-2150
PITCH	PITCH	Graphite	54-150

Table 4-6. Electrical Resistance for PAN Filament Tow

Tow	Resistance, ohms/ft
HS	12
HTS	8
HMS	6

Table 4-7. Resistance for Rayon Precursor Graphite Fabrics

Grade	Resistance in ohms per square	
	Warp	Fill
CCA-1	0.64	0.72
CCA-2	0.53	0.62
CCA-3	0.63	----
CCA-3 (HP)	0.53	----
WCA	0.39	0.53
Pluton B1 (HP)	1.7	1.7
SS2228 (Staples)	0.54	0.65

Table 4-8. Resistance for PITCH and PAN Based Fabrics

Grade	Resistance in ohms per square	
	Warp	Fill
PITCH (Continuous)	0.18	0.20
SWB-8 (PAN)	0.19	0.17
SS2271 (PAN)	0.42	0.53

Thermomechanical Effects of Lightning on Nosecone

If the 100 KAmp waveform previously proposed is evaluated for total charge transfer, it can be seen that the predicted in-flight lightning environment is about 100 coulombs. Comparing rocket attachment zones to attachment zones for aircraft, initial attachment on the nosecap (zone 1A) has a low probability of flash hang-on, as does the nose forward and mid-cone (zone 2A). Cone joints and rocket exhaust covers (zone 2B) have a high probability of flash hang-on.

The melt damage produced in zones 1A and 2A is a function of total charge transfer and dwell time. Dwell times on typical aircraft surfaces in zone 2A have been measured between 1 ms and 4 ms for unpainted aluminum and titanium structures at velocities of 35 to 240 mph.[99,100] Using the longest suggested dwell time of 4 ms, a maximum current charge transfer on the rocket nose for a single attachment is 15 coulombs. From the work of Oh and Schneider,[101] the existing hot spot data for titanium skins (a common nosecone material) indicates that a .05 inch thick structure could be heated to a temperature as high as 2400°F in zone 2A. The melting temperature of titanium is 3140°F, and that of steel is 2580°F.

Melt damage on the rocket exhaust port covers is a greater possibility because of increased dwell time. Assuming that the dwell time could embrace the full lightning strike with a total charge transfer of 100 coulombs, a small hole might be produced in the trailing edge of the cover. The work of Plumer[102] indicates that a hole produced in titanium

at an aircraft trailing edge would have a total area much less than 1 cm^2 for titanium thicknesses of .04 and greater. The most likely attachment point damage on steel or titanium exhaust port covers is estimated to be some degree of pitting around the door perimeter with no significant melt through.

Chapter 5

OFFICIAL LITERATURE

Lightning Requirement

Although rockets have been designed and used for many years, most current military documents and specifications for airborne vehicles address lightning as it relates to aircraft requirements. All major military branches and NASA are very involved in either missile or rocket programs, but little emphasis has been placed thus far on lightning documentation in the rocket field. The aim of this chapter will be to examine current military specifications in an effort to provide additional information for the majority of circuit designers who are faced with meeting military requirements in their design programs.

Current Regulations

Military specifications usually address a design requirement, and then define a test program to verify if the requirement has been satisfied. Until recently, MIL-B-5087B was the basic U.S. military specification which addressed general lightning protection and test requirements. The specification is orriented towards aircraft, but covers other military systems in general.

MIL-B-5087B also covers electrical bonding, and lightning protection for aerospace systems. Paragraph 3.3.4 titled "Class L bonding (lightning protection)(except for antenna systems)" addresses lightning protection and testing requirements. It is quoted in its entirety below.

"Lightning protection shall be provided at all possible points of entry into the aircraft, and shall be proven by test.

(a) Navigation lights
(b) Fuel filler caps
(c) Fuel gauge covers
(d) Refueling booms
(e) Fuel vents
(f) Antennas (see 6.3.1)
(g) Radomes
(h) Canopies
(i) Pitot-static booms
(j) Wiring not protected by metal or body structure

"The following bonding requirements are designed to achieve protection against lightning discharge current carried between the extremities of an airborne vehicle without risk of damaging flight controls or producing sparking or voltages within the vehicle in excess of 500 volts. These requirements are based upon a lightning current waveform of 200,000 amperes peak, a width of 5 to 10 microseconds at the 90-percent point, not less than 20 microseconds width at the 50 percent point, and a rate of rise of at least 100,000 amperes per microsecond. When flight safety is not a factor, 100,000 amperes peak with a rate-of-rise of 50,000 amperes per microsecond may be used at the discretion of the procuring activity."

Other sections of MIL-B-5087B cover lightning protection design considerations, but the paragraph quoted above was considered the standard for general lightning testing of aerospace systems according to Clifford.[103]

MIL-B-5087, dated 30 July, 1954, specified a basic peak current of 100,000 amperes, but the value was raised to 200,000 when the "B" version

was released in 1964. The 200,000 ampere value has been used in recent documents and is now considered to be at the 99 percentile level (one percent of all strikes are higher than 200,000 amps).[104]

MIL-STD 1541 (USAF) is the military standard which addresses electromagnetic compatibility (EMC) requirements for space systems. This document references 5087B in paragraph 4.6.3.2 quoted below.

"4.6.3.2 Lightning and arc-discharge protection. To prevent damage to vehicle and ground equipment from the effects of lightning strokes or arc-discharges, protection by bonding shall be provided for the complete vehicle and all external electrically conducting objects. Typical lightning stroke characteristics are defined in MIL-B-5087. Typical arc-discharges induced by space-plasma charging effects on space vehicles can have a rise time of 15 nanosecond (ns), a duration of 40 ns, and produce peak field intensities up to 1,200 volts/meter (V/m) at a distance of 30 centimeters (cm) from the discharge."
Other sections of the document include design information for the prevention of electrostatic charging, case shielding, and surface finishes.

Technical Report ET-77-9, published by the US Army Missile Research and Development Command, titled "High Level Electromagnetic (EM) Environmental Criteria for US Army Missile Systems," presents the design and test requirements needed to develop an electromagnetic hard missile system for the Army. Both direct strike and indirect (close) lightning are addressed. The document defines indirect effects as lightning electromagnetic pulse (LEMP) criteria. Testing is covered in chapter V.

There are several documents which address bonding, shielding, or grounding designs in general terms, and others which identify general EMC or Electromagnetic Pulse (EMP) design and test requirements. Unfortunately, much EMP related information is contained in classified documentation, and many organizations tend to incorporate both lightning and EMP theory in the same literature. MIL-STD 1857 is an Army EMC design practices document, and MIL-STD 461B and MIL-STD 462 are general service EMC documents. There are also a few documents which cover special equipment tests: FAA Advisory Circular AC20-53, Military Specification MIL-F-3836B, and Military Specification MIL-C-38373 concern the protection and testing of aircraft fuel systems against lightning. MIL-A-9094D specifies strenuous simulation tests of lightning arrestors which are to be used with radio receiving and transmitting antenna systems. The arrestor is used by both the Air Force and by the Naval Air Systems Command.

MIL-STD 1757 was released in June 1980. This document, titled "Lightning Qualification Test Techniques for Aerospace Vehicles and Hardware" is the result of a major effort by industry and military leaders to standardize the lightning qualification procedure. It is currently used by all Department of Defense agencies.

MIL-STD 1757 is a test document only, and does not address design criteria. It presents a set of standard test waveforms and techniques, at both vehicle and hardware box levels, to examine the direct effects of lightning. Indirect effects are not covered at present. The document

is written so tailoring can be provided for specific programs.

Other Related Documents

The Air Force's DH 1-4, although not considered a requirements document, contains a significant amount of lightning information in Chapter 7. The document primarily deals with aircraft protection techniques. However, some information is directly applicable to rocket design.

Chapter 7 is organized into six sections. General information on strike phenomena, preventive design, and damage experience is extreemly useful to all designers. Radome protection is discussed in 7A6 for aircraft applications. The remainder of the document deals with electromagnetic compatibility. Figure 5-1, shown on the next page, is a design checklist from DH 1-4.

It is suggested that the reader contact "The Lightning Flash", published by Lightning Technologies, Inc., 560 Hubbard Avenue, Pittsfield, MA 01201, if additional information on current publications is required. Lightning is a fast moving field, and a considerable volume of new information is published or contributed each year. This magazine is a good continuing source of new ideas in the lightning field.

SUB-NOTE 20(1) Guidance for Airborne System Protection

1. Do radomes have adequately tested diverter strips?
2. Does radome have conductive coating on outside surfaces?
3. Has attachment hardware for radome been tested?
4. Have electrical bonding provisions for radome been tested, and have quality controls been established?
5. Have protective devices and shielding been effectively used on wiring under radome?
6. Has a pressure relief been designed into radome in event wiring or components are vaporized?
7. Have metallic protection strips been installed on canopies to protect crew?
8. Have protection strips been tested for lightning current capacility and to ensure the ejection is not degraded?
9. Has electrical bonding of canopy protection been adequately tested?
10. Does canopy have an adequately high puncture voltage?
11. Have applied corrosion control techniques been tested to be lightning-compatible?
12. Have lightning-protected fuel tank caps been used?
13. When "wet wing" fuel tanks are used, is metallic skin thickness adequate for lightning currents?
14. Have bonding jumpers been used to obtain electrical continuity around sealed fuel tank joints?
15. Have external fuel tanks been designed with adequate and properly tested protection?
16. Have MS25083 (or equivalent) bonding jumpers been used where required for lightning protection?
17. Have bonding jumpers been installed so that they cannot be exposed to a direct arc?
18. Have MIL-A-9094 (or equivalent) arrestors been used for each antenna (including UHF)?
19. Has secondary protection been installed to eliminate the inherent 10,000-volt spike from MIL-A-9094 or equivalent arrestors?
20. Has all electrical wiring that extends outside of the skin been protected with spark gaps or other protective devices?
21. Has all wiring going into fuel tanks been adequately electrically isolated, shielded, and physically separated from wiring which might carry induced energy from lightning strike?
22. Have fuel vents and ejection mechanisms (dumps) been tested for electrical conductivity and installed at safe locations?
23. Have all control surfaces and hinges had bonding jumpers installed or tests run to prove jumpers are not needed?
24. Have diverter rods or other protection been provided for external stores?
25. Has the air intake for jet engines been tested against the blast effect of lightning strikes?
26. Have all crew stations been tested to verify that the crew cannot be subjected to hazardous induced energies?
27. Have rotor blades and associated controls been tested to demonstrate safety?
28. Have all nonmetallic structures been tested to demonstrate flight safety? (No flights should be accomplished until this testing has been satisfactorily completed.)

5 JAN 76

DH 1-4 Design Checklist

Figure 5-1

FOOTNOTES

FOOTNOTES

[1]M. Brook, C. R. Holms, and C. B. Moore, Lightning and Rockets: Some Implications of the Apollo 12 Lightning Event, p.1.

[2]Ibid, p.2.

[3]R. F. Harrington, Time Harmonic Electric Fields, Chapter 6.

[4]G. N. Watson, A Treatise on the Theory of Bessel Functions, p.76.

[5]G. Bedrosian and K. H. Lee, Diffusive Electro-Magnetic Penetration into Metallic Enclosures, p.194-198.

[6]G. A. DuBro, et al., Atmospheric Electricity-Aircraft Interaction, AGARD Lecture Series, p.2-10.

[7]T. E. James and J. Phillpott, Simulation of Lightning Strikes to Aircraft.

[8]G. A. DuBro, et al., p.2-14.

[9]C. E. Brooks, The Distribution of Thunderstorms Over the Globe, Vol. 24, p.147-164.

[10]M. A. Uman, Understanding Lightning, p.56.

[11]N. Cianos and E. T. Pierce, A Ground-Lightning Environment for Engineering Usage, p.5-6.

[12]R. G. Fleagle, The Audibility of Thunder, p.411.

[13]A. S. Dennis, Lightning Observations from Satellites.

[14]N. Cianos and E. T. Pierce, p.7.

[15]Ibid, p.7.

[16]A. S. Dennis.

[17]N. Cianos and E. T. Pierce, p.13.

[18]E. T. Pierce, Latitudinal Variation of Lightning Parameters, p.194-195.

[19]G. A. DuBro, et al., p.3-5.

[20] M. A. Uman, Understanding Lightning, p.56.

[21] D. W. Clifford, Another Look at Aircraft Triggered Lightning.

[22] D. R. Fitzgerald, Probable Aircraft Triggering of Lightning in Certain Thunderstorms, p.835.

[23] M. M. Newman, et al., Triggered Lightning Strokes at Very Close Range, p.4761.

[24] R. P. Fieux, et al., Research on Artificially-Triggered Lightning in France, p.725-733.

[25] D. W. Clifford, p.2.

[26] F. A. Fisher and J. A. Plumer, Lightning Protection of Aircraft.

[27] D. W. Clifford, p.3.

[28] Ibid.

[29] H. T. Harrison, UAL Turbojet Experience With Electrical Discharges.

[30] O. K. Trunov, Conditions of Lightning Strike on Air Transports and Certain General Lightning Protection Requirements.

[31] D. W. Clifford, p.20-1.

[32] J. E. Nanevicz, Static Electricity Phenomena: Theory and Problems.

[33] D. W. Clifford, p.7.

[34] O. K. Trunov, p.6.

[35] J. E. Nanevicz.

[36] O. K. Trunov.

[37] D. W. Clifford, p.11.

[38] J. F. Shaeffer, Aircraft Initiation of Lightning.

[39] R. F. Griffiths, The Initiation of Corona Discharges from Charged Ice Particles in a Strong Electric Field, p.3-13.

[40]G. A. DuBro, et al., p.3-3 - 3-5.

[41]D. W. Clifford, p.17.

[42]J. F. Shaeffer.

[43]D. W. Clifford, p.2-3.

[44]M. A. Uman, Understanding Lightning, p.65.

[45]F. A. Fisher, Analysis of Lightning Current Waveforms Through the Space Shuttle.

[46]D. J. Milan, Physics of Lightning, p.68-75.

[47]J. Osborn and D. Gonshor, ITP Test 20-T7 Final Report.

[48]R. R. Goulette and K. E. Felske, Electromagnetic Field Mapping of Cylinder and Missile Nosecone.

[49]N. Cianos and E. T. Pierce.

[50]M. A. Uman, Lightning.

[51]R. H. Golde (editor), Lightning.

[52]N. Cianos and E. T. Pierce, p.62.

[53]Ibid, p.88.

[54]Ibid, p.83.

[55]M. A. Uman, Lightning.

[56]C. R. Bruce and R. H. Golde, The Lightning Discharge, p.487.

[57]N. Cianos and E. T. Pierce, p.58.

[58]Ibid, p.45.

[59]Ibid, p.46.

[60]R. J. Fisher and M. A. Uman, Measured Electric Field Risetimes for First and Subsequent Lightning Return Strokes, p.399.

[61]N. Cianos and E. T. Pierce, p.34.

[62]Ibid, p.36.

[63]Conversation with E. P. Krider, University of NM., 6 March 1980.

[64]M. A. Uman, Understanding Lightning, p.43.

[65]N. Cianos and E. T. Pierce, p.37

[66]Ibid, p.35.

[67]Ibid, p.105.

[68]N. Cianos and E. T. Pierce, p.64.

[69]Electromagnetic Compatibility, AFSC Design Handbook DH1-4, 5 January 1977.

[70]Allegheny Ludlum Steel Corp., Magnetic Shielding Electrical Materials.

[71]R. M. Searing, High and Low Frequency EM Penetration of Lossy Dielectric Cylinders.

[72]R. O. McCary, Effects of Extensive Field on Switch Core, p.2.

[73]R. R. Goulette and K. E. Felske, Electromagnetic Field Mapping of Cylinder and Missile Nosecone.

[74]F. A. M. Rizk, Low Frequency Shielding Effectiveness of a Double Cylinder Enclosure, p.14-21.

[75]G. Bedrosian and K. H. Lee, p.194-198.

[76]Chromerics, EMI/RFI Gasket Design Manual, p.53.

[77]G. Bedrosian and K. H. Lee, p. 194-198.

[78]F.A.M. Rizk, p. 14-21.

[79]B. C. Gabrielson, Transfer Impedance Usage in Lightning Current.

[80]E. F. Vance, Shielding Effectiveness of Braided Wire Shields,p.71-77.

[81]Ibid.

[82]Ibid.

[83]E. F. Vance, Coupling to Shielded Cables, p.108-176.

[84]E. F. Vance, Prediction of Transients in Buried, Shielded Cables, p.29.

[85]E. F. Vance, Coupling to Shielding Cables, p.108-176.

[86]Integrated Circuit Electromagnetic Susceptibility Handbook.

[87]M. Smith and P. Mohrback, R. F. Hazards Evaluation Laboratory Testing.

[88]B. Yoda and K. Maraki, Development of EHV Cross-Linked Polyethylene Insulated Power Cables.

[89]Electromagnetic Pulse Handboook for Missiles and Aircraft in Flight, p.133.

[90]E. T. Pierce, Lightning, p.356.

[91]F. A. Fisher, p.1.

[92]Ibid, Figure 3.

[93]Ibid, p.2.

[94]Ibid, p.7-10

[95]C. F. Wagner and A. R. Hileman, Surge Impedance and its Application to the Lightning Stroke, p.1011-1022.

[96]R. H. Golde, ed.

[97]W. W. Troutman, Numerical Calculation of Pressure Pulse From a Lightning Stroke.

[98]Martin Marietta, Dynamic Buckling of Thin-Walled Ring Stiffened Conical Shroud of Variable Diameter Subject to Highly Impulsive Asymmetrical Pressures.

[99]R. O. Brick, L. L. Oh, and S. D. Schneider, The Effects of Lightning Attachment Phenomena on Aircraft Design.

[100] J. A. Plumer, Lightning Effects on General Aviation Aircraft

[101] L. L. Oh and S. D. Schneider, Lightning Strike Performance of Thin Metal Skin.

[102] J. A. Plumer, Guidelines for Lightning Protection of General Aviation Aircraft.

[103] D. W. Clifford, Lightning Test Criteria for Aircraft Avionics Systems, p.2.

[104] Ibid, p.3.

BIBLIOGRAPHY

BIBLIOGRAPHY

AFSC Design Handbook DH1-4, Electromagnetic Compatibility, Third Edition, Rev. 6, 5 July 1979.

Bedrosian, G. and K. H. Lee, Diffusive Electro-Magnetic Penetration into Metallic Enclosures, IEEE Transactions, Antenna Propagation, Vol. AP 27, March 1979.

Bogner, R. E., and A. G. Constantinides, Introduction to Digital Filtering, John Wiley and Sons, 1975.

Brick, R. O., Oh, L. L., and Schneider, S. D., The Effects of Lightning Attachment Phenomena on Aircraft Design, 1970 Lightning and Static Electricity Conference, 9-11 December, sponsored jointly by the Air Force Avionics Laboratory and the Society of Automotive Engineers, Air Force Systems Command, Wright-Patterson Air Force Base, Ohio, December 1970.

Brook, M., C. R. Holms, and C. G. Moore, Lightning and Rockets: Some Implications of the Apollo 12 Lightning Event, Naval Research Reviews, April 1970.

Brooks, C. E. P., The Distribution of Thunderstorms Over the Globe, Vol 24, Geophysics Mem., London 1925.

Clamers, J. A., Atmospheric Electricity, Oxford: Pergamon Press, 1967.

Cianos, N. and E. T. Pierce, A Ground-Lightning Environment for Engineering Usage, Stanford Research Institute, Menlo Park, CA, August 1972.

Clifford, D. W., Another Look at Aircraft Triggered Lightning, McDonnell Aircraft Company, St. Louis, MO, April 1980.

Clifford, D. W., Lightning Test Criteria for Aircraft Avionics Systems, McDonnell Aircraft Company, St. Louis, MO, June 1980.

Dennis, A. S., Lightning Observations from Satellites, Final Report, Contract NASr-49(18), Stanford Research Institute, Menlo Park, California, December 1964.

DuBro, G. A., et al, Atmospheric Electricity-Aircraft Interaction, AGARD Lecture Series, North Atlantic Treaty Organization, June 1980.

Dynamic Buckling of Thin-Walled Ring Stiffened Conical Shroud of Variable Diameter Subject to Highly Impulsive Asymmetrical Pressures, SE-0033, Martin Marietta Company, Denver, CO, November 1979.

Electromagnetic Pulse Handbook for Missiles and Aircraft in Flight, Sandia Laboratories, September 1972.

FAA Advisory Circular No. 20-53, Protection of Aircraft Fuel Systems Against Lightning, October 1967.

Felske, K. E. and R. R. Goulette, Electromagnetic Field Mapping of Cylinder and Missile Nosecone, Bell-Northern Research, RADC-TR-81-179, Ottawa, Canada, July 1981.

Fieux, R. P., et al, Research on Artificially-Triggered Lightning in France, IEEE Transactions on Power Apparatus and Systems, Vol. PAS-97, No. 3, May-June 1978.

Fisher, F. A., Analysis of Lightning Current Waveforms Through the Space Shuttle, Aircraft Lightning Protection Note 75-1, General Electric Company, Pittsfield, MA, January 1975.

Fisher, F. A. and J. A. Plumer, Lightning Protection of Aircraft, NASA Reference Publication 1008, October 1977.

Fisher, F. J. and M. A. Uman, Measured Electric Field Risetimes for First and Subsequent Lightning Return Strokes, Journal of Geophysical Research, Vol. 77, No. 3, 1972

Fitzgerald, D. R., Probable Aircraft Triggering of Lightning in Certain Thunderstorms, Monthly Weather Review, Vol. 95, 1967

Fleagle, R. G., The Audibility of Thunder, Journal of the Acoustic Society of America, Vol. 21, 1949.

Golde, R. H. (editor), Lightning, Vols. 1 and 2, Academic Press, London, York, 1977.

Griffiths, R. F., The Initiation of Corona Discharges from Charged Ice Particles in a Strong Electric Field, Journal of Electrostatics, Vol. 1, 1975, pp.3-13.

Harrington, R. F., Time Harmonic Electric Field, McGraw Hill, New York, 1961

Harrison, H. T., UAL Turbojet Experience with Electrical Discharges, UAL Meteorology Circular No. 57, January 1967.

Integrated Circuit Electromagnetic Susceptibility Handbook, MDC Report E1999, McDonnell Douglas Astronautics Company, St. Louis, MO, 5 January 1979.

James, T. E. and J. Phillpott, Simulation of Lightning Strikes to Aircraft, Culham Laboratory Report CLM-R111, Abingdon, Oxfordshire, U.K., 1971.

Kraus, J. D., Antennas, McGraw-Hill, New York, 1950.

Lightning Test Waveforms and Techniques for Aerospace Vehicles and Hardware, Society of Automotive Engineers, Warrendale, Pennsylvania, 5 May 1976.

Malan, D. J., Physics of Lightning, The English Universities Press, Ltd., London, 1963.

McCary, R. O., Effects of Extensive Field on Switch Core, General Electric CRD, Philadelphia, PA, June 1976.

Muhleisen, R. P., Phenomenology of Lightning/Aircraft Interaction, AGARD Conference on Atmospheric Electricity, Menlo Park, CA, June 1980.

Muller, E., H. Steinbigler and J. Weisinger, On the Numerical Calculations of Induced Voltages Surfaces Neighboring Lightning Conductors, edited translation by Foreign Technology Division, Wright-Patterson Air Force Base, September 1977.

Nanevicz, J. E., Static Electricity Phenomena: Theory and Problems, Conference on Certification of Aircraft for Lightning and Atmospheric Electricity Hazards, ONERA-Chatillon, France, September 1978.

Newman, M. M., et al, Triggered Lightning Strokes at Very Close Range, Journal of Geophysical Research, Vol. 72, pp. 4761, 1967.

Nussbaum, A., Electromagnetic Theory for Engineers and Scientists, Prentice-Hall, 1965.

Oh, L. L. and Schneider, S. D., Lightning Strike Performance of Thin Metal Skin, Session III: Structures and Materials, Proceedings of the 1975 Conference on Lightning and Static Electricity, 14-17 April 1975, at Culham Laborator, England, the Royal Aeronautical Society of London, 1975.

Osburn, J. D., et al, ITP Test 20-T7 Final Report, Martin Marietta Corporation, Denver, CO, December 1981.

Pearlston, C. B., Case and Cable Shielding, Bonding, and Grounding Considerations in Electromagnetic Interference, IRE Transactions on RFI, October 1962.

Pierce, E. T., H. R. Arnold and A. S. Dennis, Very Low Frequency Atmospheric Due to Lightning Flashes, Final Report, Contract AF33(657)-7009, Stanford Research Institute, Menlo Park, California, July 1962.

Pierce, E. T., Latitudinal Variation of Lightning Parameters, Journal of Applied Meteorology, Vol. 9, 1970.

Pierce, E. T., Lightning, Academic Press, New York, 1977.

Pierce, E. T., Lightning Discharges to Tall Structures, EOS, Vol. 51, No. 4, April 1970.

Plumer, J. A., Guidelines for Lightning Protection of General Aviation Aircraft, FAA-RD-73-98, Federal Aviation Administration, Department of Transportion, Washington, D.C., October 1973.

Plumer, J. A., Lightning Effects on General Aviation Aircraft, FAA-RD-73-99, Federal Aviation Administration, Department of Transportation, Washington, D. C., October 1973.

Rizk, F. A. M., Low Frequency Shielding Effectiveness of a Double Cylinder Enclosure, IEEE Transactions, Electromagnetic Compatibility, Vol. EMC-19, No. 1, February 1977.

Schelkunoff, S. A., The Electromagnetic Theory of Coaxial Transmission Lines and Cylindrical Shields, Bell Laboratories Technical Journal, Vol. 3, Whippany, NJ, October 1934.

Searing, R. M., High and Low Frequency EM Penetration of Lossy Dielectric Cylinders, R-I, Autonetics Division, 80-278-066-EM-197, Anaheim, CA, 10 October 1960.

Shaeffer, J. F., Aircraft Initiation of Lightning, 1972 Lightning and Static Electricity Conference, USAF Report AFAL-TR-72-325, December 1972.

Smith, M. and P. Mohrbach, RF Hazards Evaluation Laboratory Testing, TSR-B2344-1, Franklin Institute, Philadelphia, PA, July 1966.

Sparling, R. H., Seven Rules for Long Term RFI Shielding, The Electronic Engineer, October 1967.

Troutman, W. W., Numerical Calculation of Pressure Pulse From a Lightning Stroke, Journal of Geophysical Research, Vol. 74, No. 18, August 1969.

Trunov, O. K., Conditions of Lightning Strike on Air Transports and Certain General Lightning Protection Requirements, 1975 Lightning and Static Electricity Conference, Culham Laboratory, England, April 1975.

Uman, M. A., Lightning, McGraw-Hill, New York, 1969.

Uman, M. A., Understanding Lightning, Bek Technical Publications, Carnegie, PA, 1971.

Vance, E. F., Coupling to Shielded Cables, John Wiley and Sons, 1978.

Vance, E. F., Prediction of Transients in Buried, Shielded Cables, Technical Report, Stanford Research Institute, Menlo Park, CA, 14 March 1973.

Vance, E. F., Shielding Effectiveness of Braided Wire Shields, IEEE Transactions Electromagnetic Compatibility, Vol. EMC-17, No. 2, May 1975.

Wagner, C. F. and A. R. Hileman, Surge Impedance and Its Application to the Lightning Stroke, Transactions of AIEE, Part III, Power Apparatus and Systems, February 1962.

Watson, G. N., A Treatise on the Theory of Bessel Functions, Cambridge University Press, London, 1961.

Yoda, B. and K. Muraki, Development of EHV Cross-Linked Polyethylene Insulated Power Cables, IEEE Power System Conference on Underground Transmission, Pittsburg, PA, May 1972.

APPENDIX A

Appendix A

The BLM Lightning Monitoring System

This information is a summary of an interview of Mr. Duane Herman, the lightning operations program manager for the BLM office at the Interagency Fire Center in Boise, Idaho, during May 1980. The interview reviewed the BLM lightning monitoring and measuring system reported in "An Automatic Locating System for Cloud-to-Ground Lightning," by E. Philip Krider, A. E. Pifer, and Martin A. Uman. This system, covering most western states, detects and locates lightning within about a 300 mile range with an accuracy capability within a mile or two, and is used for fire detection.

The direction finding (DF) equipment used has incorporated electronics that differentiate local interference and the field waveshapes that are characteristic of lightning return strokes. The lightning field characteristics that must be satisfied are rise time, width, and subsidiary peak structure. The amplitude and direction data from each DF site are used in the triangulation process as the information is fed from 2, 3, or 4 DF stations to a position analyzer. The position snalyzer is a preprogrammed microcomputer that computes maps and records lightning strikes. Unfortunately, the BLM does not use the amplitude data in their program.

The output of this program enables a more accurate assessment of the real lightning threat than previously anticipated by thunderstorm day information. A typical lightning flash map was presented by Dr. Krider and is shown in Figure A-1. Figure A-2 was recorded as part of

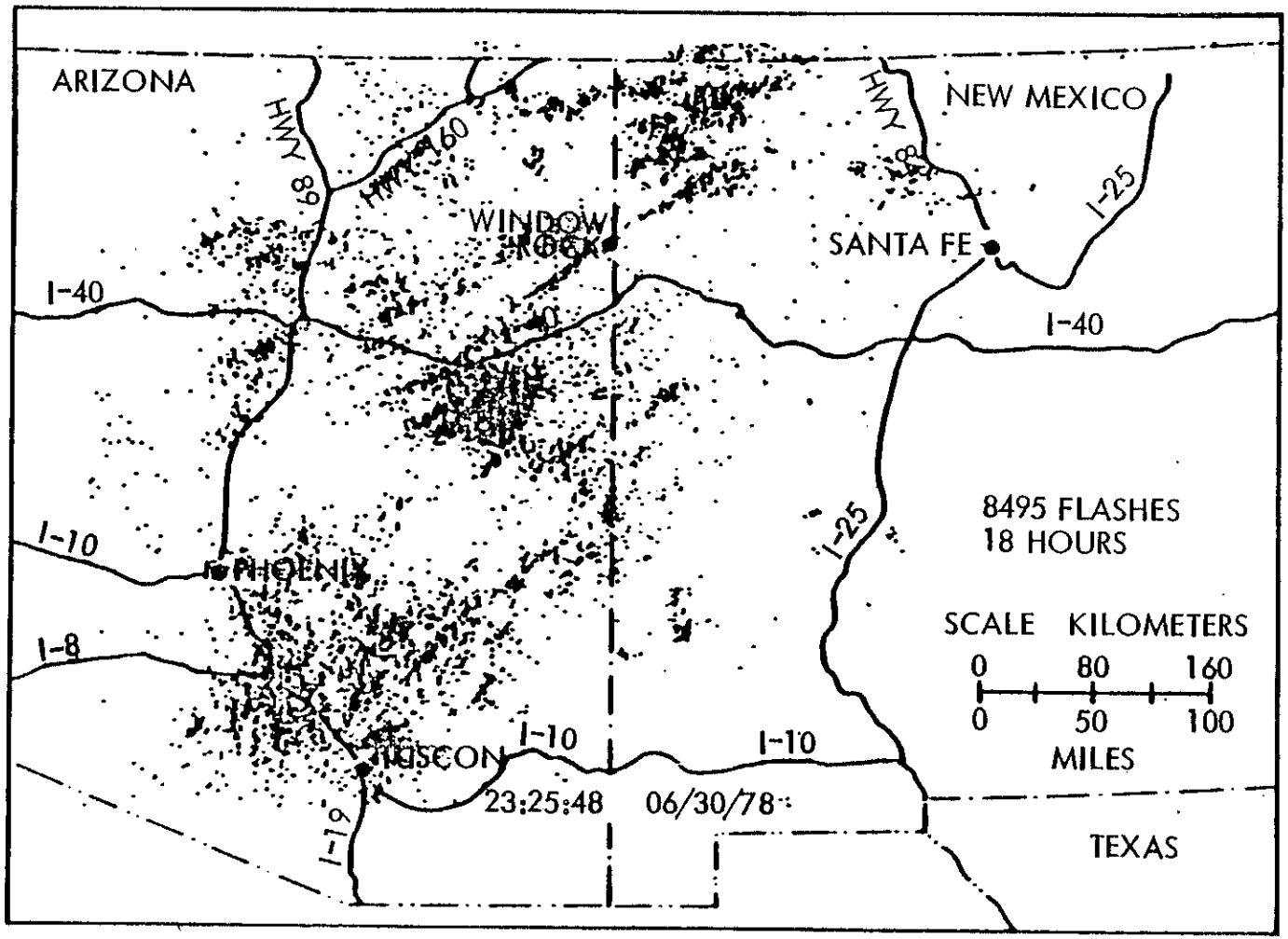

A Lightning Map; The Location of Each Flash is Plotted as a Small Dot

Figure A-1

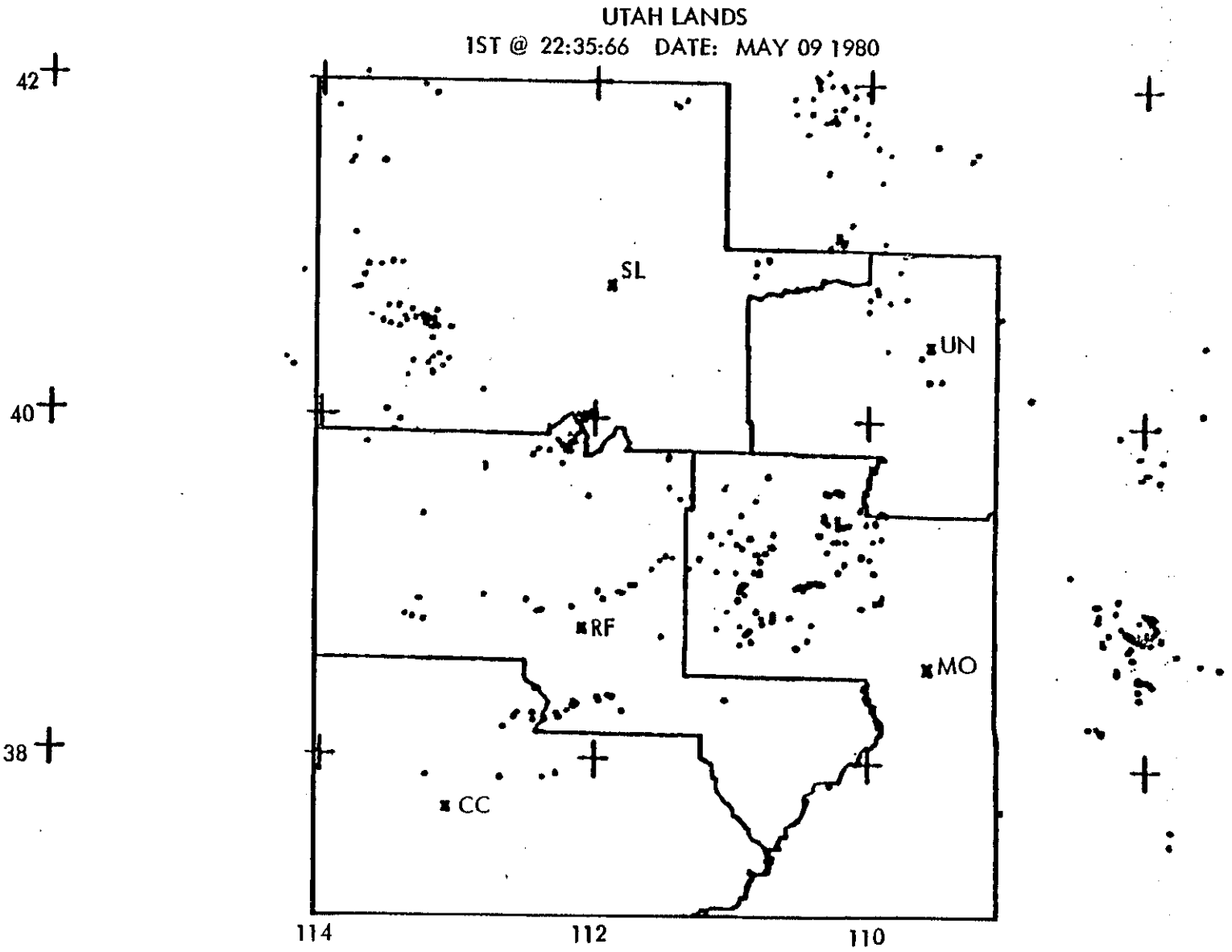

Grand Junction Position Analyzer

Figure A-2

the checkout of the Grand Junction position analyzer on May 9, 1980.

Figure A-3 is a sequential real time recording of 300 lightning flashes basically in remote parts of Colorado. The significance of this data is that the flash activity recorded as a cloud to ground discharge occurred during a snow storm. This would not have been recorded as a thunderstorm day.

Rockets are affected by cloud-to-ground, intra- and intercloud, and triggered lightning flashes. Only cloud-to-ground flashes are recorded by the BLM system. However, it appears that the natural cloud-to-ground thunderstorm day data base can be greatly improved by using the data that would be available via the fielded BLM system.

The following is a summary of the BLM system and its possibilities:

1) The BLM does not have an adequate archiving system.

2) BLM works in "real-time" and presently does not accumulate the scientific data.

3) BLM operates only 4 to 6 months per year. They normally have 1 one-shift operation (8-hour day) even though the equipment is capable of 24-hour per day operation with high reliability and high MTBF experience - one electronic failure at a DF in the 1979 season.

4) BLM personnel familiar with the software and hardware feel that with only minor software modifications the amplitude of each stroke could be determined and recorded.

5) The position analyzers that provide information are located at Grand Junction, Colorado; Elko, Nevada; Las Vegas, Nevada; and Suanville, California. Figure A-4 shows the area of coverage for the Las Vegas net.

6) The thunderstorm day information is based on two types of data:

   a) Thunder is heard by an observer;

   b) The observer reports it.

   These are fairly reliable criteria for inhabited areas. However, the results in desert and mountain areas are reported infrequently as the hearing range is approximately 15 miles and the observers are limited in number. The number of lightning flashes measured in desert areas is estimated by the BLM project manager to be 10 to 100 times greater than that anticipated by the thunderstorm day criteria.

7) Lightning strokes occur in many desert and mountain areas that lack trees and brush. Because there is little or no flammable material, the BLM firefighters have no interest in such areas.

8) Current BML equipment would need to be modified to assess inter- and intracloud flashes as an ancillary function. (The equipment is presently designed to reject all but cloud-to-ground flashes.)

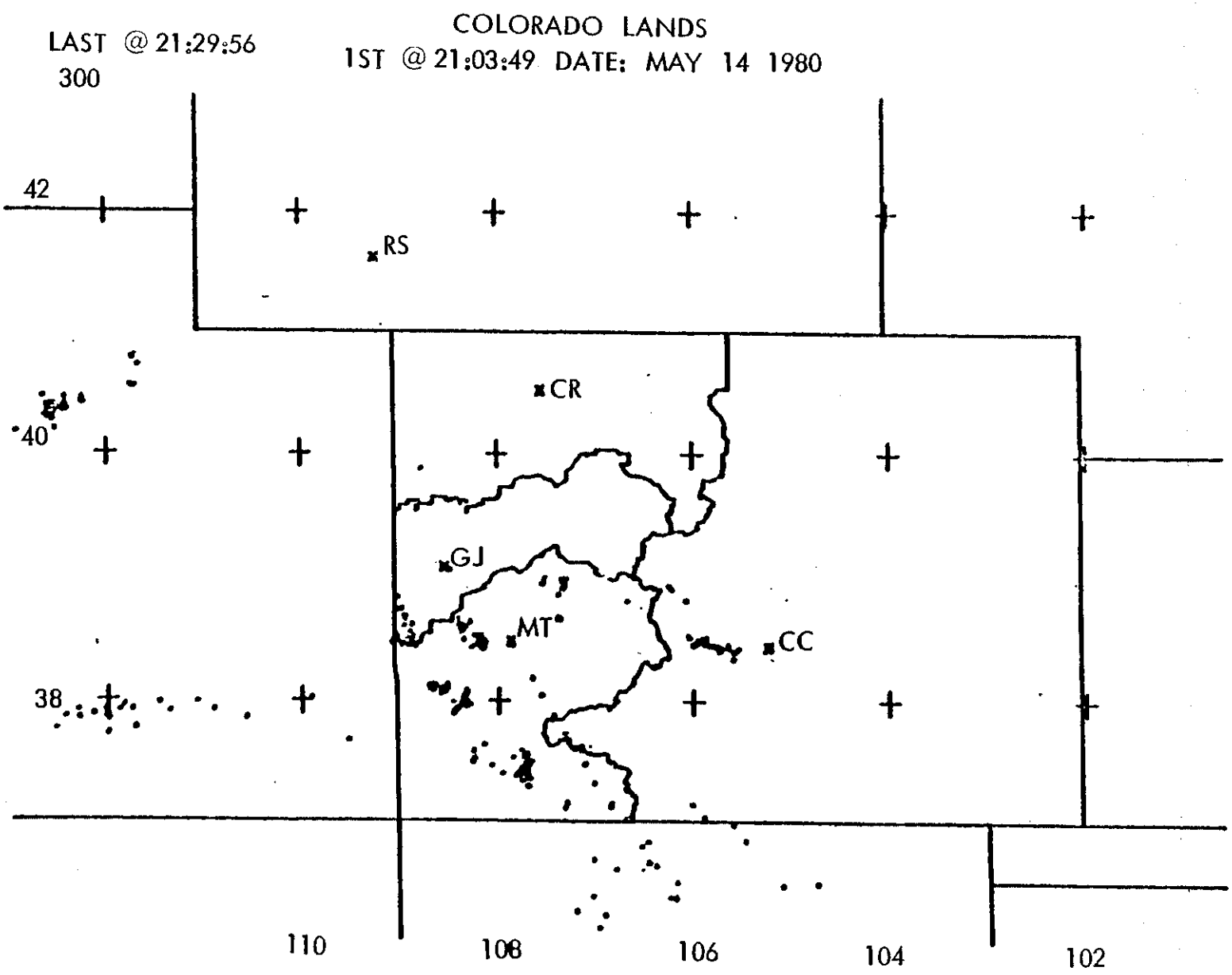

Figure A-3 **Lightning Flash Activity**

Figure A-4. **Las Vegas Net**
(Las Vegas, NV., Ely, NV., Cedar City, UT., Phoenix, AZ.)

APPENDIX B

APPENDIX B

Oscillations at Transmission Line Interfaces

The following example is taken from General Electric Aircraft Lightning Protection Note 75-1.

Figure B-1 is a transmission line of 1000 ohms surge impedance mating with a short length of line of surge impedance of 200 ohms. This in turn is mated with a continuation of the 1000 ohm transmission line. The time required for a wave to travel the length of the 200 ohm line is ΔT. Coming into the junction from the left is a current wave of amplitude 1.0. At this junction the transmission coefficient is $\gamma = 1.667$ and the reflection coefficient is $\delta = 0.667$. Accordingly, a transmitted wave of 1.667 amplitude enters the 200 ohm line and a reflected wave is launched from right to left of amplitude 0.667. On either side of the vertical separation lines, the voltage must be equal. The incident voltage (to the left of the separation line) is equal to the sum of the incident and reflected components for 1.667 amplitude. The wave that is transmitted into the 200 ohm section of line then propagates to the right to the next transition point where a reflection of amplitude -1.111 occurs, and a transmitted wave of amplitude 0.556 is propagated to the right and out of the paper.

The first reflection travelling right to left, then meets the first transition point at a time $2\Delta t$ after the incident wave hit the first junction. At that time, there is generated a second reflection travelling right to left of amplitude 0.741 and a transmitted wave going right to left of 0.370. At any time, the magnitude of the wave at the tirst tran-

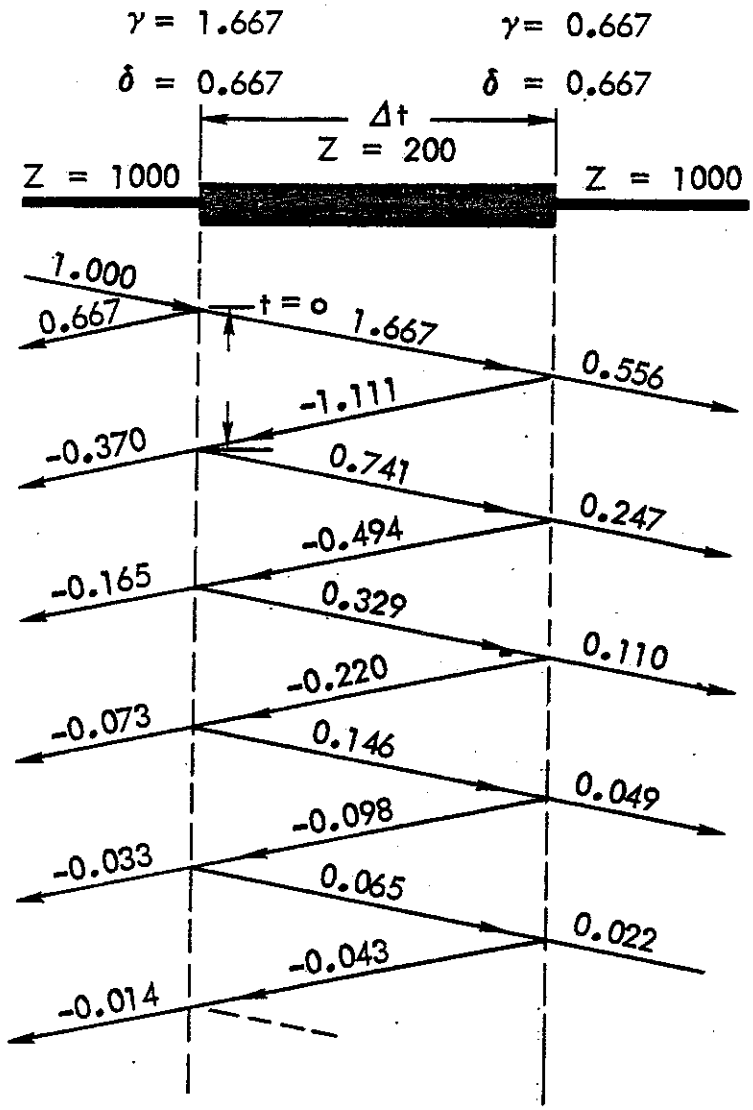

Figure B-1. Amplitude of Reflections

sition is the sum of all of the wave components on either side of the first vertical demarcation line. Accordingly, at time $2\Delta t$ the amplitude at the first transition point is 1.0 + 0.667 - 0.370 or 0.1297. The amplitude at any other point and at any other time is likewise the sum of all the transmitted and reflected wave components above that point at that time. For instance, at the midpoint of the 200 ohm line, the current is zero until a time $1\Delta t$. This time, the amplitude jumps to 1.667 and remains there until a time $3\Delta t$, when the amplitude becomes 1.667 - 1.111 or 0.556. This bookkeeping process of keeping track of the transmitted and reflected wave components may be continued as long as necessary.

The total pattern of development of these waves for the conditions of Figure B-1 (and assuming Δt equals 0.1 microseconds) is shown on Figure B-2. The voltage at the input of the 200 ohm line is seen to rise to an amplitude of 0.167 and decay in a series of steps reaching essentially its final amplitude after about 1 microsecond. Current does not begin to come out of the line until 0.1 microsecond, at which time it begins to jump to its final value in a series of steps. The current at the midpoint of the 200 ohm line oscillates back and forth with a period $2\Delta t$ = 0.2 microseconds, or a frequency of 5 MHz.

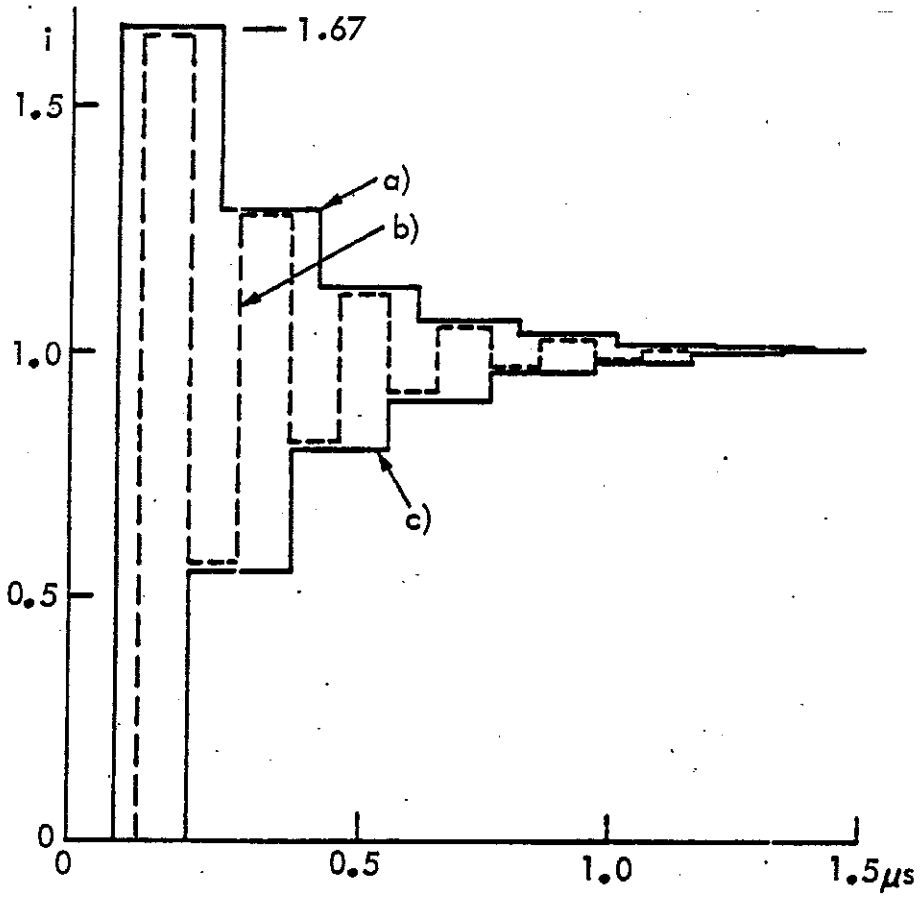

RESPONSE TO STEP FUNCTION CURRENT

a) INPUT CURRENT

b) CURRENT AT CENTER OF 200 Ω LINE

c) OUTPUT CURRENT

Figure B-2. Response to Step Function Current